



UMEÅ UNIVERSITY

Unraveling the importance of thiol
compounds on mercury speciation, uptake
and transformation by the iron-reducer
Geobacter sulfurreducens

Mareike Franziska Gutensohn

This work is protected by the Swedish Copyright Legislation (Act 1960:729)

Dissertation for PhD

ISBN: 978-91-8070-089-4 (print)

ISBN: 978-91-8070-090-0 (pdf)

Cover art: Mareike Franziska Gutensohn

Electronic version available at: <http://umu.diva-portal.org/>

Printed by: CityPrint i Norr AB

Umeå, Sweden 2023

To all alpacas

Table of Content

Abstract	iii
Sammanfattning på svenska	iv
Thesis at a glance	v
Definitions	vii
Abbreviations	viii
List of publications	x
Author´s contributions	xi
Introduction	1
Mercury in the environment	1
Transformation of mercury	3
Methylation of Hg(II)	3
Reduction of Hg(II)	4
Uptake of Hg(II)	5
Chemical speciation of mercury	5
Thiol compounds	6
Dissolved thiols	6
Membrane surface thiols	7
Aim of this thesis	9
Experimental approaches	10
Experimental systems	10
Model organism <i>Geobacter sulfurreducens</i>	10
<i>Geobacter sulfurreducens</i> preparation	10
Dissolved thiols	11
Membrane surface thiols	13
Instrumental analysis	15
LC-MS/MS	15
ICP-MS	16
X-ray absorption spectroscopy	17
Additional methods	19
Data analysis	20
Results and discussion	21
Dissolved thiols	21
Iron as a driver for thiol formation	21
Turnover of thiol compounds - conversion of cysteine to penicillamine	23
Mercury speciation, losses, and methylation	25

Cell physiology during Hg(II) methylation assays	29
Concluding remarks: Dissolved thiols and cell physiology driving Hg(II) methylation	31
Surface thiols on the outer and inner membrane.....	32
Mercury speciation on the outer and inner membrane.....	32
Concentration of membrane surface thiols.....	34
Mercury partitioning.....	35
Reduction of Hg(II)	36
Methylation of Hg(II)	38
Concluding remarks: Interaction of Hg with the inner and outer membrane	41
Conclusion	42
Outlook.....	46
Acknowledgement	48
References.....	49
Appendix.....	64

Abstract

The biogenic methylation of inorganic, divalent mercury (Hg(II)) by methylating microorganisms leads to formation and bioaccumulation of monomethyl mercury (MeHg) in the environment and can cause severe damage to ecosystems and human health. Diverse microorganisms carry the gene sequence *hgcAB* and are able to methylate Hg(II) intracellularly. The interplay of biological, chemical and physical parameters is driving mercury (Hg) transformation by microorganisms. The chemical speciation of Hg(II) with thiol compounds, both with dissolved low molecular mass (LMM) thiols and thiols present on microbial membrane surfaces, is one key factor for Hg availability and transformation. In this work the role of thiol compounds with respect to Hg speciation, uptake and transformation was studied by the iron-reducing model organisms *Geobacter sulfurreducens*. The turnover of dissolved thiols and the role of outer and inner membrane thiols was studied with novel experimental strategies.

In Paper I and II the formation of thiol compounds was studied under varying nutrient conditions. It was shown that the formation of LMM-thiol compounds was impacted by divalent iron, Fe(II). Furthermore, we showed the turnover of the small LMM-thiol cysteine to the branched LMM-thiol penicillamine, which was further amplified by the addition of exogenous cysteine or nutrients. This turnover of small to branched LMM-thiols impacted the Hg(II) speciation in methylation assays and the relative contribution between cysteine and penicillamine was important for Hg(II) availability, uptake and methylation. In addition, the partition of Hg(II) between the cell-adsorbed and dissolved phase was shifted towards the latter at higher LMM-thiol concentrations. Nutrient concentrations impacted cell physiology due to a shift to an active metabolism and a faster metabolization of LMM-thiols. We concluded that the interplay between thiol metabolism, Hg(II) speciation and cell physiology are key parameters for Hg(II) methylation by *G. sulfurreducens*. In Paper III The outer and inner membrane was characterized independently by two X-ray absorption spectroscopy techniques. The determination of the Hg speciation by both X-ray absorption spectroscopy techniques showed coherent results for both the outer and inner membrane of *G. sulfurreducens*. The concentration of thiol membrane groups was higher on the inner compared to the outer membrane. The differences between the outer and inner membrane suggested that thiol concentration and Hg coordination environment likely impact the Hg(II) internalization. The role of membrane thiols for Hg(II) uptake and transformation was further investigated in Paper IV by selectively blocking these functional groups. Partitioning and uptake of Hg was not affected by blocking the outer and inner membrane thiols of whole cell and spheroplast samples, respectively. However, the Hg(II) methylation was decreased by blocking thiols at the outer membrane, but no effect was observed by blocking thiols at the inner membrane. Blocking of membrane surface thiols changed the physiology in whole cells but not in spheroplasts. This result suggested weaknesses of the applied blocking approach. In addition, Hg(II) reduction was studied on the outer and inner membrane and showed the formation of liquid and gaseous elemental Hg, Hg(O), in Paper III and IV, respectively.

Overall, this work showed the central role of dissolved and cell-associated thiol compounds for Hg(II) uptake and the transformation reactions. Herby, concentration, compositions and distribution of thiols are crucial and impact the Hg(II) speciation, partitioning, uptake and availability for Hg(II) methylation and reduction. In addition, cell physiology is impacting the methylation potential and the turnover of LMM-thiol compounds. The role of membrane surface thiols for Hg(II) uptake was not fully identified, however such thiols were for the first time characterized selectively for the outer and inner membrane by X-ray absorption spectroscopy.

Sammanfattning på svenska

Biogen metylering av oorganiskt, divalent kvicksilver (Hg(II)) förekommer i specifika mikroorganismer och leder till bildning och bioackumulering av monometylkvicksilver (MeHg) i miljön som kan orsaka allvarliga skador på ekosystem och människors hälsa. Vissa mikroorganismer bär på gensekvensen *hgcAB* och kan via dessa gener metylera Hg(II) intracellulärt. Metyleringen drivs av ett komplext samspel mellan biologiska, kemiska och fysikaliska parametrar. Kemiska komplex av Hg(II) (speciering) med tiolföreningar, både lösta tioler med låg molekylmassa (LMM) och tioler som finns på mikrobiella membranytor, är en nyckelfaktor för att förstå kvicksilvers (Hg) tillgänglighet och transformationsprocesser. I denna avhandling har tiolföreningarnas roll studerats med avseende på Hg-speciering, upptag och transformationer i den järnreducerande bakterien *Geobacter sulfurreducens*. Omsättningen av lösta tioler och betydelsen av tioler på ytan av de yttre och inre cellmembranen har studerades med nya experimentella strategier.

I manuskript I och II studerades bildningen av tiolföreningar under varierande näringstillstånd. Resultaten visade att bildningen av LMM-tiolföreningar påverkades av divalent järn, Fe(II). Vidare visade vi att cystein, en LMM-tiolförening med liten storlek och enkel kemisk struktur, omvandlas till penicillamin, en LMM-thiolförening med mer "grenad" kemisk struktur. Process förstärktes ytterligare genom tillsats av exogen cystein eller andra näringsämnen. Omvandlingen från liten till grenad LMM-tiol påverkade Hg(II)-specieringen i metyleringsexperiment och den relativa fördelningen mellan dessa tioler visade sig vara viktig för tillgänglighet, upptag och metylering av Hg(II). Dessutom skiftades fördelningen av Hg(II) mellan den celladsorberade och lösta fasen mot den senare vid högre koncentrationer av LMM-tioler. Halterna av näringsämnen påverkade cellfysiologin och ökade cellmetabolismen vilket ledde till en snabbare nedbrytning av LMM-tioler. Vi drog slutsatsen att samspelet mellan tiolmetabolism, Hg(II)-speciering och cellfysiologi är nyckelparametrar för Hg(II)-metylering av *G. sulfurreducens*. Det yttre och det inre membranet karaktäriserades separat i manuskript III genom två olika tekniker baserade på röntgenabsorptionsspektroskopi. Bestämningen av Hg-specieringen med båda teknikerna för röntgenabsorptionsspektroskopi visade överensstämmande resultat för både det yttre och det inre membranet hos *G. sulfurreducens*. Koncentrationen av membranbundna tiolgrupper var högre på det inre jämfört med det yttre membranet. Skillnaderna mellan det yttre och det inre membranet tyder på att tiolkoncentration och koordinationsmiljön för Hg(II) sannolikt påverkar Hg(II)-upptaget. Membrantiolers roll för Hg(II)-upptag och omvandling undersöktes ytterligare i manuskript IV genom att selektivt blockera dessa funktionella grupper. Fördelning och upptag av Hg påverkades inte av blockering av de yttre och inre membrantiolerna. Hg(II)-metyleringen minskade när tioler på det yttre membranet blockerade men inte vid selektiv blockering av tioler på det inre membranet. Blockering av membrantioler förändrade fysiologin i hela celler men inte i sfäroplaster. Detta resultat antydde begränsningar i den tillämpade blockeringsmetoden. Även Hg(II)-reduktion studerades på det yttre och inre membranet och resultaten visade bildningen av både flytande och gasformigt elementärt Hg, Hg(O), i manuskript III respektive IV.

Vårt arbete visade att lösta och cellbundna tiolföreningar spelar en central roll för upptag och transformationsreaktioner av Hg(II). Koncentration, sammansättning och fördelning av tiolföreningar har stor påverkan på specieringen, fördelningen och cellupptaget av Hg(II) och därmed för tillgängligheten av Hg(II) för metylering och reduktion. Dessutom påverkar cellfysiologin metyleringspotentialen och omsättningen av LMM-tiolföreningar. Tioler på membranytor karaktäriserades för första gången selektivt för det yttre och inre membranet genom röntgenabsorptionsspektroskopi, även om deras fullständiga funktion för cellupptag av Hg(II) inte bestämdes.

Thesis at a glance

Paper I	Metabolic turnover of cysteine-related thiol compounds at environmentally relevant concentrations by <i>Geobacter sulfurreducens</i>
Objective	<ul style="list-style-type: none"> • Investigate the time-dependent response of thiol turnover linked to the growth state • Effect of essential and toxic trace metals on thiol turnover • Effect of exogenous thiols on metabolic turnover of thiols
Experimental set-up	<ul style="list-style-type: none"> • Alterations of growth medium and assay buffer composition • Exposure to Fe(II) and Hg(II) • Monitoring extra- and intracellular thiol compounds • Trace isotopically labeled exogenous thiols
Main findings	<ul style="list-style-type: none"> • Control of thiol formation and excretion linked to growth state and external condition • Iron dependent thiol formation • Di-methylation of cysteine to penicillamine

Paper II	The combined effect of Hg(II) speciation, thiol metabolism and cell physiology on methylmercury formation by <i>Geobacter sulfurreducens</i>
Objective	<ul style="list-style-type: none"> • Examine the effect of endogenous and exogenous thiols on time-dependent changes of Hg(II) speciation and their impact on Hg(II) methylation • Impact of cell physiology on Hg(II) methylation
Experimental set-up	<ul style="list-style-type: none"> • Hg(II) methylation assays under altering nutrient load with endogenous and exogenous thiol addition • Monitor Hg species • Monitor cell physiology • Thermodynamic and kinetic modelling
Main findings	<ul style="list-style-type: none"> • Short term: Thiols enhance dissolved Hg(II) fraction and Hg(Cys)₂ complexes enhance MeHg formation • Long term: Thiol turnover from small to branched Hg(RS)₂ complexes lead to stalled MeHg formation • Nutrient addition enhances MeHg formation and physiology of cells

Paper III	Determination of mercury speciation and thiol concentration on the outer and inner membrane of <i>Geobacter sulfurreducens</i> by EXAFS and HERFD-XANES
Objective	<ul style="list-style-type: none"> Investigate the Hg speciation on the outer and inner membrane surface of <i>G. sulfurreducens</i> by EXAFS and XANES Determine the membrane surface thiol concentration of the outer and inner membrane
Experimental set-up	<ul style="list-style-type: none"> Hg titration of whole cells (outer membrane) and spheroplasts (inner membrane) under starved assay condition (no electron donor or acceptor) Examine membranes by X-ray absorption spectroscopy: EXAFS and HERFD-XANES
Main findings	<ul style="list-style-type: none"> Coherent Hg speciation result by EXAFS and HERFD-XANES Membrane surface thiol concentration higher on the inner membrane compared to the outer membrane Liquid Hg(0) formation

Paper IV	The role of outer and inner membrane surface thiols on Hg(II) uptake, methylation and reduction by <i>Geobacter sulfurreducens</i>
Objective	Study the mechanistic role of outer and inner membrane surface thiol functional groups on: <ul style="list-style-type: none"> Hg partitioning Hg(II) uptake and methylation Hg(II) reduction
Experimental set-up	<ul style="list-style-type: none"> Blocking of outer (whole cell) and inner membrane (spheroplast) surface thiols Cell wash and sample purging Monitor Hg partitioning and species Monitor cell physiology
Main findings	<ul style="list-style-type: none"> MeHg formation higher for whole cells compare to spheroplasts Formed MeHg remain cell-associated Hg(0) formation independent of membrane surface thiols Blocking of membrane surface thiols alter cell physiology

Definitions

Availability – In this thesis, a mercury (Hg) molecule, which is internalized across the cell membrane and intracellularly methylated. Overall, availability of metals in the environment is impacted by their concentration, speciation, partitioning, pH, redox potential, and organic matter content.^{1, 2}

Cell-associated – The sum of Hg, that is adsorbed to the cell membrane and in the peri- and cytoplasm of the cell.

Cell physiology – In general the understanding of the principle of cellular reproduction.³ In this thesis the term cell physiology is globally used and comprises cell number changes, biochemical composition and/or cell viability.

Low molecular mass thiols – Small organic molecules (≤ 1000 Dalton) containing a thiol functional group (-SH), which are highly reactive molecules, controlling redox homeostasis in cells.⁴⁻⁶

Metabolites – A molecule that is a substrate, product, or essential component of a metabolic reaction, which is an end- or by-products of a metabolic pathway.⁷

Partitioning – The distribution of Hg among the dissolved, cell-adsorbed, intracellular and gaseous phases. In this case, the partitioning between the phases refers to a dynamic system and not to an equilibrium state.

Speciation – The “distribution of an element among defined chemical species in a system”, where the chemical species is specified as the “specific form of a chemical element defined as to isotopic composition, electronic or oxidation state, and (or) complex or molecular structure”.⁸

Abbreviations

ATR-FTIR	Attenuated total reflectance Fourier transform infrared spectroscopy
Cl ⁻	Chloride
-COOH	Carboxyl group
Cys	L-cysteine (chemical formula: C ₃ H ₇ NO ₂ S)
CysN	Cysteamine (chemical formula: C ₂ H ₇ NS)
DOM	Dissolved organic matter
EDTA	Ethylenediaminetetraacetic acid
ESI	Electro spray ionization
EXAFS	Extended X-ray absorption fine structure
ext	exterior
Fe(II)	Divalent iron
GC	Gas chromatography
GSH	Glutathione
Hg	Mercury (all species)
Hg(o)	Elemental Hg (gaseous or liquid)
Hg(II)	Divalent, inorganic Hg
HgS	Mercury sulfide
HERFD	High-Energy-Resolution-Fluorescence-Detected
IDA	Isotope dilution analyses
ICP-MS	Inductively coupled plasma mass spectrometry
<i>k</i> _{meth}	Rate constant for Hg(II) methylation
LC-MS/MS	Liquid chromatography tandem mass spectrometry
LCF	Linear combination fitting
LMM	Low molecular mass
LOD	Limit of detection
log <i>K</i>	Equilibrium constant
<i>M</i>	Molar concentration, mol L ⁻¹
MeHg	Monomethyl mercury (chemical formula: CH ₃ Hg)
Mem	Membrane (outer or inner)
N ₂	Nitrogen (gaseous or liquid)
-NH ₂	Amine group
NOM	Natural organic matter
-OH	Hydroxyl group
PBS	Phosphate buffer saline
PEN	D-Penicillamine (chemical formula: C ₅ H ₁₁ NO ₂ S)
PHMB	4-(hydroxymercuri)benzoate acid sodium salt (chemical formula: C ₇ H ₅ HgNaO ₃)
qBBr	Monobromo(trimethylammonio)bimane bromide (chemical formula: C ₁₃ H ₁₉ Br ₂ N ₃ O ₂)

R	Rest of a molecule consisting of a group of carbon and hydrogen atoms any size
RO/N	Rest of molecule with oxygen (-OH, -COOH) or nitrogen (NH ₂) functional group
-SH	Thiol group
SPE	Solid phase extraction
XANES	X-ray absorption near edge structure
XAS	X-ray absorption spectroscopy

List of publications

This thesis is based on the following papers and manuscripts and referred to in the text by their corresponding Roman numerals.

- I. **Mareike Gutensohn**, Jeffra K. Schaefer, Torben J. Maas, Ulf Skjallberg and Erik Björn. (2023) Metabolic turnover of cysteine-related thiol compounds at environmentally relevant concentrations by *Geobacter sulfurreducens*. *Frontiers in Microbiology*. 13:1085214. doi: 10.3389/fmicb.2022.1085214
- II. **Mareike Gutensohn**, Jeffra K. Schaefer, Elena Yunda, Ulf Skjallberg and Erik Björn. (2023) The combined effect of Hg(II) speciation, thiol metabolism and cell physiology on methylmercury formation by *Geobacter sulfurreducens*. *Environmental, Science & Technology*. doi: 10.1021/acs.est.3c00226
- III. **Mareike Gutensohn**, Morgane Desmau, Olivier Proux, Erik Björn, Ulf Skjallberg. Determination of mercury speciation and thiol concentration on the outer and inner membrane of *Geobacter sulfurreducens* by EXAFS and HERFD-XANES
Manuscript
- IV. **Mareike Gutensohn**, Jeffra K. Schaefer, Ulf Skjallberg and Erik Björn. The role of outer and inner membrane surface thiols on Hg(II) uptake, methylation and reduction by *Geobacter sulfurreducens*
Manuscript

Publication by the author during the doctoral education but not part of the thesis

- V. Elena Yunda, **Mareike Gutensohn**, Madeleine Ramstedt and Erik Björn. (2023) Methylmercury formation in biofilms of *Geobacter sulfurreducens*. *Frontiers in Microbiology*. 14:1079000. doi: 10.3389/fmicb.2023.1079000

Paper I was published as open access under the Creative Commons CC-BY license (the current version is CC-BY, version 4.0).

Paper II was reprinted with permission from *Environmental Science & Technology*. Copyright © 2023, American Chemical Society. All rights reserved.

Author's contributions

Paper I

The author had a lead role in planning the study, carried out the experimental work and the instrumental analyses, performed a major part of the data processing and contributed to manuscript preparation and revision.

Paper II

The author had the idea for the study, planned the study, carried out the experimental work and the instrumental analyses, performed the data processing and had a lead role in writing and revising the manuscript.

Paper III

The author had a key role in planning the study and writing the proposal, carried out the experimental work and major part of the instrumental analyses, performed minor parts of the data processing and had a lead role in writing the manuscript.

Paper IV

The author developed the idea for the study, planned the study, carried out the experimental work and the instrumental analyses, performed the data processing and was responsible for writing the manuscript.

Introduction

Mercury in the environment

Mercury (Hg) is one of the top ten chemicals of major public health concerns according to the World Health Organization.⁹ It is the heavy metal with the highest toxicity.¹⁰ Hg exposure to humans occurs predominantly through the consumption of food like fish and rice.¹¹⁻¹³ Hg pollution is spread across the whole globe, including in highly remote areas.¹⁴ The main sources for Hg pollution are anthropogenic origin with ~80% of the global input dominated by gold mining, coal combustion and cement production.¹⁶ Natural sources are contributing with ~20% to the global Hg emission including volcanic activity and weathering of rocks.¹⁶ The earth's crust contains on average 0.085 ppm Hg.¹⁷ The release of Hg from anthropogenic or natural sources is either in the form of gaseous elemental Hg (Hg(0)) or by inorganic divalent Hg (Hg(II)).¹⁸ Anthropogenic releases of other Hg forms, like organometallic Hg has occurred for example through chemical accidents and usage of Hg containing compounds in agriculture.¹⁹⁻²¹

The first described environmental Hg pollution by a point source occurred in the 1950s at the Minamata bay in Japan by a chemical company.¹⁹ This dramatic accident caused severe Hg poisoning of thousands of people through the consumption of MeHg-containing fish and shellfish and consequently led to an increased mortality.^{22, 23} In the beginning of the 20th century, mercury became a popular fungicide due to its high efficiency in controlling microorganism growth.²⁴⁻²⁶ In Sweden, the intensive use of Panogen, a Hg-containing seed-dressing pesticide, had severe mass mortality effects on the seed-eating bird population in the 1950s.²¹ Moreover, in the 1950s and 1960s extensive emission of Hg by chlor-alkali plants and by metal production to the atmosphere led to extensive Hg pollution of the terrestrial and aquatic ecosystem in Sweden.²⁰ In 1966 Hg-containing pesticides were restricted in Sweden²⁷ and since 2009 the use of Hg and Hg-containing products is banned.²⁸ Moreover, the severe effects of Hg on human health and ecosystems led to a global goal to protect humans and ecosystems from Hg exposure. This resulted in developing the international document "Minamata convention on Mercury" in 2013 and 128 states signed the agreement.²⁹ It is a leading document for the global ban of hazardous chemicals.

Since the mid-20th century scientists have focused on understanding the complex biogeochemical cycling of Hg in the environment (Figure 1).³⁰ The physiochemical properties of Hg are unique as reflected by the low melting and boiling point.³¹ The electronic configuration of Hg is with a filled d and f orbital and due to its weak interaction, it is the only liquid metal at room temperature.³¹ The three oxidation states of Hg are: 0, +1 and +2 and Hg occurs in different forms: elemental as Hg(0), either gaseous or liquid, inorganic as Hg(II) or Hg(I) (metastable) and organic as e.g., monomethyl mercury (MeHg, CH₃Hg⁺).³¹ The different forms are distributed in the hydrosphere, atmosphere, geosphere and biosphere (Figure 1).¹⁵ Transportation and deposition of Hg in the atmosphere and remobilization of different Hg forms in soil and sediment cause a continuing spread of Hg in the environment.¹⁵ The residence time of Hg(0) in the atmosphere is >1 year and therefore allows long-range atmospheric transport.³² Hg(II) is

the dominant form of Hg in soil and sediments, whereas MeHg is the dominant form in the biosphere.³⁰ Both biotic and abiotic processes contribute to transformation and transport of Hg. Microorganisms are key transformers of Hg with reduction of Hg(II), methylation of Hg(II) and demethylation of MeHg.³³ The biogenic formation of MeHg leads to bioaccumulation and biomagnification across the food web in aquatic systems and leads to high MeHg concentration with up to 85% of the total Hg in end predators.³⁴⁻³⁷ Trophic transfer through the food web is more efficient for MeHg species.^{35, 38} Overall, the organometallic forms of Hg show a higher toxicity compared to inorganic Hg with a higher mobility and a higher bioaccumulation.³⁹

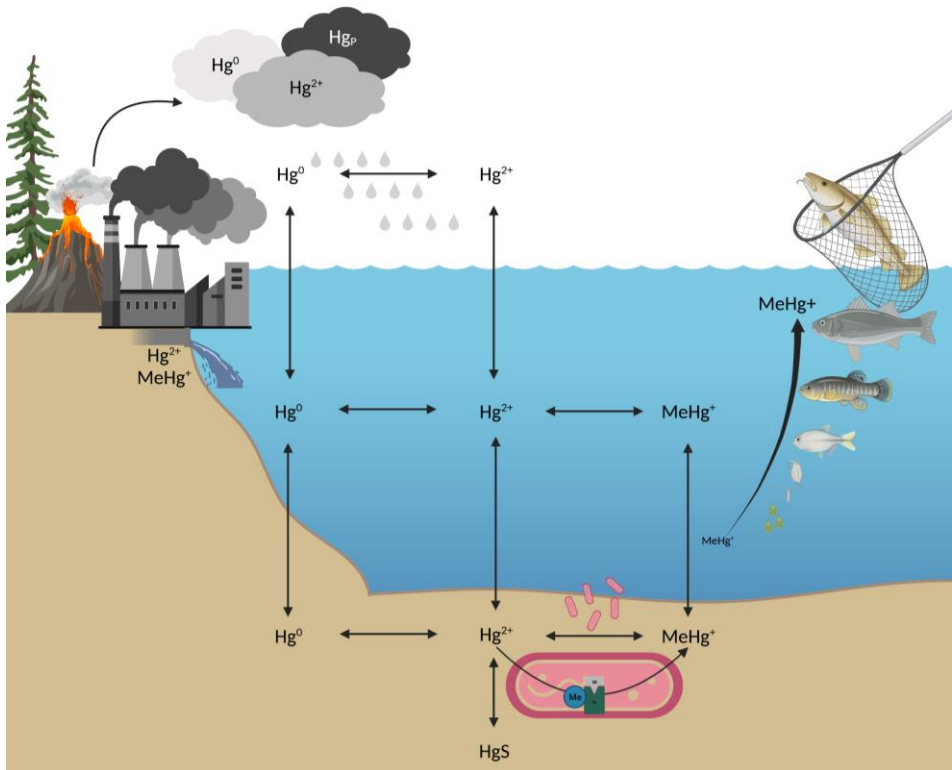


Figure 1: Key pathways of the biogeochemical transformation of Hg in the environment. Sources of Hg are anthropogenic or natural origin in the form of Hg(II), Hg(0) and particulate Hg (Hg_P). The biogenic Hg(II) methylation by the enzyme cluster HgcAB in anaerobic microorganisms is the major mechanism for MeHg formation and leads subsequently to the bioaccumulation of MeHg in the food web. (Created with BioRender.com)

The biotransformation of Hg(II) to MeHg through microorganisms is a crucial step of the biogeochemical cycling of Hg in the environment. The mechanistic understanding of Hg(II) availability, uptake and methylation in methylating microorganisms and the identification of its driving parameters are still not fully identified.^{2, 40, 41} The overall methylation potential of an organism is a complex interplay of various biological-, chemical- and physical-parameters, which are impacting Hg(II) availability, uptake and methylation as illustrated in Figure 2.²

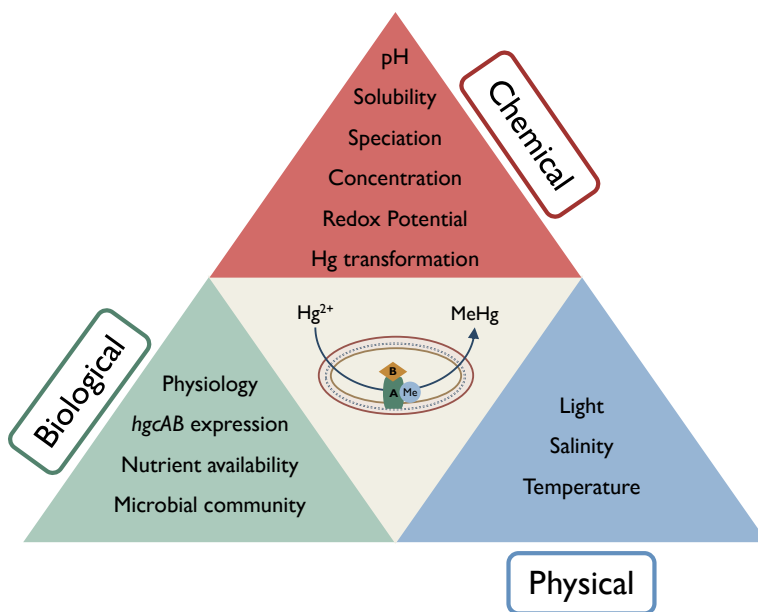


Figure 2: Driving biological-, chemical- and physical parameters impacting the biogenic methylation of Hg(II) in the environment. The available Hg(II) pool is additionally impacted by Hg transformation reactions like Hg(II) reduction and MeHg demethylation.

Transformation of mercury

Methylation of Hg(II)

Jensen and Jernelöv first described the biogenic methylation of Hg(II) in sediments in the 1960s.⁴² During the last decades, a variety of Hg(II) methylating organisms were identified, which are dominated by sulfate-reducers, iron-reducers, firmicutes, methanogens and archaea.^{43, 44} As major model organism for Hg(II) methylation studies, the sulfate-reducer *Pseudodesulfobivrio mercurii* ND132 (ND132, formerly classified as *Desulfobivrio desulfuricans*) and the iron-reducer *Geobacter sulfurreducer* are commonly used.^{43, 45-64} Since the discovery of Hg(II) methylating organisms, the biochemical pathway of biogenic Hg(II) methylation has been of great interest.⁶⁵⁻⁷⁰ In 2013, Parks and co-workers identified the gene sequence *hgcAB*, a significant breakthrough for understanding the mechanism of biogenic Hg(II) methylation and to further identify Hg(II) methylating organisms.⁷¹ The *hgcAB* gene cluster consists of a

membrane associated corrinoid-binding protein HgcA, which transfers the methyl group to Hg(II), and a ferredoxin like protein HgcB, which transfers electrons to the HgcA enzyme unit.^{71, 72} The methylation of Hg(II) is an anaerobic process and is inhibited under ambient oxygen levels.⁷² Previously, the methylation of Hg(II) was ascribed to anaerobic organisms in anoxic environment, i.e. sediment or soil.^{43, 44} Recently organisms in the oxic environment were identified, which carry the gene sequence *hgcAB* and show the potential to methylate Hg(II) in oxic environments.^{73, 74} The gene expression of *hgcAB* is constitutive and it is not induced by Hg exposure.^{45, 75} In addition, field and laboratory studies showed that Hg(II) methylation is enhanced with increased microbial activity and biomass production.⁷⁵⁻⁷⁸ The physiological role of MeHg formation is unknown since its formation has no selective advantage towards Hg resistance.^{45, 71}

Abiotic methylation

Biotic MeHg formation is the major source for MeHg in the environment.^{14, 15} However abiotic Hg(II) methylation occurs under specific environmental condition if suitable methyl donors are present.⁷⁹ Possible methyl donors are methyl iodide, dimethylsulfide, fluvic and humic acids and organometallic compounds like methyl cobalamin.^{39, 79} The abiotic transfer of a methyl group onto Hg(II) in the environment is dependent on pH, temperature, and available complexing agents.⁷⁹ Overall, the contribution of abiotically formed MeHg in the environment is of minor importance.^{39, 80}

Demethylation of MeHg

In parallel to MeHg formation, demethylation of MeHg occurs via abiotic and biotic mechanisms in the environment. The most efficient biotic demethylation mechanism is via the *mer* operon system. The mercury resistance gene *merAB* detoxifies Hg(II) or MeHg into the relatively inert volatile Hg(0) form through reduction.⁸¹⁻⁸³ It is the only known large-scale Hg detoxification system in microorganisms and it is not linked to the *hgcAB* gene cluster.⁸⁴ The *mer*-operon system is predominantly present in aerobic microorganisms.⁸⁴ As an additional demethylation mechanism by microorganism the oxidative demethylation is known.⁸⁵ Moreover, abiotic demethylation by photochemistry at a wavelength between 200-400 nm has been described, and this is the dominating demethylation process in surface waters.^{86, 87}

Reduction of Hg(II)

Transformation of Hg(II) to Hg(0) also occurs through biotic and abiotic mechanisms. Biotic Hg(II) reduction by microorganisms occurs either via the *mer*-resistance operon or via cytochromes. In microorganisms with the *mer*-resistance operon, Hg(II) uptake and reduction occur via the *merT* and *merA* operon, respectively, and are highly efficient in contaminated sites.^{81, 88-90} Hg(II) reduction via cytochromes was shown in the model organisms *G. sulfurreducens* and is linked to outer membrane cytochromes, and deletion of five dominant outer-membrane c-type cytochromes decreased the formation of Hg(0).^{57, 60} Moreover, a variety of algae show the potential to reduce Hg(II).⁹¹⁻⁹³ Abiotic reduction of Hg(II) occurs either by photoreduction or by organic and inorganic ligands. Photoreduction is dependent on the intensity of ultraviolet radiation and the presence of ligands in surface waters.⁹⁴⁻⁹⁷ Under anoxic dark condition, Hg(II) can be reduced to Hg(0)

by reduced natural organic matter (NOM).⁹⁸⁻¹⁰⁰ Additionally, Hg(II) reduction occurs on sulfide and iron mineral surfaces.¹⁰¹⁻¹⁰³

Uptake of Hg(II)

The uptake of Hg(II) across the cell membrane is a pivotal step for Hg(II) methylation. Microorganisms carrying the *mer* resistance operon are able to take up Hg(II) and MeHg by the *merR* and *merT* transportation system.⁸¹ However, the majority of methylating microorganisms do not carry the *mer*-resistance operon and the uptake of Hg(II) in those methylating organisms is linked to another mechanism.⁴¹ Overall, the molecular mechanism of Hg(II) internalization for Hg(II) methylating organisms is still unidentified and passive, facilitated and active uptake mechanisms have been discussed.^{40, 41, 52, 104-106} The passive diffusion transport pathway hypothesized internalization of lipophilic, uncharged Hg(II) complexes in the form of dissolved Hg-sulfide complexes, predominantly as Hg(SH)_{2(aq)}, Hg(S)_{2(aq)}, HgCl₂ or nonionized Hg(RS)₂ species, across the cell membrane.^{41, 104, 105, 107-111} HgS nanoparticles are proposed to be available for sulfate-reducing microorganisms as shown in sediments and laboratory studies.^{48, 112-115} The uptake mechanism of the sulfate-reducing model organism ND132 is assumed to be passive⁵⁶ and follows the principle of the biotic ligand model.^{116, 117}

Facilitated and active uptake of Hg(II) occurs through membrane transporters.^{40, 41, 106} Active uptake is energy dependent.^{40, 41} For the iron-reducing model organism *G. sulfurreducens*, Hg(II) uptake is ascribed to an active uptake mechanism.^{52, 53} In addition, it is suggested that metal transporters for other trace metals like Cd(II) and Zn(II) are used for Hg(II) uptake by *G. sulfurreducens*.^{53, 118}

The Hg(II) uptake by *G. sulfurreducens* is hypothesized to consist of multiple processes across the outer and inner membrane, shown by fractionation effects of Hg stable isotopes.⁵⁴ It is proposed that dissolved Hg(II) is the available Hg pool for uptake and is internalized across the outer membrane into the periplasm, most likely as a Hg(RS)₂ complex.⁵⁴ The transport into the periplasm is the rate limiting step, based on slower observed uptake kinetics for whole cells compared to spheroplasts (cells without the outer membrane) through a transporter system in *G. sulfurreducens*.⁵³ The crossing of the periplasmic membrane is assumed to be linked to either free Hg(II) ions or Hg-cysteine complexes via membrane transporters.^{53, 54} In a last step Hg(II) dissociates from the transporter and Hg(RS)₂ complexes are formed intracellularly and provide the Hg(II) for the methylation by the HgcAB enzyme cluster. However, it is not clear if Hg(II) is passing the outer and inner membrane as a free Hg(II) ion or if Hg(II) is complexed to ligands like cysteine.^{53, 54} Overall, the speciation of Hg(II) with low molecular mass (LMM) thiol compounds such as Hg(RS)₂ complexes have been suggested to play an important role for Hg(II) uptake.^{49, 51, 52, 54, 114, 119-121}

Chemical speciation of mercury

In the environment, metals occur in different physical and chemical forms: elemental (gaseous, solid, liquid), in minerals (solid), free dissolved cation (aqueous phase) or

complexed with inorganic or organic compounds (aqueous or solid phase).³¹ The distribution between divalent (Hg(II)), monovalent (Hg(I)) and elemental Hg (Hg(0)) is the chemical species of Hg related to the oxidation state.³¹ The speciation of Hg(II) is the composition of its different complexes, for instance HgCl₂, Hg(RS)₂ and Hg(SH)₂, in a natural system.³¹ Chemical and biological properties of Hg are largely determined by the speciation, which impacts availability, uptake and consequently methylation.^{40, 117, 122, 123} Hg is a class B element, soft Lewis acid, and forms stable complexes with soft Lewis bases like sulfur and halides or weaker complexes with OH-ligands.¹²⁴ Chemical speciation of Hg in the environment is controlled under anoxic condition by the competition between reduced sulfur ligands, both organic and inorganic, like sulfides or thiols (RSH).¹²⁵ Hg(RS)₂ complexes are thermodynamically more stable compared to HgCl₂ or Hg(OH)₂ species.¹²⁵ The thermodynamic stability constants increase in the order from Hg(OH)₂ < HgCl₂ < Hg(RS)₂ with a log K of -6.2, 13.8 and 37-40.1, respectively.^{126, 127} Both spectroscopic and thermodynamic modelling show that two coordinated Hg(RS)₂ complexes dominate due to their thermodynamic stability compared to one coordinated complexes HgSR⁺. Moreover, under great excess of non-steric-hindered RSH compounds relative to Hg(II), three and four coordinated Hg(RS)_{3/4} complexes are formed under neutral and alkaline pH.^{31, 128} The speciation of Hg(II) is commonly determined by LC-ICPMS, GC-ICPMS or X-ray absorption spectroscopy.^{129, 130} Additionally, thermodynamic speciation modelling, a well-established approach, is applied to determine the speciation in the environment based on the thermodynamic stability constants of each species.^{31, 104, 131, 132}

Thiol compounds

Dissolved thiols

The speciation of Hg(II) with thiol compounds is crucial for Hg(II) availability.^{2, 40, 51, 52, 120} LMM-thiols are formed and build up in the suboxic to anoxic environment, in sediments, hypolimnetic bottom waters, pore waters and as well in biofilms, and reach high nanomolar concentration.¹³³⁻¹³⁷ Moreover, microbial activity in anoxic sediments, in pore waters and in water is controlling the concentration and turnover of thiols in the environment.^{136, 138, 139}

Several studies showed that addition of LMM-thiols enhance Hg(II) uptake and methylation in Hg(II) methylation studies in planktonic cell assays with *G. sulfurreducens* and ND132.^{47, 51, 52, 119, 120, 140, 141} In particular, cysteine is one of the well-studied LMM-thiols in *G. sulfurreducens* assays and is enhancing MeHg formation in the range of 1-100 μM cysteine compared to controls.^{51, 52, 120} The mechanisms for the observed enhancement effects are not identified. However, several studies ascribed this enhancement effect on Hg(II) uptake and methylation to the high availability of Hg(LMM-RS)₂ complexes.^{51, 52, 58, 136} In addition, cysteine degrades to α-HgS(s) and β-HgS(s) on cell surfaces in the presence of Hg and high cysteine concentration (>1000 μM).^{121, 142} HgS and nanoparticulate HgS are available for sulfate-reducing microorganisms and subsequently MeHg is formed.^{47, 48, 77, 114, 143} In contrast, formation of MeHg is inhibited by HgS for *G. sulfurreducens*.^{51, 120} Overall, high thiol additions should be critically considered, since microorganisms show a growth-inhibitory effect for concentrations above 200 μM Cys,¹⁴⁴ due to the redox activity

of thiol compounds and therefore their intracellular concentration is tightly controlled to prevent toxic effects.¹⁴⁵⁻¹⁴⁸ In addition to the concentration range of thiol compounds the composition of thiol compounds is crucial for Hg(II) availability and methylation. The MeHg formation by *G. sulfurreducens* is decreased in the presence of branched LMM-thiols, like penicillamine, or dissolved organic matter (DOM).^{52, 62, 63, 149} The impact of LMM-thiols on MeHg formation is organism specific since the model organism ND132 shows enhanced methylation for both branched LMM-thiols and DOM.^{52, 62, 63, 149}

In a recent study, the biogenic formation of LMM-thiols in *G. sulfurreducens* assays were shown and both Hg(II) uptake and methylation was increased even at thiol concentrations as low as ~100 nM.¹²⁰ In addition, environments like natural biofilms and wetland soils showed a correlation between the methylation potential and the LMM-thiol concentration.¹³⁵⁻¹³⁷ The Hg(II) speciation with LMM-thiol compounds could not alone describe the Hg(II) methylation potential in various studies and microbial activity was considered as an additional key factor.^{77, 120, 136, 150} Indeed, a correlation between methylation potential and metabolic activity or biomass production was observed in several studies.^{75, 77, 150} Specifically, nutrient availability and NOM composition are known driving parameters for enhanced methylation in the natural environment.^{48, 78, 150, 151} So far only one study investigated the relationship between metabolic activity and Hg(II) speciation and this study showed, that under high microbial activity the Hg(II) speciation is controlling MeHg formation under sulfidic conditions.⁷⁷

Previous studies focused on Hg(II) uptake and methylation in defined media composition with a single microbial strain^{51, 52, 59, 60, 120, 152} or studied Hg(II) methylation in natural sample environment.^{77, 78, 135-137, 150, 153} In several studies the combination of Hg(II) speciation and microbial activity is highlighted,^{77, 120, 136, 137} however these two factors were not systematic in a joint approach investigated. Overall, LMM-thiols are formed and accumulated in anoxic environments and determine the Hg(II) speciation. In addition, nutrient availability is impacting microbial activity of methylators. Both factors, chemical and biological, consequently impact the Hg(II) methylation potential.² However, their combined effect on MeHg formation is not known and it is a crucial next step to investigate in a joint approach the formation and turnover of LMM-thiols, their impact on Hg(II) speciation, and to understand the role of microbial activity.

Membrane surface thiols

In addition to the chemical speciation of Hg(II) with dissolved LMM-thiols, cell-associated thiol groups located in cell membrane proteins impact the Hg(II) speciation, partitioning and uptake of Hg(II).^{54, 61, 103, 152, 154, 155} Cell membrane thiols compete with dissolved LMM-thiols and DOM compounds outside the cell for complexing Hg(II).^{58, 152, 155, 156} The thermodynamic stability constant of Hg with thiols groups of the dissolved phase and the cellular phase are in the same order of magnitude.¹⁵⁵ The stability constant $\log K$ for Hg(NOM-RS)₂, Hg(Cys)₂, Hg(Cys)(NOM-RS), Hg(Cys)(Mem-RS) and Hg(Mem-RS)₂ are in the range of 37.5 to 40.0.^{126, 155, 157} In contrast, Hg(II) complexes with mixed ligation consisting of one thiol group and one hydroxyl (-OH) or carboxyl (-COOH) group, like Hg(NOM-RS)(NOM-RO), Hg(Mem-RS)(Mem-RO) or Hg(OH)(RSH), show lower thermodynamic stability constants with $\log K$ of 26, 25.6 and 18.5, respectively.^{126, 155, 158}

Since the thermodynamic constant of cell membrane and dissolved thiols are in the same order of magnitude, the concentration of both membrane surface and dissolved thiols are impacting the partitioning of Hg between the dissolved and cellular phase.^{52, 58, 61, 63, 152, 156, 159} To improve the understanding of cell membrane thiols on Hg(II) uptake, the cell membrane thiol concentration of *G. sulfurreducens* was estimated by fluorescence spectroscopy, potentiometry and extended X-ray absorption fine structure (EXAFS).^{152, 154, 155, 160} The three recent studies showed cell membrane thiol concentration between 20–240 $\mu\text{mol g}^{-1}$ wet mass (380–2000 $\mu\text{mol g}^{-1}$ C).^{152, 154, 155}

The role of Hg(II) adsorption as a sink or source for Hg(II) uptake and methylation is controversially discussed.^{49, 54, 60, 61} Previously, availability of metals was described by a simplified approach, the biotic ligand model, which assumes a chemical equilibrium between the metal, metal complexes and the metal bound to biological surfaces.¹¹⁶ However, this model failed to predict metal availability, since metal-biota interactions are not in equilibrium, metal adsorption is organism specific and dependent on the binding environment of the biological surface.^{117, 161} Recent studies showed the importance of both the metal speciation and the concentration of cell membrane thiols for metal availability.^{49, 57, 60, 61, 152, 162} On the one hand, one study showed a positive relationship between cell membrane thiols and Hg(II) methylation⁶⁰ and on the other hand Hg(II) adsorbed to cell membrane thiols inhibited Hg(II) uptake and methylation by decreasing the dissolved Hg(II) pool.^{49, 54, 61} Additionally, the competing process Hg(II) reduction is dependent on the Hg to cell thiol ratio and is enhanced by high Hg to cell thiol ratios.^{57, 60} A recent study by Thomas et al. showed, that blocking of cell membrane thiols did not decrease MeHg formation and Hg partitioning between the cellular and dissolved phase was not impacted, instead the Hg(II) methylation was only driven by the dissolved thiol concentration.¹⁵² Especially, Hg speciation analyses by X-ray absorption spectroscopy highlighted the importance of the Hg coordination environment for Hg(II) uptake and methylation.^{152, 162}

Recent studies focused on cell surface thiols of either the outer membrane^{58, 60, 61, 141, 152, 154, 163} or cell membrane fragments,¹⁵⁵ but did not differentiate between the outer and inner membrane. However, several studies ascribed the uptake across the outer and inner membrane as two separate processes.⁵²⁻⁵⁴ The hypothesized uptake mechanism emphasized both dissolved and cell membrane thiols as crucial parameters, while dissolved thiols enhance Hg(II) uptake and cell membrane thiols decrease Hg(II) uptake.⁵⁴

So far, the thiol concentration and the Hg speciation of the outer membrane have been determined for MeHg methylating organisms.^{152, 154, 155, 162} Studies determined thiol concentration and Hg speciation on the inner membrane (spheroplast) of ND132 and *Geobacter bemidjensis Bem* and in these studies Hg(0) oxidation and demethylation processes were studied.^{55, 164} The thiol concentration and the Hg speciation on the inner membrane and their impact on Hg(II) availability and Hg(II) uptake is unknown for the model organism *G. sulfurreducens*. It is crucial to investigate the Hg speciation for both the outer and the inner membrane to further understand the role of membrane thiols on the inner and outer membrane with respect to Hg(II) availability and uptake.

Aim of this thesis

As described in the introduction, the biogenic methylation of Hg(II) is the dominant source of MeHg in the environment. A broad variety of methylating microorganisms and the methylating enzyme cluster HgcAB have been identified. However, the specific mechanisms for Hg(II) internalization are not identified. In this work the purpose is to identify crucial biological and chemical parameters impacting Hg(II) availability and transformation by the iron-reducing model organism *G. sulfurreducens*. This thesis was carried out under the premise that thiol compounds are a key factor controlling Hg(II) speciation, uptake, methylation and reduction.

The overall aim of this thesis is to unravel the importance of thiol compounds on Hg(II) speciation, uptake and transformation by the iron-reducer *G. sulfurreducens*. The focus is on dissolved thiol compounds of endogenous and exogenous origin (Paper I and II) and on membrane thiol compounds of the outer and inner membrane (Paper III and IV).

The specific aims for the four projects were to investigate:

- I. the turnover of LMM-thiols under varying cell growth and assay condition.
- II. the combined effect of Hg(II) speciation with LMM-thiol compounds and the cell physiology on MeHg formation under varying assay condition over time.
- III. the chemical speciation of cell-adsorbed Hg on the outer and inner membrane and to determine the concentration of membrane surface thiols.
- IV. the role of membrane surface thiols on the outer and inner membrane for the internalization and transformation of Hg(II).

Experimental approaches

Experimental systems

Model organism Geobacter sulfurreducens

G. sulfurreducens is an obligately anaerobic, iron-reducing, gram-negative, Thermodesulfobacteriota, which was firstly isolated and described in the 1990s from a petroleum-contaminated lake sediment by Caccova et al.^{165, 166} It is used in different research fields including bioremediation of environmental contaminants or electricity production.¹⁶⁷⁻¹⁶⁹ Among other mercury methylating organisms *G. sulfurreducens* is one major model organism for mechanistic studies on Hg(II) reduction, uptake, and methylation.^{51-54, 57, 59, 60, 62, 64, 118, 120, 170} A variety of electron-donors and acceptors can be used for the growth of *G. sulfurreducens*.^{75, 165, 171} Growth medium, in which the formation of sulfide by *G. sulfurreducens* is prevented,¹⁶⁵ are preferred in mechanistic Hg(II) methylation studies to avoid uncontrolled formation of Hg-sulfide species.^{113, 120, 126} *G. sulfurreducens* is an ideal model organism to study Hg(II) methylation, due to possible mass cultivation,¹⁷² fast Hg(II) methylation,⁵¹⁻⁵³ no demethylation,^{50, 58} and the fact that its genome has been sequenced,¹⁷³ mutant strains can be generated (e.g. $\Delta hgcAB$).^{57, 58}

***Geobacter sulfurreducens* preparation**

In all experiments of this thesis, *G. sulfurreducens* PCA (ATCC 51573) was grown in a pH buffered minimum growth medium (pH=6.8) containing acetate and fumarate as an e-donor and an e-acceptor, respectively,⁵¹ as recommended by the provider the German Collection of Microorganisms and Cell Cultures.¹⁷⁴ The detailed growth medium composition is provided in the appendix (Table A1). Growth medium was freshly prepared for each experiment with Milli-Q-water (>18 M Ω .cm, Merck Millipore) in acid-clean glass serum vials, purged with N₂, crimp sealed with butyl rubber stopper and subsequently autoclaved. *G. sulfurreducens* cells were grown to mid- or late-exponential growth phase (OD₆₆₀=0.15-0.2), were harvested under N₂ atmosphere in an anaerobic glove chamber (Saffron Scientific Equipment Ltd.), collected by centrifugation (4000×g, 8 min, 5 °C) washed twice with anoxic, carbon-free assay buffer and resuspended in assay buffer. Assay buffers were prepared in the same manner as growth media, except that Teflon-stoppers were used to crimp seal the vials (assay buffer composition: Table A1). On each experimental day, freshly harvested *G. sulfurreducens* cells were used for various experiments as described in the following sections. Cell density was monitored in growth media and assay buffer by UV-vis absorption spectroscopy (UV-1201 spectrophotometer, Shimadzu) at a wavelength of $\lambda=660$ nm.

Spheroplast formation

Spheroplast assays of *G. sulfurreducens* were studied in Paper III and IV alongside whole cell assays. Spheroplast formation followed the protocol by Coppi et al.¹⁷⁵ After successful spheroplast formation an additional washing step by centrifugation was added (2 times, 15000×g, 10 min, 5 °C) with spheroplast assay buffer solution (Table A1) to reduce the amount of outer membrane and peptidoglycan residuals. The spheroplast formation was

verified by fluorescence and electron microscopy (Paper III and IV). Protein concentrations were measured in each spheroplast assay with the BCA protein assay kit (Pierce, Thermo Scientific) and used as a normalization factor (Paper IV).

Dissolved thiols

Paper I and II focused on the role of extracellular thiols, biogenic and exogenous origin. The main experiment for Paper I and II was based on the same experimental approach. Paper I focused on the turnover of thiols under varying conditions and Paper II focused on the effect of Hg(II)-speciation with dissolved thiol compounds on MeHg formation combined with the effect of cell physiology. The general experimental workflow of study I and II is illustrated in Figure 3.

The formation of LMM-thiols by *G. sulfurreducens* was studied in growth medium under addition of varying concentrations of divalent iron (Fe(II)) (0–3.7 μM , medium composition: Table A1). Between inoculation and stationary growth phase, samples were collected for extra- and intracellular LMM-thiol analyses at multiple time points.

The turnover of biogenic and exogenous thiols was studied in three different assay buffers: “*standard assay*”, “*metabolite assay*” and “*nutrient assay*” with increasing nutrient concentration. The standard assay buffer is an established assay buffer used in studies of Hg(II) uptake and methylation with low e-donor and e-acceptor concentrations of 1 mM acetate and fumarate, respectively (Table A1).⁵¹ The metabolite and nutrient assay buffer consist of 90% (v/v) standard assay and 10% (v/v) spent or growth medium, respectively. The spent medium was obtained during the late-exponential growth ($\text{OD}_{660}=0.17\text{--}0.2$) under iron depleted growth condition with 1.5 μM Fe(II), filtered through a syringe filter (0.2 μm pore size, PES) and the collected filtrate was added to the assay buffer. All cell assays were performed in the presence of 30 nM Hg(II) (as $\text{Hg}(\text{NO}_3)_2 \cdot \text{H}_2\text{O}$ TraceCERT®, Sigma Aldrich) and exogenous addition of 0–1000 nM cysteine (L-Cysteine, $\geq 97\%$, Sigma Aldrich). Assays were pre-equilibrated with Hg(II), cysteine, spent medium and/or growth medium for ~ 1 h under incubation conditions (30 °C, dark). Cell assays were started by inoculation of washed cells to a final cell density of $\sim 10^8$ cells mL^{-1} (corresponding to $\text{OD}_{660}=0.02$). The redox state of cell assays was observed by the color change from pink to clear of the redox indicator resazurin (clear color indicating a redox potential of ≤ 100 mV). The assays were incubated for 24 h at 30 °C in the dark and subsamples for total Hg, dissolved Hg, MeHg and dissolved LMM-thiols analyses were taken at multiple time points. All measured and calculated Hg fractions of Paper II are summarized in Table A2.

For Paper I, the turnover of thiol compounds was further studied in assays with 1000 nM isotopically labeled L-cysteine (L-Cysteine- $^{13}\text{C}_3$, ^{15}N , ≥ 99 atom %, $\geq 98\%$ (CP), Sigma Aldrich) and 500 nM D-penicillamine (98–101%, Sigma Aldrich). Intra- and extracellular LMM-thiol concentration were measured at multiple time points. A control assay without cells was performed by filtering a standard assay buffer after 24 h, subsequently spiked with isotopically labeled L-cysteine (final concentration 1000 nM) and samples were collected for dissolved LMM-RSH analysis at multiple time points.

For Paper II, the experimental approach for standard and metabolite assay as described above was further modified for additional experiments. *G. sulfurreducens* cells were inoculated in Hg(II) free standard and metabolite assay buffers and cells were aged for 6 h. Hg(II) was added at time point 6 h. In a separate experiment metabolite medium was added (10% v/v) after 6 h to a standard assay. Samples for MeHg, total Hg, dissolved Hg and dissolved LMM-thiols were collected at multiple time points. The impact of sulfide on Hg(II) methylation was studied by addition of sulfide below the limit of detection (120 nM) with a final sulfide concentration of 100 nM ($\text{Na}_2\text{S}\times 9\text{H}_2\text{O}$, Sigma Aldrich). Abiotic and biotic demethylation of MeHg was monitored by the addition of Me^{204}Hg with a final concentration of 3 nM. The overall cell physiology was monitored by the changes of cell density over time by UV-vis and by recording ATR-FTIR spectra of the different assay systems at multiple time points.

All experiments were performed in triplicates ($n=3$). Detailed description of sample analyses and data treatment is described in *Instrumental analysis* and *Data analysis*.

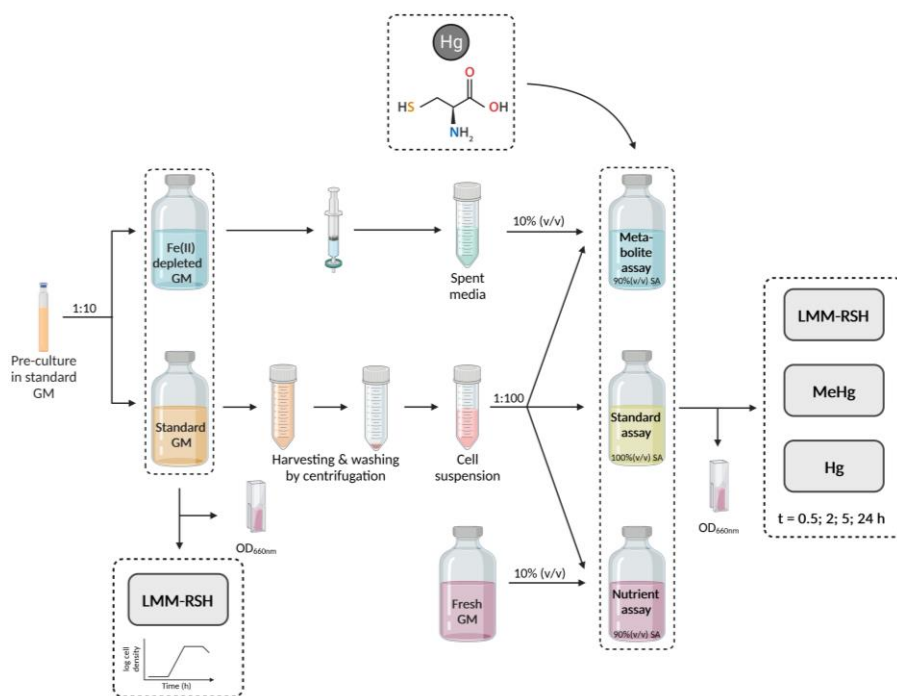


Figure 3: Experimental design of Paper I and II. Incubation of growth culture and assays at 30°C in the dark. GM: growth medium; SA: Standard assay buffer. (Created with BioRender.com)

Membrane surface thiols

In Paper III and IV, both whole cells and spheroplasts of *G. sulfurreducens* were studied to investigate the outer and inner membrane, respectively. Paper III focused on the Hg speciation and the concentration of surface thiols. In Paper IV, the focus was on the role of cell surface thiols for Hg(II) reduction, uptake, and methylation.

Mercury speciation on the membrane surface

Samples for EXAFS and High-Energy-Resolution-Fluorescence-Detected X-ray absorption near edge structure (HERFD-XANES) measurements were prepared in the same manner. Assay buffers were prepared as described above without the addition of the e-donor and e-acceptor to prevent Hg(II) uptake and methylation and to probe Hg speciation on the membrane surface (assay buffer composition: Table A1).^{52, 53} Whole cells and spheroplasts were incubated for 10 min with 0.28–420 μM Hg(II) (pre-equilibrated for ~ 1 h, dark, 30°C) in glass assay vials. The final Hg concentration in the sample pellet was 0.3–920 $\mu\text{mol g}^{-1}$ dry mass. A sample aliquot for total and dissolved Hg analyses was collected from the assay vial. Whole cells and spheroplasts were collected by centrifugation, washed 2 times with 0.1 M NaClO₄ (for spheroplasts: 0.1 M NaClO₄ in 0.35 M sucrose). Pelleted samples were immediately frozen with liquid N₂ and stored frozen at -30°C until analysis. A subsample of the cell pellet was taken for Hg analyses with the direct mercury analyzer. Further description of EXAFS and HERFD-XANES analysis are described in *X-ray absorption spectroscopy*.

Blocking of membrane surface thiols

Blocking of cell surface thiols in Paper IV was performed with a thiol-specific brominated bimane compound, which was used in previous studies to determine the thiol concentration in dissolved organic matter and on bacteria cell surfaces.^{152, 154, 164, 176-182} Monobromo(trimethylammonio)bimane bromide (qBBr, $\geq 90\%$, Sigma Aldrich) reacts with the thiol functional group through nucleophilic substitution, an S_N2 reaction mechanism between the thiol and the alkyl bromide (Figure 4).^{177, 183, 184} Based on the positive charge of qBBr, it is assumed that cell membrane crossing is prevented and in addition qBBr is selectively reacting with thiol functional groups.^{164, 176, 182, 185, 186} In a previous study by Thomas et al. this method was firstly applied to selectively blocked cell surface thiols of *G. sulfurreducens* for Hg(II) methylation assays.¹⁵²

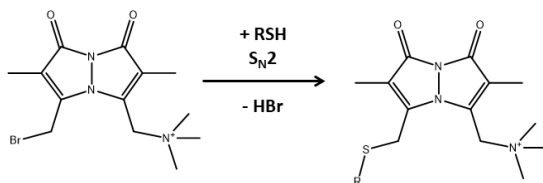


Figure 4: Reaction mechanism between the thiol group (RSH) and the alkyl bromine monobromo(trimethylammonio)bimane (qBBr) via an S_N2 reaction.

The partitioning of Hg was studied with and without qBBr derivatized membrane surface thiols on whole cells and spheroplasts. Whole cells and spheroplast were prepared as described in *Geobacter sulfurreducens* preparation. Cell surface thiols were derivatized with an aliquot of a freshly prepared 8 μM qBBr stock solution in anoxic 5 mM PBS buffer and incubated in a shaking incubator (30 rpm, dark, 30 °C) for 1 h. To derivatize all outer or inner membrane surface thiols, samples were incubated with a four times higher qBBr concentration than outer or inner membrane surface thiol concentration to ensure blocking of all membrane surface thiol groups. The outer and inner membrane surface thiol concentrations were based on Paper III.¹⁸⁷ After qBBr derivatization, whole cells and spheroplasts were washed twice by centrifugation (4000 \times g, 8 min, 5 °C and 15000 \times g, 10 min, 5°C for whole cells and spheroplasts, respectively) to remove excess qBBr. Cell assays were started by the addition of whole cells and spheroplast to the assay vials. Prior to cell addition, assay buffers were equilibrated with 30 nM Hg(II) (~1h, dark, 30 °C). The final protein concentration was 22-45 $\mu\text{g mL}^{-1}$ protein for whole cells and corresponding to a cell density of 3-4 $\times 10^8$ cell mL^{-1} (OD_{660} =0.06-0.08). The final spheroplast protein concentration was 15-25 $\mu\text{g mL}^{-1}$ protein. The following seven Hg samples were collected after 0.5 and 4 h incubation time: total Hg, dissolved Hg, total non-purgeable Hg, dissolved non-purgeable Hg, total MeHg, dissolved MeHg and intracellular Hg (Figure 5). The dissolved Hg and MeHg samples were collected by filtration of the sample through a syringe filter (0.2 μm pore size, PES). Non-purgeable Hg samples were collected after purging the sample for 10 min with N_2 . The intracellular Hg samples were collected after washing whole cells and spheroplasts with a specific cell washing procedure for *G. sulfurreducens* according to Schaefer et al. 2011 and 2014, respectively.^{51, 53} Sample collection is illustrated in Figure 5. Based on the seven measured Hg fractions, ten Hg fractions were calculated for Paper IV as displayed in TableA2. All experiments were performed in quintuplicates (n=5). Additionally, the overall cell physiology was examined by fluorescence microscopy and by recording ATR-FTIR spectra of the whole cells and spheroplasts with and without qBBr derivatized membrane surface thiols. Details of sample analyses are described in *Instrumental analysis*.

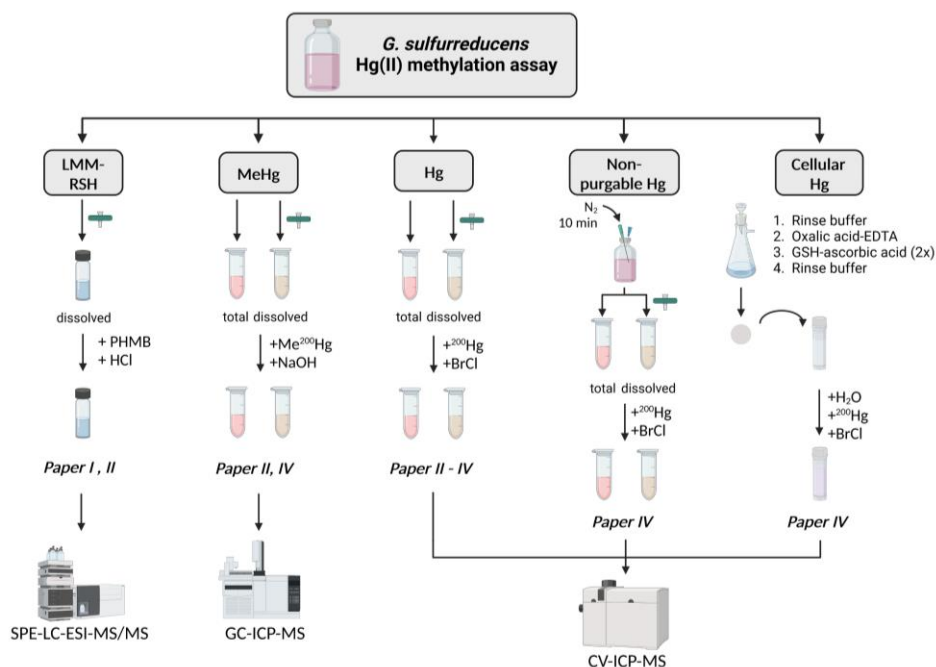


Figure 5: Sample preparation scheme for thiol samples and the different Hg fractions. LMM-thiols were determined by solid-phase extraction liquid chromatography electrospray ionization tandem mass spectrometry (SPE-LC-ESI-MS/MS). MeHg was analyzed by gas chromatography inductively coupled plasma mass spectrometry (GC-ICP-MS) Hg, non-purgeable Hg and cellular Hg samples were analyzed by cold vapor inductively coupled plasma mass spectrometry (CV-ICP-MS). (Created with BioRender.com)

Instrumental analysis

LC-MS/MS

LMM-thiol samples were immediately derivatized with 4-(hydroxymercuri)benzoate (PHMB) after collection, pH was adjusted to 3 with HCl and the samples were subsequently analyzed. Derivatized samples were not stored longer than 1 day in the fridge (8°C, dark) prior to analysis. The concentration of LMM-thiols was analyzed by liquid chromatography (Agilent Zorbax SB-C8, 2.1×100 mm, 3.5 μm) electrospray ionization tandem mass spectrometry (LC-ESI-MS/MS, TSQ Quantum Ultra electrospray ionization triple quadrupole mass spectrometer, Thermo Fisher Scientific) prior to online pre-concentration with solid-phase extraction (Waters, Oasis HLB, 2.1×20 mm, 15 μm) by selective reaction monitoring as described in Liem-Nguyen et al.¹⁸⁸

The method was developed for a variety of LMM-thiols present in the environment and showed a low LOD for samples in a complex sample matrix (e.g., growth medium) within the low nanomolar range.¹⁸⁸ The reactive thiol group is derivatized with PHMB, which leads to a sample stability of up to one month.¹⁸⁸ The selection of analyzed LMM-thiols was based on a previous study by Adediran et al. and are illustrated in Figure 6.¹²⁰ Further,

samples were not reduced prior to PHMB derivatization to detect possible disulfides in the sample and only the reduced sulfide form, thiols, was analyzed.

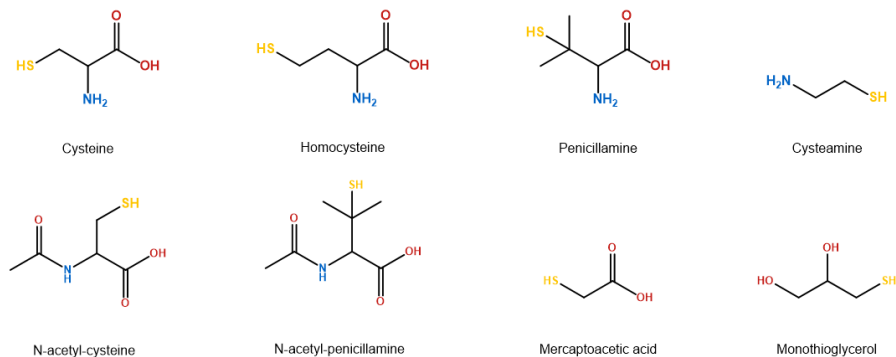


Figure 6: Molecular structure of the eight LMM-thiols analyzed by SPE-LC-ESI-MS/MS in Paper I and II.

ICP-MS

Isotope dilution analysis (IDA) techniques were used to analyze Hg and MeHg concentration by inductively coupled plasma mass spectrometry (ICP-MS). An isotope enriched ^{200}Hg and Me^{200}Hg standard was used for Hg and MeHg analyses, respectively. The ^{200}Hg was commercial obtained (ORNL batch 185091, 96.41%, Oak Ridge National Laboratory, TN, USA) and Me^{200}Hg was synthesized in-house after Snell et al. from the ^{200}Hg (ORNL batch 185091).¹⁸⁹ IDA is a definitive method with an enriched isotope as an internal standard since it is corrected for losses and degradation of the analyte and is therefore a stable method with great accuracy and precision.^{190, 191} One crucial aspect for reliable analyses is to achieve an isotope equilibrium in the sample and the usage of a traceable primary standard.¹⁹⁰ The concentration of the enriched isotope standards were determined before their usage by reverse isotope dilution analyses. The concentration of ^{200}Hg and Me^{200}Hg were determined by using a Hg analytical standard (TraceCERT®, $1000 \pm 4 \text{ mg L}^{-1} \text{ Hg}$) in nitric acid and a 1.44 mM MeHg stock solution in 0.1 M HCl prepared gravimetrically from MeHgCl (PESTANAL®, analytical standard, $\geq 98.0\%$), respectively.

In short, for Hg analyses, samples were spiked with an aliquot of ^{200}Hg (96.41%, Oak Ridge National Laboratory, TN, USA) and digested with 0.02 M BrCl for >48 h in the dark. On the analysis day, a small aliquot of 4.3 M $\text{NH}_2\text{OH}\cdot\text{HCl}$ was added to the sample to remove excess BrCl, followed by reduction of Hg(II) with SnCl_2 and analyses were performed on a cold vapor system (CETAC HGX-200, Teledyne CETAC Technologies) coupled to ICP-MS (Agilent 8900 Triple Quadrupole Inductively Coupled Plasma Mass Spectrometry, Agilent technologies). The method is based on the EPA method 1631E.¹⁹²

For MeHg analyses, samples were spiked with an aliquot of Me^{200}Hg solution and digested with 0.6 M NaOH ~24 h in the dark (alkaline digestion adapted from Carrasco and Vassileva).¹⁹³ On the analysis day, the sample pH was adjusted to 4.5 with 5 M HCl,

buffered with an aliquot of 2 M $\text{CH}_3\text{COONH}_4$, derivatized with $\text{NaB}(\text{C}_2\text{H}_5)_4$, purged with N_2 for 10 min and trapped on TENAX adsorbent. Derivatized MeHg was analyzed by thermal desorption (TD-100 Thermal Desorber, Markes international) gas chromatography (GC) coupled to ICP-MS (Agilent GC 7890B and Agilent 7700 ICP-MS, Agilent technologies). The method is described in detail in Lambertsson et al.¹⁹⁴

X-ray absorption spectroscopy

With X-ray absorption spectroscopy (XAS) core electrons, in case of Hg of the L-shell, are excited.¹²⁹ Herby, the element in its intact environment is analyzed without prior chemical treatment to prevent chemical changes.¹²⁹ In general, X-ray absorption spectroscopy requires relatively high concentrations of the element (as compared to natural environmental conditions) and it is not an absolute measurement.¹²⁹ An XAS spectrum consists of three regions: (I) pre-edge, (II) near-edge (also known as X-ray absorption near-edge spectroscopy, XANES) and (III) extended near-edge fine structure spectroscopy, EXAFS (Figure 7).¹²⁹ Briefly, the three regions provide information about: (I) unallowed transitions, (II) oxidation state and geometry of the absorbing element and (III) number, type, and distance of the nearest neighbor/-s to the absorbing atom.¹²⁹ In this study HERFD-XANES spectra were collected by measuring the Hg $L_{\alpha 1}$ fluorescence line.¹⁹⁵ HERFD-XANES data were analyzed by optimizing linear combination fits (LCF) of pre-selected model compounds, which were characterized by EXAFS. Hg L_{III} -edge EXAFS spectra were collected as total fluorescence and analyzed by fitting *ab initio* models of known structures generating information about coordination number, CN, bond distance, R, and Debye-Waller factors (thermal and structural disorder), σ .

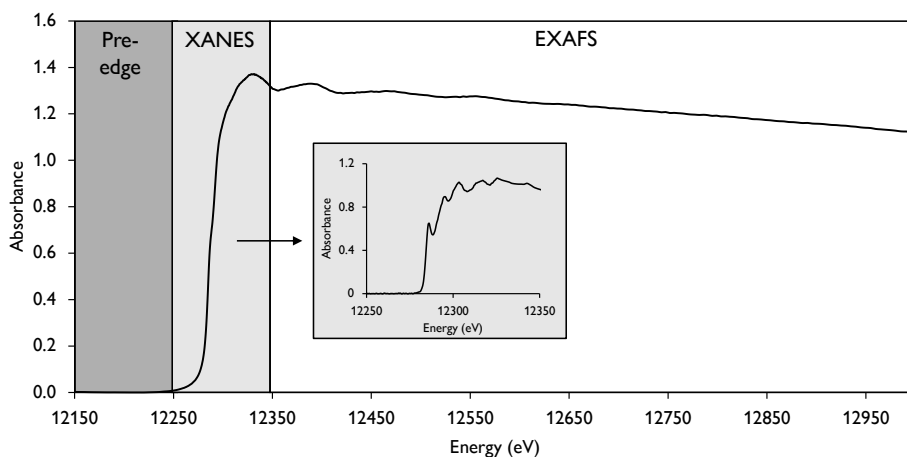


Figure 7: Mercury L_{III} -edge spectra illustrating the (I) pre-edge (>12250 eV), (II) XANES (12250-12350 eV) and (III) EXAFS (12350–13000 eV) regions. The normalized EXAFS and HERFD-XANES spectra were obtained at the bending magnet FAME BM30 and at the FAME-UHD BM16, respectively. Whole cell samples were exposed to $5.3 \mu\text{M}$ Hg with a final Hg concentration of 25 and $13 \mu\text{mol g}^{-1}$ dry mass for EXAFS and HERFD-XANES samples, respectively.

Extended X-ray absorption fine structure spectroscopy

EXAFS measurements were performed at the bending magnet FAME BM30 and the undulator beamline P65 at the European Synchrotron Radiation Facility (ESRF, Grenoble, France)¹⁹⁶ and at the Deutsches Elektronen-Synchrotron (HASYLAB/DESY Petra III, Hamburg, Germany),¹⁹⁷ respectively. Samples and reference samples were kept frozen in a helium-cryostat during measurements at 15 K. At BM30 a Si(220) double crystal monochromator modulated the photon flux energy to a beam size of $100 \times 300 \mu\text{m}^2$ and a 30-element Canberra detector was used in fluorescence mode. At beamline P65 a Si(111) double crystal monochromator modulated the photon flux energy to a beam size of $0.3 \times 1.5 \text{ mm}^2$ and a PIPS detector was used in fluorescence mode. The K-edge for selenium was used for internal energy calibration. Spectra were collected at the Hg L_{III}-edge at 12284 eV and the range of measurement was from -200 eV below to $+800 \text{ eV}$ above the edge. Five to 15 spectra were recorded for each sample. Samples were monitored for radiation damage by comparing multiple scans at the same sample spot. No radiation damage was noted. Spectra were averaged by the Athena software and data reduction and modelling was performed by WinXAS and FEFF software programs. A detailed description of the data treatment procedure is found in Paper III.

High energy-resolution-fluorescence-detected X-ray absorption near edge structure spectroscopy

HERFD-XANES measurements were performed on the FAME-UHD BM16 at the ESRF. Samples and reference samples were kept frozen in a helium-cryostat during measurements at 15 K. A Si(220) double crystal monochromator modulated the photon flux to a beam size of $200 \times 100 \mu\text{m}^2$ with an energy-resolution of $\sim 0.6 \text{ eV}$. Spectra were collected at the Hg L_{III}-edge ($12\,284 \text{ eV}$) and the range of measurement was from -140 eV below to $+420 \text{ eV}$ above the edge. The Hg L_{α1} fluorescence line was detected by twelve spherically bent Si(555) crystal analyzers.¹⁹⁵ The diffracted intensity of samples and model compounds was measured by a Silicon Drift Detector and the reference (Au foil) by a Hybrid Pixel detector. An Au foil was used for calibration of the monochromator. Eight pre-selected reference compounds were used for fitting the normalized HERFD-XANES spectra by LCF. A detailed description of the method and the data treatment can be found in Paper III.

Model compounds

For both EXAFS and HERFD-XANES measurements, various Hg model compounds were prepared. Hg(Cys)₂ (pH 3, 7, 11), Hg(Cys)₃ (pH 11) and Hg(Cys)₄ (pH 11) model complexes were prepared according to Jalilehvand et al.¹²⁸ Additionally, pellets of solid Hg(acetate)₂ and of the mineral metacinnabar (β-HgS) were prepared. Liquid Hg(0) reference spectrum was collected on the FAME-UHD BM16 at the ESRF and kindly provided by Marie-Pierre Isaure.¹⁶² A detailed description of the model compound preparation can be found in Paper III.

Additional methods

The different studies were complemented with additional methods to support the results of the core methods.

Sulfide was measured with the methylene blue method in growth cultures and cell assay by UV-vis absorption spectroscopy (UV-1201 spectrophotometer, Shimadzu) in Paper I and II.^{198, 199}

The cell physiology of *G. sulfurreducens* whole cells and spheroplasts was examined by attenuated total reflectance Fourier transform infrared spectroscopy (ATR-FTIR) on a Bruker Vertex 80v FTIR spectrometer. ATR-FTIR is a powerful method to evaluate changes in microbial activity based on biochemical fingerprints by monitoring the evolution of the intensity of infrared bands assigned to, for example, proteins, nucleic acids, or polysaccharides.^{200, 201} (Paper II, IV)

Additionally, fluorescence and electron microscopy techniques were applied to characterize *G. sulfurreducens* cells, to verify spheroplast formation and cell viability after qBBr derivatization of membrane surface thiols. For fluorescence microscopy, whole cells and spheroplasts were stained with SYTO 9 (BacLight™ Bacterial Viability Kits, Invitrogen™) and examined at its specific excitation and emission wavelength with $\lambda_{ex/em}=504/543$ nm on a Leica Widefield Thunder microscope (Leica Microsystems). Further, for qBBr derivatized membrane surface thiols, the fluorescence signal was examined at $\lambda_{ex/em}=380/475$ nm. Whole cells and spheroplasts were examined by transmission electron microscopy with a Talos L120C (FEI) after fixation, embedding in resin and sectioning in thin slices. (Paper III, IV)

Beside IDA Hg analyses, total Hg in frozen or freeze-dried cell samples were analyzed with a direct mercury analyzer (DMA-80, Milestone) by combustion atomic absorption spectroscopy. (Paper III)

Data analysis

Thermodynamic speciation modelling

The speciation of the dissolved Hg(II) was predicted by thermodynamic modelling in winSGW based on Liem-Nguyen et al.^{126, 202} The input data contained the measured LMM-thiol concentration and calculated dissolved Hg(II) and MeHg at multiple time points. The log K values of each compound are based on literature values as reported in Paper II (see Paper II supporting information).

Kinetic modelling for MeHg formation

Two kinetic first order rate models were applied to describe the MeHg formation of the three different assay systems in Paper II. The models were based on either the concentration of total dissolved Hg(II) (model 1) or on the concentration of specific Hg(LMM-RS)₂ species (model 2). The cumulative MeHg formation was determined for each time interval, based on the time-resolved dataset of dissolved Hg(II) and Hg(II) speciation. The rate constant for Hg(II) methylation, k_{meth} , was optimized for the measured MeHg concentration of the time interval 0.5-6 h. For the model based on Hg(LMM-RS)₂ species, the three dominant species were included with Hg(Cys)₂, Hg(CysN)₂ and Hg(PEN)₂. The rate constants $k_{\text{meth}}(\text{Hg}(\text{LMM-RS})_2)$ were based on Schaefer et al.⁵² Both models take into account changes in the cell density and dissolved Hg(II) concentration, whereas the chemical speciation of dissolved Hg(II) was only considered in model 2.

Model 1:

$$[\text{MeHg}] = \sum_{i=0}^n [\text{Hg(II)}_{\text{aq}}]_{\text{initial}} \times (1 - e^{-k_{\text{meth}}(\text{Hg(II)}_{\text{aq}}) \times \Delta t})$$

Model 2:

$$\begin{aligned} [\text{MeHg}] = & \sum_{i=0}^n [\text{Hg}(\text{Cys})_2]_{\text{initial}} \times (1 - e^{-k_{\text{meth}}(\text{Hg}(\text{Cys})_2) \times \Delta t}) \\ & + \sum_{i=0}^n [\text{Hg}(\text{CysN})_2]_{\text{initial}} \times (1 - e^{-k_{\text{meth}}(\text{Hg}(\text{CysN})_2) \times \Delta t}) \\ & + \sum_{i=0}^n [\text{Hg}(\text{PEN})_2]_{\text{initial}} \times (1 - e^{-k_{\text{meth}}(\text{Hg}(\text{PEN})_2) \times \Delta t}) \end{aligned}$$

Results and discussion

Dissolved thiols

The formation of LMM-thiols by microorganisms is observed in various anoxic environments.^{120, 135-139, 203} The speciation of Hg(II) with ligands like LMM-thiols is known to be an important driver for availability, internalization, and methylation of Hg(II).^{2, 40, 51, 52, 120} Paper I and II focused on the formation and the turnover of thiol compounds in different experimental systems with altered nutrient concentrations and their impact on Hg(II) speciation and methylation. This chapter focuses on the following four research questions, which were addressed in detail in Paper I and II.

- i. How is the turnover of LMM-thiols dependent on growth medium and on assay buffer composition, respectively?
- ii. How is the fate of LMM-thiols impacted by exogenous thiol addition?
- iii. Is Hg(II) methylation controlled by LMM-thiol compounds and their complexes with Hg(II)?
- iv. How does the assay medium composition impact the cell physiology and subsequently the MeHg formation potential?

Iron as a driver for thiol formation

Overall, Fe(II) is an essential micronutrient and microorganisms developed strategies to acquire Fe(II).²⁰⁴ The effect of the essential micronutrient Fe(II) on the formation of LMM-thiols by *G. sulfurreducens* was tested in growth medium with Fe(II) addition between 0-3.7 μM . The standard growth medium contains a Fe(II) concentration of 3.7 μM .^{51, 174} The study focused on the eight dominant LMM-thiol detected in *G. sulfurreducens* in a previous study (Figure 6).¹²⁰

Overall, the extracellular concentration of thiols was higher compared to the intracellular concentration when normalized to cell density (Figure 8, Paper I). Under Fe(II) depleted condition, tested in the range 0.5–2 μM Fe(II), cell growth was not significantly impacted compared to standard Fe(II) concentration of 3.7 μM (repeated measure ANOVA, $p > 0.05$) (Figure 8 and Paper I). The cell growth was impacted by 0 μM Fe(II) addition as shown by a reduced cell growth yield (Paper I). The intra- and extracellular LMM-thiol concentration showed a growth phase response in thiol formation (Figure 8). Of the eight thiols that were analyzed, the thiols with the highest detected extracellular concentration in the growth medium with 3.7 μM Fe(II) were cysteine and mercaptoacetic acid with ~ 0.4 and 0.9×10^{-18} mol cell⁻¹, respectively, during the late exponential growth phase (Paper I). Mercaptoacetic acid was detected in the late exponential growth phase and therefore suggested to be a secondary metabolite (Paper I). Cysteine showed the most distinct changes in intra- and extracellular concentration over time with altering Fe(II) exposure (Figure 8 and Paper I). The intracellular cysteine concentration increased with Fe(II) concentration and reached $\sim 0.35 \times 10^{-18}$ mol cell⁻¹ with 3.7 μM Fe(II) during the log phase ($t=24$ h). In contrast, the extracellular cysteine concentration followed a different pattern with the highest concentration reached with 1.5 μM Fe(II), reaching 8.0×10^{-18} mol cell⁻¹ cysteine with 1.5 μM Fe(II) during the late log phase ($t=60$ h). For

growth cultures exposed to 0.5 and 3.7 μM Fe(II), the extracellular cysteine concentration was 3.7 and 0.5×10^{-18} mol cell $^{-1}$, respectively, in the late log growth phase (t=60 h). The intracellular cysteine concentration was tightly controlled during the growth cycle and was regulated in a concentration range of 0.01 to 0.35×10^{-18} mol cell $^{-1}$ (corresponding to 10 to 200 μM cysteine intracellular) The intracellular cysteine concentration reached its maximum in the mid log phase and decreased during the late log phase (Figure 8 and Paper I). The decrease in intracellular cysteine coincided with an extracellular increase and showed a tight coupling between the intra- and extracellular concentration (Figure 8).

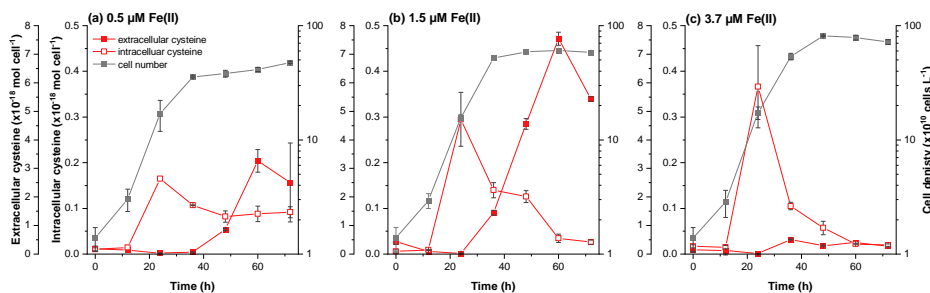


Figure 8: Extra- and intracellular cysteine concentrations normalized to the cell density of *G. sulfurreducens* in growth medium over time with (a) 0.5, (b) 1.5 and (c) 3.7 μM Fe(II) addition. Growth curve of *G. sulfurreducens* illustrated in gray. Error bars represent standard error ($n=3$). (Adapted from Paper I)

Extracellular cysteine concentration was enhanced under Fe(II) depleted growth conditions and resulted in the highest extracellular cysteine concentration with 1.5 μM Fe(II) (Paper I). The effect of Fe(II) on cysteine formation suggested that there was a relationship between cysteine and Fe(II) homeostasis, although the mechanism behind this interplay was not identified. *G. sulfurreducens* regulated cysteine homeostasis and regulated it by cysteine production and cellular export. The control of the intracellular cysteine concentration is crucial, due to its reactivity and subsequent ability to cause toxic effects in the cytosol.¹⁴⁵⁻¹⁴⁸ However, our results suggested that cysteine is involved in Fe(II) transfer and distribution to iron proteins of surface membrane and periplasm proteins. It was shown by previous transcriptomics studies, that iron limitation led to an upregulation of specific genes, including genes that are part of the cysteine biosynthesis.²⁰⁵ Additionally, cysteine could be involved in Fe(II) complexation and uptake during growth, similar to the excretion of siderophores.^{206, 207}

In the following experiments the enhanced formation of the LMM-thiol cysteine produced under Fe(II) depleted growth condition, 1.5 μM Fe(II), by *G. sulfurreducens* was used to modify the standard assay buffer by adding 10% (v/v) spent media and investigate thiol turnover and Hg(II) methylation under varying conditions (see *Experimental systems-Dissolved thiols*).

Turnover of thiol compounds - conversion of cysteine to penicillamine

The turnover of LMM-thiols by *G. sulfurreducens* was investigated in three assay systems: (I) standard, (II) metabolite and (III) nutrient assay with and without addition of cysteine (see *Experimental systems-Dissolved thiols*). This thesis highlights selected key results, while in Paper I and II, the detailed thiol turnover was described for all three assay systems. All eight LMM-thiols were detected in the three assay systems with concentrations up to 13×10^{-18} mol cell⁻¹ (Figure 6, Paper I). The determined concentrations in the standard assays without cysteine addition were in agreement with a recent study showing the formation of LMM-thiols in *G. sulfurreducens* assays with 0.9 and 1.1×10^{-18} mol cell⁻¹ for Paper I after 6 and 48 h, respectively, and 1.0 and 1.2×10^{-18} mol cell⁻¹ thiols for Adediran et al. after 6 and 48 h, respectively (Paper I).¹²⁰

Overall, the most notable differences were observed in the extracellular media for the small LMM-thiol cysteine and branched LMM-thiol penicillamine. In standard assays without cysteine addition, low concentrations of cysteine were formed, $\sim 0.025 \times 10^{-18}$ mol cell⁻¹ (Figure 9a). In assays with addition of 600 nM exogenous cysteine, the cysteine concentration decreased during the first 6 h, from 6.3 to 0.09×10^{-18} mol cell⁻¹, and reached steady state concentration after >6 h with $\sim 0.9 \times 10^{-18}$ mol cell⁻¹ (Figure 9b). The penicillamine concentration increased over time in standard assays (Figure 9a,b). However, without cysteine addition penicillamine concentration increased between 6 and 24 h, whereas for assays with exogenous cysteine addition the increase in penicillamine concentration occurred already in the initial time interval (0.5 to 2 h, Figure 9b). Overall, with exogenous cysteine higher cysteine and penicillamine concentrations were observed over time (Paper I). The decrease of cysteine and increase of penicillamine concentrations pointed towards a link between the metabolism of these two LMM-thiols.

Standard assays with $1 \mu\text{M}$ isotopic labeled cysteine (L-cysteine-¹³C₃, ¹⁵N) addition showed the same pattern in concentration change as with 600 nM cysteine, with a decrease and increase in isotopic labeled cysteine and penicillamine, respectively (Figure 9b,c). This result proposed the turnover of cysteine to penicillamine by *G. sulfurreducens*. Control experiments excluded the possibility of abiotic turnover of cysteine to penicillamine (Paper I). In this study the reaction mechanism of the di-methylation of cysteine to penicillamine by *G. sulfurreducens* was not identified (Figure 9d). The biological methylation was likely linked to methyltransferases. For example, radical S-adenosylmethionine enzymes might be involved in the transfer of two methyl groups on the C-3 atom of cysteine,²⁰⁸ as reported for the C-methylation of arginine and glutamine in methyl-coenzyme M reductase.^{209, 210}

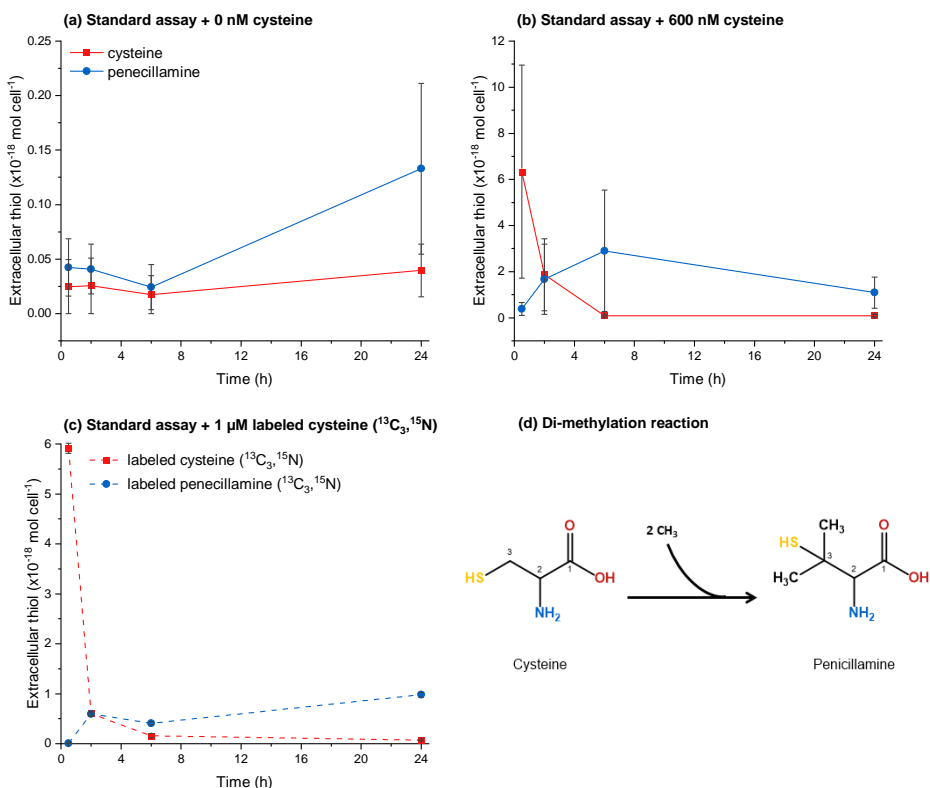


Figure 9: (a) and (b) Extracellular cysteine and penicillamine concentration normalized to cell density over time in standard assays with washed *G. sulfurreducens* cells. (a) and (b) with 0 and 600 nM cysteine addition, respectively, and 30 nM Hg(II). (c) Extracellular isotopically labeled cysteine and penicillamine concentration normalized to cell density over time in standard assay buffer with 1 μM isotopically labeled cysteine (*L*-Cysteine-¹³C₃,¹⁵N) addition. Error bars represent standard error (*n*=3). (d) Reaction scheme illustrating the di-methylation of cysteine at the C-3 atom to penicillamine. (Adapted from Paper I)

The intracellular concentration of cysteine and penicillamine was tightly controlled during the incubation time and exogenous cysteine and penicillamine addition led to enhanced intracellular LMM-thiols after 0.5 h, which subsequently decreased and were maintained at low levels for incubation times >2 h (Paper I). Overall, the intracellular thiol concentrations were in the same range for *G. sulfurreducens* cells in assay buffer and growth medium (Paper I).

The turnover of cysteine to penicillamine was also observed in metabolite and nutrient assays, however the LMM-thiol concentrations (sum of the eight measured LMM-thiols) varied among the different systems during the incubation time and was impacted by cysteine, metabolite, and nutrient addition (Paper I and II). In nutrient assays the exogenous addition of cysteine led to a fast metabolization, and subsequently low LMM-thiol concentrations were detected (sum LMM-thiols: 50-420 nM during incubation time, Paper I and II). In addition, metabolite assays showed an overall high LMM-thiol

concentration due to addition of spent media (sum LMM-thiol: 300-1700 nM during incubation time, Paper I and II).

In addition, the impact of 0–200 nM Hg(II) on the formation of LMM-thiols by *G. sulfurreducens* was tested and showed that LMM-thiol formation was not affected by Hg(II) during a 48 h incubation period with average thiol concentration for all Hg(II) exposure levels of 31 ± 6 and 114 ± 5 nM after 2 and 48 h incubation, respectively (Paper I). However, previous studies showed an upregulation of specific thiol synthesis pathways due to heavy metal exposure which resulted in changes in the free LMM-thiol concentrations.^{211–213} In the present study the overall extracellular LMM-thiol concentration was not impacted by Hg(II), however up- or downregulation of genes were not studied and cannot be ruled out.

Mercury speciation, losses, and methylation

Impact of thiol turnover on mercury speciation

The dissolved Hg(II) speciation was calculated in Hg(II) methylation assays at multiple time points based on the measured LMM-thiol and dissolved Hg(II) concentrations calculated by thermodynamic speciation modelling. The most dominant three species in *G. sulfurreducens* assays were Hg(Cys)₂, Hg(CysN)₂ and Hg(PEN)₂ with varying concentrations during the incubation time (Figure 10 and Paper II). Cysteine and nutrient addition impacted the Hg(II) speciation species at different time points. In the initial time frame (0.5 to 2 h), Hg(II) complexes with small thiols, Hg(Cys)₂ and Hg(CysN)₂, were the dominating species in the extracellular media, except for the nutrient assay (Figure 10). The speciation changed over time and for extended incubation time ($t \geq 6$ h) branched Hg(II) species, Hg(PEN)₂, were dominating. The shift of small to branched LMM-thiols was amplified by the addition of cysteine as described in the previous section “*Turnover of thiol compounds - conversion of cysteine to penicillamine*” and showed consequently the same pattern for the Hg(II) speciation with higher contribution of Hg(PEN)₂ for incubation times > 2 h (Figure 9 and 10, Paper I and Paper II).

Mercury losses and partitioning

Dissolved LMM-thiols were impacting the recovery and partitioning of Hg in the three assay systems. Overall, Hg(II) recovery in the different systems was in the range of 65–85% at time point 0.5 h and further decreased to 51–71% after 24 h (Paper II). Losses of Hg(II) were likely a combination of reduction and volatilization of Hg(II)^{57, 60} and adsorption to the glass vessel.^{214, 215} The Hg partition between the dissolved and cell-associated phase changed over time and higher concentrations of LMM-thiols drove the partitioning towards the dissolved phase and decreased the losses of Hg by ~12% (Paper II). In assays with a higher LMM-thiol concentration, the available Hg pool increased due to Hg partition towards the dissolved phase and consequently a greater fraction of Hg(II) was available for uptake and methylation (Paper II). Previous studies showed that cell-associated Hg(II) was less available than dissolved Hg(II) for Hg(II) uptake and methylation by *G. sulfurreducens*⁵⁴ and a positive relationship between dissolved Hg(II) and Hg(II) methylation was shown.^{58, 60}

Methylmercury formation

The formation of MeHg by *G. sulfurreducens* was studied in the three different assay systems. The formation of MeHg without cysteine addition increased in the order: standard assay < metabolite assay \approx nutrient assay (Figure 10, Paper II). In standard assays, the formation of MeHg was not affected by cysteine addition, whereas MeHg formation increased for metabolite assays and decreased for nutrient assays (Figure 10, Paper II).

The speciation of Hg(II) with LMM-thiols is discussed as one of the driving parameters for Hg(II) availability and the subsequent uptake and methylation of Hg(II) in *G. sulfurreducens* assays.^{2, 51, 52} However, only specific LMM-thiols, like cysteine, enhances Hg(II) methylation in assays with *G. sulfurreducens*, whereas branched LMM-thiols, like penicillamine, do not.^{51, 52, 120} The high concentration of Hg(Cys)₂ and Hg(CysN)₂ in the initial time interval (0.5 to 2 h) and the observed high Hg(II) methylation suggested that Hg(II) methylation was driven by the Hg(II) speciation in the dissolved phase (Figure 10, Paper II). The higher Hg(II) methylation formation in metabolite assays compared to standard assays was likely due to a shift in the partition towards the dissolved phase and not linked to the Hg(II) speciation in the dissolved phase, which was similar. Although, metabolite assays were dominated by Hg(Cys)₂, whereas standard assays by Hg(CysN)₂ after 0.5 h (Figure 10a,b), both Hg-complexes showed a similar Hg(II) methylation rate in previous studies.⁵²

At incubation time >6 h, stalled MeHg formation was observed with a low net formation of MeHg of 0.2–2.8 nM MeHg within 18 h (Figure 10, Paper II). The stalled Hg(II) methylation at extended time points (>6 h) was likely linked to the presence of Hg(II) species, that are less available for Hg(II) uptake and methylation, i.e. Hg(PEN)₂, and concentration changes in the dissolved Hg(II) pool. In addition, in metabolite assays with 100 and 600 nM cysteine, the concentration of the substrate Hg(II) decreased substantially over time, due to a high Hg(II) methylation potential, and the lack of the substrate (dissolved Hg(II)) caused stalled net MeHg formation at t>6 h (Figure 10d, Paper II).

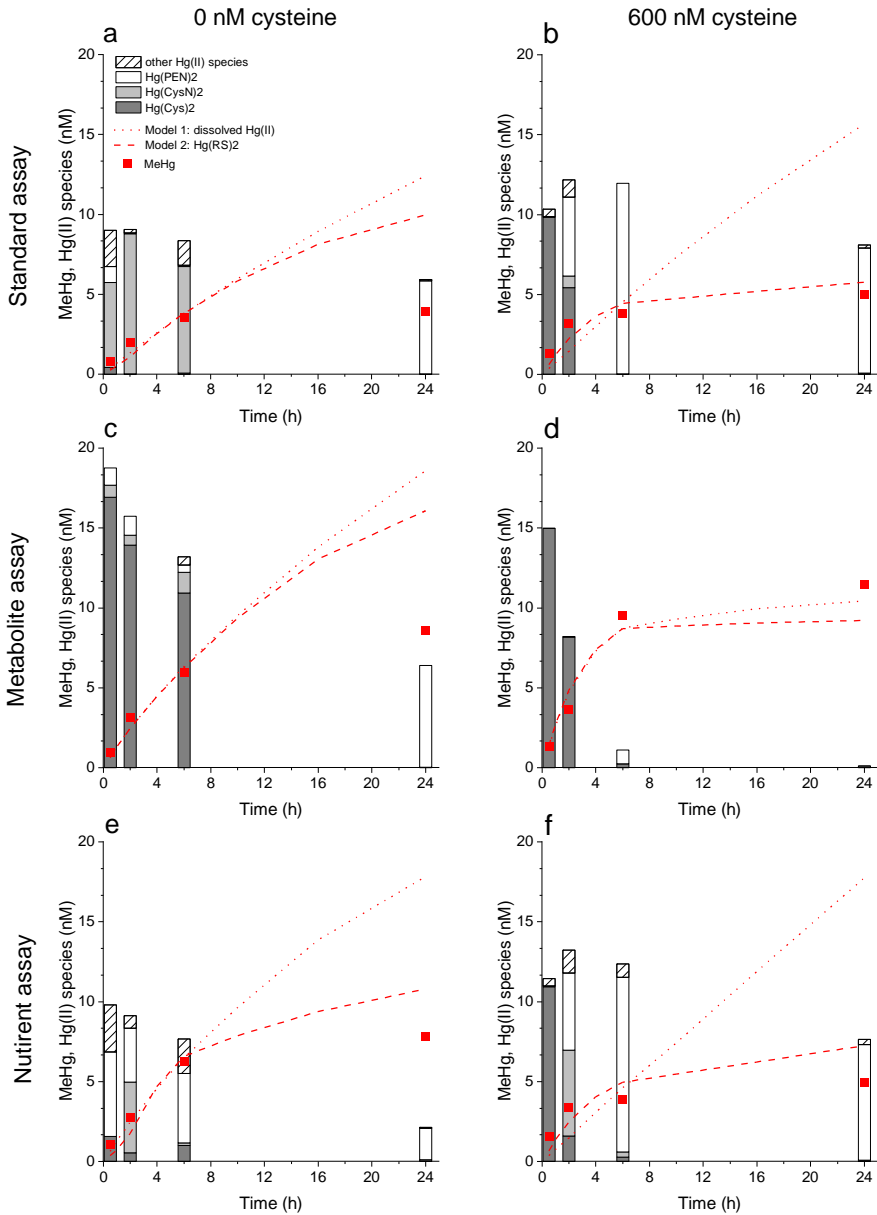


Figure 10: Composition of Hg(II) species (bar plots) in the dissolved phase at the four time points (0.5, 2, 6 and 24 h) in three different *G. sulfurreducens* assay systems after addition of 30 nM Hg(II): (a), (b) standard assay, (c), (d) metabolite assay and (e), (f) nutrient assay with 0 and 600 nM cysteine addition, respectively. The three dominant Hg(II) species are: Hg(Cys)₂, Hg(CysN)₂ and Hg(PEN)₂. Measured MeHg concentration over time (red squares). Modelled MeHg formation over time by the rate model 1 based on the total dissolved Hg(II) concentration (red dotted line) and by the rate model 2 based on the Hg(II)-speciation (Hg(RS)₂) (red dashed line). (Adapted from Paper II)

Modelling methylmercury formation

All assays were impacted by two major changes during the incubation time: (i) changes in the chemical speciation of Hg(II) with LMM-thiols and (ii) changes in the total concentration of dissolved Hg(II) driven by Hg(II) methylation and LMM-thiols. Both changes are crucial parameters for the overall Hg(II) methylation potential as discussed in the previous paragraph. A species-specific Hg(II) methylation rate model was developed to further clarify the importance of the Hg(II) speciation for Hg(II) uptake and methylation and the decrease in the dissolved Hg(II) pool. A first-order exponential rate model based on the dissolved Hg(II) speciation (model 2) was developed. This model takes into account the changes in dissolved Hg(II) concentration and the changes in Hg(II) speciation over time. To separate the effect of changes in the dissolved Hg(II) concentration, an additional model based on the total dissolved Hg(II) concentration (model 1) as the substrate for Hg(II) methylation was developed. In all three assay systems with the addition of 600 nM cysteine, model 2 described the MeHg formation fairly well, whereas model 1 overpredicted the MeHg formation in standard and nutrient assays. The predicted low MeHg formation at extended time points was driven by the shift in Hg(II) speciation from complexes with small to branched LMM-thiols, due to the metabolic turnover of cysteine to penicillamine and the 20×times lower Hg(II) methylation rates of Hg(PEN)₂ complexes compared to Hg(Cys)₂.⁵² In the metabolite assay the shift in chemical speciation was not observed and both models predicted the MeHg formation fairly well since the stalled MeHg formation at extended time points was likely due to a depletion of the dissolved Hg(II) pool. In assays without exogenous cysteine addition, MeHg formation was overpredicted at t > 6 h by both models with an overall better performance by model 2. It is likely that the Hg(II) speciation was more complex than calculated by the performed speciation model, since the Hg(II) speciation modelling was based on the eight measured LMM-thiols in this study. Additionally, unidentified ligands might further impact Hg(II) speciation and subsequently MeHg formation at extended time points if those ligands form complexes with Hg(II) with a lower availability for Hg(II) uptake and methylation than Hg(Cys)₂. Branched LMM-thiols and DOM are known to decrease the availability of Hg(II) for *G. sulfurreducens*.^{52, 62, 63, 149} Overall, the formation of MeHg could be better described by model 2 based on the Hg(II) speciation at each time point and showed, how time-dependent changes in Hg(II) speciation, caused by bacterial thiol metabolism, is a major parameter controlling MeHg formation.

In addition, the formation of sulfide in Hg(II) methylation assays might have contributed to stalled MeHg formation at t > 6 h, since sulfide inhibited MeHg formation as shown by additional experiments and in previous studies (Paper II).^{51, 120} However, in case of sulfide formation, the formation was below the detection limit of 120 nM sulfide, but this concentration would impact the Hg(II) speciation with HgS as the dominant species. MeHg formation was inhibited by low exogenous sulfide addition, 100 nM, between 0-6 h and showed low formation between 6-24 h (Paper II). Overall, the formation of sulfide could not be fully excluded at incubation time > 6 h. Moreover, MeHg demethylation could contribute to the observed time trend in MeHg formation since steady-state between Hg(II) methylation and MeHg demethylation is often observed in environmental samples at longer incubation times.^{216, 217} MeHg was not demethylated by *G. sulfurreducens* as shown in Paper II and other previous studies (Paper II).^{50, 58}

The species-specific Hg(II) methylation rate constant k_{meth} determined by model 2 for Hg(Cys)₂ was comparable to previous studies with 0-100 nM cysteine concentration with $0.5\text{-}0.7 \times 10^{-12}$ L cell⁻¹ h⁻¹ and $0.1\text{-}0.34 \times 10^{-12}$ L cell⁻¹ h⁻¹ for standard assays in this study and previous studies, respectively (Paper II).^{52, 53, 120} For metabolite assays with 600 nM cysteine the determined k_{meth} was 1.6×10^{-12} L cell⁻¹ h⁻¹ and this value was previously reported for standard assays with 10 μM cysteine (Paper II).⁵² However, nutrient assays showed the highest k_{meth} with 3.3×10^{-12} L cell⁻¹ h⁻¹ (no cysteine addition) which indicated that nutrients drive Hg(II) methylation, and cysteine addition, 600 nM, had a countereffect on the k_{meth} , resulting in a lower rate of 0.85×10^{-12} L cell⁻¹ h⁻¹ (Paper II). Overall, these results showed, that the addition of cysteine enhances k_{meth} , but in addition the turnover of cysteine during the incubation time was affecting the Hg(II) methylation potential and this effect was more distinct in assays with higher nutrient concentrations.

Cell physiology during Hg(II) methylation assays

The MeHg formation in nutrient assays did not follow the same pattern as standard and metabolite assays, since the highest MeHg formation potential was observed in assays without cysteine addition and added cysteine was rapidly metabolized. This result suggested that cell physiology was impacted by the nutrient addition, since the concentrations of the electron donor (acetate) and acceptor (fumarate) were highest for nutrient assays with 3.9 nM and 1.9 nM, respectively (Table A1). The biochemical composition of *G. sulfurreducens* cells was monitored during the 24 h incubation by ATR-FTIR. The polysaccharide region (1189–956 cm⁻¹), ascribed to the polymer glycogen showed the most pronounced changes. In general, glycogen is a dynamic energy storage polymer and utilized under altering environmental conditions to provide short term benefits and facilitate nutrient uptake.²¹⁸⁻²²⁰ Overall the consumption of glycogen increased with increasing nutrient concentration in the order standard assay < metabolite assay < nutrient assay. A small increase in the nucleic acid and phospholipids region (1240–1220 cm⁻¹) was observed and indicated active cell growth. In fact, the cell number increased in all assay systems within 24 h by a factor of 1.2, 1.5 and 2.8 for standard, metabolite, and nutrient assays, respectively (Paper II). The small nutrient concentration increases in metabolite and nutrient assay buffer composition impacted the cell physiology and led to an increase in the metabolic activity as revealed by changes of the biochemical composition in the ATR-FTIR spectra and additional changes in cell density (Figure 11, Paper II). The enhanced metabolic activity in the nutrient assay was likely the driving factor for enhanced MeHg formation without cysteine addition (Figure 10e). These results further showed that the two parameters, Hg(II) speciation and metabolic activity, are not necessarily additive and higher metabolic activity led to a higher turnover of LMM-thiols (Figure 10f, Paper I and II).

During the initial time frame (0.5–6 h) the highest amount of MeHg was formed, which corresponded primarily to the time frame of net-synthesis of glycogen. MeHg formation was decreased at extended incubation time (t>6 h) during glycogen consumption. This relationship indicated a possible link of the cell physiology to MeHg formation potential. However, additional experiments showed, that ageing of cells for 6 h prior to Hg(II) addition did not impact the Hg(II) methylation potential and similar concentrations of MeHg were formed after a total incubation time of 24 h with *G. sulfurreducens* cells

compared to non-aged assays (Paper II). The metabolic shift of glycogen synthesis and consumption did thus not impact the Hg(II) methylation.

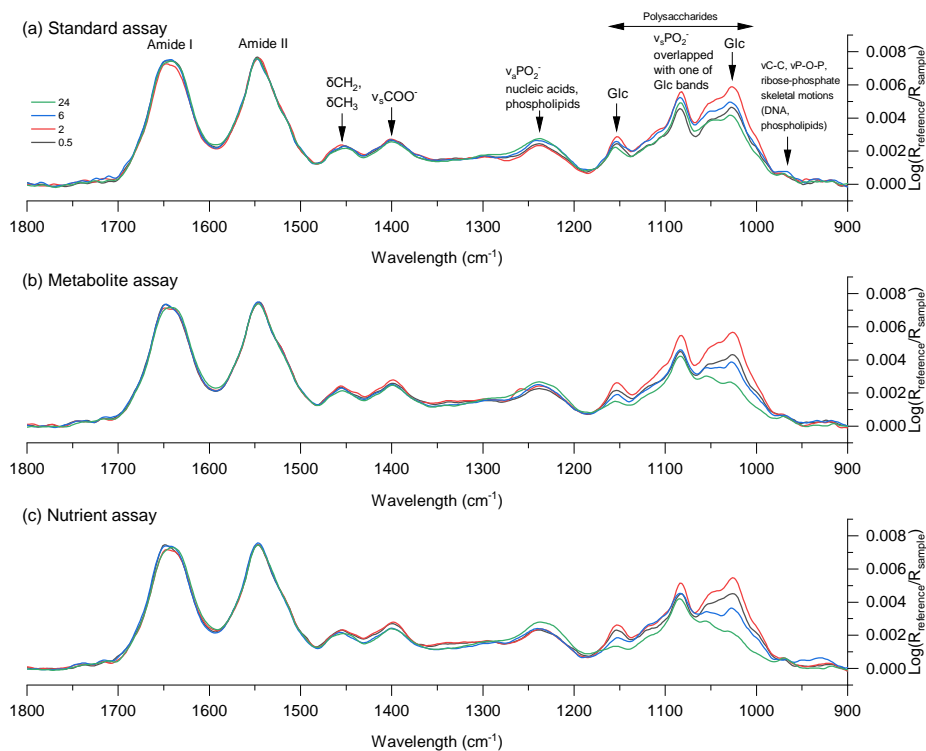


Figure 11: Evolution of the ATR-FTIR spectra of *G. sulfurreducens* cells (pelleted) in the different assay systems: (a) standard assay, (b) metabolite assay and (c) nutrient assay after 0.5, 2, 6 and 24 h with 30 nM Hg(II). For each sample, the corresponding supernatant was used as a reference spectrum and all spectra were normalized to the amide II band at 1548 cm^{-1} . Assignments of the different infrared bands are based on Quilès et al.²⁰¹ (Reproduced from Paper II with permission from Environmental Science & Technology. Copyright © 2023, American Chemical Society)

Concluding remarks: Dissolved thiols and cell physiology driving Hg(II) methylation

Overall, the formation of LMM-thiols by *G. sulfurreducens* during growth and in washed cell assays showed a highly dynamic pattern. The LMM-thiol metabolism was impacted by Fe(II) and led to high formation of LMM-thiols under Fe(II) depleted condition. Moreover, in washed cell assays a turnover of small to branched LMM-thiols was observed based on a di-methylation of cysteine to penicillamine as verified by isotopic labeled cysteine exposure experiments. This turnover of cysteine to penicillamine was amplified by the addition of cysteine. In Hg(II) methylation assays, the Hg(II) speciation was impacted by the turnover of LMM-thiols. The shift of small to branched Hg(II)-thiol complexes resulted in high Hg(II) methylation in the initial time period based on small Hg-thiol species, i.e. Hg(Cys)₂, and into stalled net MeHg formation at extended time intervals based on branched Hg-thiol complexes, i.e. Hg(PEN)₂. Additionally, LMM-thiols shifted the Hg partitioning from the cell-associated to the dissolved phase and increased the available Hg(II) pool. Besides the role of LMM-thiols in driving the Hg(II) speciation and the Hg(II) partitioning, the overall cell physiology impacted the Hg(II) methylation potential. However, the effects of cell physiology and LMM-thiols were not additive, since high metabolic activity led to a faster turnover of small to branched LMM-thiols. Moreover, cells maintain their potential to methylate Hg(II) despite metabolic shifts from net synthesis to net consumption of glycogen. Overall, the relative concentration of cysteine and penicillamine was the major driving factor for Hg(II) availability and methylation in *G. sulfurreducens* assays under non-sulfidic conditions. The monitoring of the LMM-thiol composition is crucial to predict and understand the Hg(II) methylation potential.

Surface thiols on the outer and inner membrane

Membrane surface thiols are considered as crucial functional groups for Hg(II) adsorption, reduction, and internalization.^{57, 60, 154, 155} The coordination environment of Hg with membrane functional groups is proposed to determine Hg(II) availability and consequently uptake and methylation of Hg(II).^{55, 152, 154, 155, 162, 164} Paper III focused on characterizing these features for the outer and inner membrane by EXAFS and HERFD-XANES. Paper IV investigated the role of outer and inner membrane thiol groups with respect to Hg partition and uptake and Hg(II) methylation and reduction. This chapter focuses on the following four research questions which were addressed in detail in Paper III and IV.

- i. What is the Hg speciation on the surface of the outer and inner membrane?
- ii. What is the cell surface thiol concentration on the outer and inner membrane?
- iii. Is Hg partitioning controlled by surface thiols on the outer and inner membrane?
- iv. Are Hg(II) transformation processes, i.e. methylation and reduction, impacted by membrane surface thiols?

Mercury speciation on the outer and inner membrane

The speciation of Hg was determined by EXAFS and HERFD-XANES on the outer and inner membrane probed on whole cells and spheroplasts, respectively. The results were overall in good agreement for the two techniques (Figure 12, Paper III). At low Hg(II) addition (samples with final Hg concentration $<13 \mu\text{mol g}^{-1}$), the speciation was dominated by two coordinated Hg-thiol structures (determined as $\text{Hg}(\text{Mem-RS})_2$ and $\text{Hg}(\text{Cys})_2$ with EXAFS and HERFD-XANES, respectively, see Table A3). With increasing Hg concentration, the speciation shifted towards less stable Hg species with hydroxyl (-OH), carboxyl (-COOH) or amine (-NH₂) functional groups, as shown by the presence of $\text{Hg}(\text{Mem-CO/N})_2$ and $\text{Hg}(\text{acetate})_2$ for EXAFS and HERFD-XANES, respectively. The Hg speciation by HERFD-XANES showed a better fit for the model compound $\text{Hg}(\text{Cys})_2$ at pH 11 for lower Hg concentration and for $\text{Hg}(\text{Cys})_2$ at pH 3 at higher Hg concentration. The reason for an increasing contribution of $\text{Hg}(\text{Cys})_2$ at lower Hg to sample thiol concentration is unclear, however small and increasing contribution of $\text{Hg}(\text{Cys})_{3/4}$ structures were suggested at decreasing Hg to sample ratio and cannot be excluded (Paper III). In addition, liquid Hg(0) was detected, and the formation of Hg(0) is further discussed in the section *Reduction of Hg(II)*.

The Hg speciation was dominated by $\text{Hg}(\text{Mem-RS})_2$ species on the outer and inner membrane at Hg concentrations relevant for Hg(II) uptake and methylation studies by both techniques, EXAFS and HERFD-XANES (Figure 12, Paper III). The XANES results of this study were not in alignment with previous XANES studies. Several studies by XANES showed that the speciation on cell membranes was dominating by $\beta\text{-HgS}$ and $\text{Hg}(\text{RS})_{3/4}$ species,^{142, 152, 162} whereas by EXAFS, $\text{Hg}(\text{RS})_2$ species were the dominated determined species.^{154, 155} In our study there was no indication for 3/4-coordinated Hg-thiol complexes, neither by EXAFS nor by HERFD-XANES at higher Hg to sample ratios (Paper III). Small contribution of $\text{Hg}(\text{Cys})_3$ by HERFD-XANES could be not excluded in samples with low Hg concentration, however the model compound $\text{Hg}(\text{Cys})_3$ was not improving the model fit (Paper III). The differences among the studies were likely

due to different experimental approaches, since for example Thomas et al. investigated the speciation of Hg associated to metabolically active *G. sulfurreducens* cells during a 2 h incubation time with and without addition of dissolved thiol ligands.¹⁵² In contrast, Hg(II) internalization and methylation was prevented in our study due to the absence of the electron donor and acceptor.⁵² The Hg speciation was further probed selectively on the outer and inner membrane surface under short incubation times (10 min). These differences suggested that the initial complexation of Hg with the cell membrane is 2-coordinated ($t < 10$ min) while the longer incubation time in previous studies lead to 3/4-coordinated Hg complexes and these complexes are predominantly formed in the presence of dissolved LMM-thiol ligands.^{152, 163} In addition, cell-associated Hg speciation might be controlled by the type of microorganisms, since HgS species are determined especially for sulfate-reducing microorganisms.¹⁶²

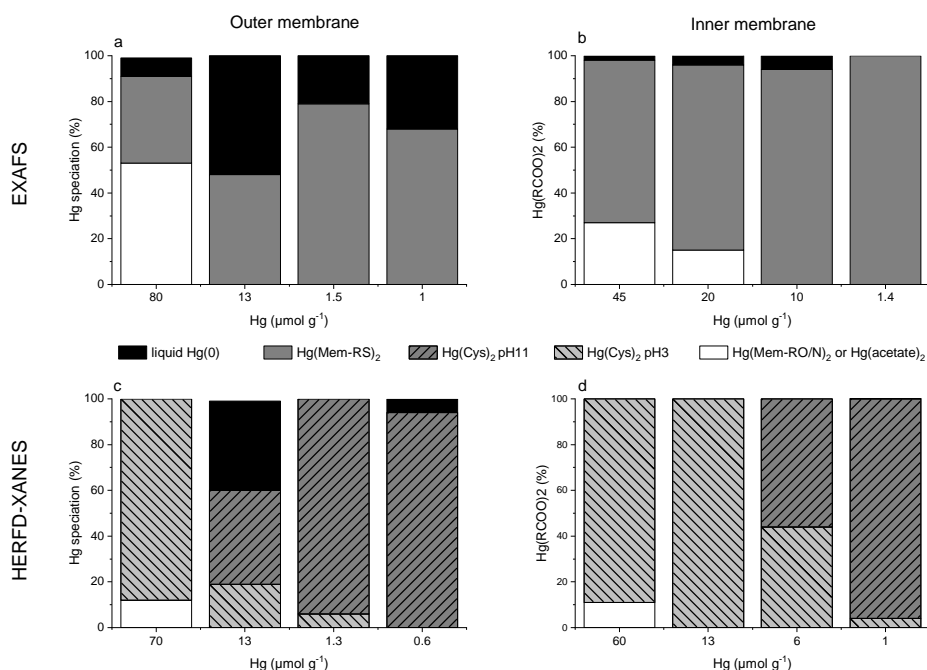


Figure 12: Mercury speciation on the outer (a, c) and inner (b, d) membrane surface of *G. sulfurreducens* by (a, b) EXAFS and (c, d) HERFD-XANES. The outer membrane was probed by starved whole cells. The inner membrane was probed by starved spheroplasts. Selected samples with final Hg concentration of 0.6 to 80 $\mu\text{mol g}^{-1}$ dry mass are shown. The definition of the different Hg species for EXAFS and HERFD-XANES are described in Table A3. (Adapted from Paper III)

Concentration of membrane surface thiols

The outer and inner membrane of *G. sulfurreducens* was titrated with increasing Hg concentration to determine the surface thiol concentration. This experimental approach was previously used to determine the concentration of thiol compounds by EXAFS in whole cells, cell fragments and NOM.^{154, 155, 157}

The concentration of surface thiol groups on the inner membrane was by a factor of six higher compared to the outer membrane with 120 and 20 $\mu\text{mol g}^{-1}$ wet mass (corresponding to 1490 and 240 $\mu\text{mol g}^{-1}$ C), respectively. The results for the outer membrane were lower compared to previous studies with *G. sulfurreducens* which showed thiol concentrations between 67.8–240 $\mu\text{mol g}^{-1}$ wet mass based on fluorescence spectroscopy, potentiometric titration, and EXAFS (Table 2). In addition, our study distinguished between the outer and inner membrane, prevented Hg(II) internalization and methylation, and probed under short incubation time.⁵² Hg internalization was not prevented in the study by Mishra et al., which showed a four times higher membrane thiol concentration based on EXAFS,¹⁵⁴ and contribution of inner membrane, periplasm or cytosol thiols cannot be excluded. Moreover, the study of Song et al. measured the membrane thiol concentration based on membrane fragments, however these results were in between the determined concentration of outer and inner membrane (Table 2).¹⁵⁷ The deviation of surface thiols groups could be additional linked to variation in growth conditions, since growth state and medium composition impact the thiol surface concentration.^{179, 221}

In addition to the total concentration, two types of exterior membrane surface thiols were identified and quantified based on their complex formation with Hg. Two types of Hg complexes on the exterior of the outer and inner membrane were described: (i) $\text{Hg}(\text{Mem}_{\text{ext}}\text{-R}^{\text{II}}\text{S})_2$ and (ii) $\text{Hg}(\text{Mem}_{\text{ext}}\text{-R}^{\text{I}}\text{S})(\text{Mem}_{\text{ext}}\text{-RO/N})$ based on Song et al.¹⁵⁵ $\text{Mem}_{\text{ext}}\text{-R}^{\text{II}}\text{S}$ describes two membrane thiol groups, which are located sufficiently close to each other to form a linear two coordinated $\text{Hg}(\text{Mem}_{\text{ext}}\text{-R}^{\text{II}}\text{S})_2$ structure. Whereas $\text{Mem}_{\text{ext}}\text{-R}^{\text{I}}\text{S}$ describes a membrane thiol group which is not located close enough to another membrane thiol functional group to form the two-coordinated Hg(II)-thiol complex and is therefore involved in a mixed complex with hydroxyl, carboxyl or an amine functional group, $\text{Hg}(\text{Mem}_{\text{ext}}\text{-R}^{\text{I}}\text{S})(\text{Mem}_{\text{ext}}\text{-RO/N})$. On the inner membrane a high total concentration of cell surface thiols was determined, however only 30 $\mu\text{mol g}^{-1}$ of surface thiols were situated close enough to be involved in a two-coordinated Hg(II) structure, $\text{Hg}(\text{Mem}_{\text{ext}}\text{-R}^{\text{II}}\text{S})_2$, whereas 700 $\mu\text{mol g}^{-1}$ were involved in mixed-ligation Hg(II) complexes with one membrane surface thiol, $\text{Hg}(\text{Mem}_{\text{ext}}\text{-R}^{\text{I}}\text{S})(\text{Mem}_{\text{ext}}\text{-RO/N})$ (Paper III). In contrast, on the outer membrane 80 $\mu\text{mol g}^{-1}$ of thiols were involved in $\text{Hg}(\text{Mem}_{\text{ext}}\text{-R}^{\text{II}}\text{S})_2$ structures and 40 $\mu\text{mol g}^{-1}$ in $\text{Hg}(\text{Mem}_{\text{ext}}\text{-R}^{\text{I}}\text{S})(\text{Mem}_{\text{ext}}\text{-RO/N})$ structures. A previous study on cell membrane fragments (of both the outer and inner membranes) by Song and co-workers showed a distribution of 5% Hg-Mem-R^{II}S and 95% Hg-Mem-R^IS,¹⁵⁵ comparable to what we reported for the inner membrane with 4% and 96%, respectively. Both the concentration of membrane thiol compounds and their complexation with Hg are considered crucial for Hg(II) availability and uptake. The thermodynamic stability of $\text{Hg}(\text{Mem}_{\text{ext}}\text{-R}^{\text{II}}\text{S})_2$ is much higher compared to $\text{Hg}(\text{Mem}_{\text{ext}}\text{-R}^{\text{I}}\text{S})(\text{Mem}_{\text{ext}}\text{-RO/N})$ with a $\log K$ of 39.1 and 25.6, respectively.¹⁵⁵ The two types of formed Hg complexes with the membrane and the differences in their stability constant might have implications for the

uptake of Hg(II) across the outer and inner membrane. The high proportion of Mem_{ext}-R^IS at the inner membrane may lead to a predominance of kinetically favored Hg(Mem_{ext}-R^IS)(Mem_{ext}-RO/N) or two coordinated Hg(II) complexes with one dissolved ligand, Hg(Mem_{ext}-R^IS)(RS) or Hg(Mem_{ext}-R^IS)(RO/N). Complexes with RO/N functional groups are less stable than the Hg(Mem_{ext}-R^{II}S)₂ and may facilitate a fast internalization of Hg(II) into the cytosol. These concepts are coherent with previous observations that the Hg(II) uptake kinetics across the inner membrane is faster compared to the outer membrane for *G. sulfurreducens*.⁵³ Moreover, dissolved thiol ligands and DOM may decrease the formation of Hg(Mem_{ext}-R^{II}S)₂ in Hg(II) methylation assays and it is assumed that Hg(Mem_{ext}-R^{II}S)(RS) complexes are formed with increasing concentration of dissolved thiol ligands,¹⁵⁵ since the concentrations of dissolved thiols typically present in *G. sulfurreducens* assays are sufficient to compete with membrane surface thiols (Paper I and II).¹²⁰

Table 2: Comparison of thiol concentrations of different *G. sulfurreducens* fractions determined by fluorescence spectroscopy, potentiometric titration, and EXAFS. (Adapted from Paper III)

<i>Geobacter sulfurreducens</i>	Wet	Dry		Method	Reference
	μmol g ⁻¹	μmol g ⁻¹	μmol g ⁻¹ C		
Whole cells - outer membrane	20	120 [§]	240	Hg L _{III} -edge EXAFS	Paper III
Spheroplasts - inner membrane	120	730 [§]	1490	Hg L _{III} -edge EXAFS	Paper III
Membrane fragments (average of the inner and outer membranes)	-	-	380*	Hg L _{III} -edge EXAFS	Song et al. ¹⁵⁵
Whole cells [#]	240	-	2000*	Fluorescence (qBBr)	
Whole cells [#]	67.8	-	550*	Potentiometric titration	Mishra et al. ¹⁵⁴
Whole cells [#]	75	-	608*	Hg L _{III} -edge EXAFS	
Whole cells [#]	55.5	-	466*	Fluorescence (qBBr)	Thomas et al. ¹⁵²

[§] expressed in relation to mass of whole cells, *numbers reproduced from Song et al.¹⁵⁵, [#] expected to represent the outer membrane

Mercury partitioning

In Paper IV, the role of membrane surface thiols for Hg(II) uptake and transformations was investigated by derivatizing membrane surface thiols with qBBr. The partitioning of total Hg (sum of Hg(II), Hg(o) and MeHg) between dissolved, cell-adsorbed, and intracellular fraction was determined for whole cells with and without blocking after 0.5 and 4 h incubation. The Hg partitioning was not altered by blocking the membrane surface thiols, but the cell-adsorbed Hg fraction decreased for both samples from 240 to 155 pmol Hg between 0.5 and 4 h (Figure 13a, Paper IV). The intracellular amount remained constant with ~85 pmol Hg at both time points and in both sample types. The Hg partitioning for spheroplasts did not change over time with a higher intracellular Hg fraction compared to whole cells with 180 pmol Hg (Figure 13e, Paper IV).

The total Hg was dominated by Hg(II) and represented after 0.5 h around 60% and 80% of total Hg for whole cells and spheroplasts, respectively, and no differences between

blocking and non-blocking were observed (Paper IV). The partitioning between Hg(II) dissolved and cell-associated (sum of surface adsorbed and intracellular) Hg(II) changed over time with a higher relative amount of dissolved Hg(II) for whole cells (Paper IV). The dissolved Hg(II) amount was constant for spheroplast and whole cells with 200 pmol (Figure 13b,f, Paper IV).

Overall, the partitioning of total Hg was not significantly impacted by blocking of cell surface thiols with qBBr in whole cells and spheroplasts (repeated measure ANOVA, $p > 0.05$). Thomas and co-workers also showed no impact on the partition between dissolved and cell-associated Hg for blocked and non-blocked membrane surfaces thiols.¹⁵² In general, it is assumed, that qBBr is selectively derivatizing cell surface thiol functional groups and that, due to its molecule size and positive charge the internalization of qBBr is prevented and cell properties are not affected.^{154, 176, 178, 181, 182, 186} Potentiometric titration showed changes of the acidity constants between qBBr treated and untreated cells and therefore it is assumed to be a direct measure of the thiol concentration in membranes.^{154, 181} However, one study hypothesized the possibility that qBBr only partly derivatized membrane surface thiols and sites which are inaccessible for qBBr, due to its size, might still be available for binding Hg(II).¹⁸¹ This in turn could explain our result, since no changes in the partition between blocked and non-blocked samples were observed. In addition, Hg partition varied between whole cells and spheroplast with a higher amount of internalized Hg for the latter (Figure 13) and this suggested that a higher amount of intracellular Hg has implication for Hg(II) methylation.

Reduction of Hg(II)

Hg losses

In all samples, average Hg losses average losses of $20 \pm 4\%$ were observed between the time of Hg(II) addition and the first measurement time point 0.5 h (Paper IV). Further Hg losses were observed between 0.5 and 4 h with $4 \pm 1.3\%$. The losses for whole cells and spheroplasts were in a similar range as in Paper III with $19 \pm 12\%$ for the initial losses (Paper III). In addition, these losses were in line with Paper II and other studies with *G. sulfurreducens*.^{57, 60, 152} Losses of Hg are ascribed to evasion of gaseous Hg(0)^{57, 60} and Hg adsorption onto glass vial walls,^{214, 215} as discussed in section *Mercury speciation, losses, and methylation*.

Formation of liquid Hg(0)

In Paper III, the formation of liquid Hg(0) was observed in all outer membrane samples by EXAFS, except IM 1.4, with contribution to the Hg speciation between 5-52% whereas low contribution of liquid Hg(0) was determined for the inner membrane samples with 2-7% (Figure 12 and Paper III). In comparison, liquid Hg(0) was fitted only in four samples by HERFD-XANES and contributed to the Hg speciation between 9-59% (Figure 12, Paper III). Further, liquid Hg(0) was also detected in a set of freeze-dried samples analyzed by EXAFS and freeze drying did not lead to volatilization of Hg(0) (Paper III).

Isaure and co-workers were the first to show the presence of liquid Hg(0) in bacteria samples exposed to Hg with a speciation contribution of 29-41% of cell-associated Hg by

HERFD-XANES.¹⁶² Important to note is, that this was also the first study which used liquid Hg(o) as a reference compound for LCF fitting of HERFD-XANES spectra of Hg exposed bacteria sample. The formation of Hg(o) was however puzzling, since it was reported that the potential to reduce Hg(II) by the studied microorganisms was low.¹⁶² In contrast, *G. sulfurreducens* is known to reduce Hg(II) to Hg(o) as shown by several studies and commonly detected as the difference between purgeable and non-purgeable Hg.^{57, 60} In this study, liquid Hg(o) was detected, and this result raised the question whether the origin of gaseous and liquid Hg(o) was based on the same mechanism. The formation of gaseous Hg(o) was previously linked to the presence of cytochromes in the outer membrane.^{57, 60} A higher amount of liquid Hg(o) was formed on the outer membrane compared to the inner membrane in our study (Figure 12). In general, a high number of cytochromes is known for *G. sulfurreducens*, both in the inner and outer membrane as well as in the periplasm.^{222, 223} The lower formation of Hg(o) on the inner membrane might be a consequence of an interrupted e-transfer due to the removal of the outer membrane and the periplasm.

Formation of gaseous Hg(o)

In Paper IV, the reduction of Hg(II) was further investigated, whether Hg(II) reduction potential differs among whole cells and spheroplasts and if cell surface thiols were impacting this transformation. In all samples gaseous Hg(o), quantified as purgeable Hg was formed after 0.5 and 4 h (Figure 13). The formation of Hg(o) was fast and the amount of formed Hg(o) was significant higher for whole cells with 140 pmol Hg(o) compared to spheroplasts with 80 pmol Hg(o) (repeated measure ANOVA, $p < 0.05$). Whole cells showed a similar distribution of Hg(o) between the dissolved and cell-associated phase for qBBr treated and untreated samples with a higher Hg(o) amount in the dissolved phase, 95 pmol (Figure 13). Overall, no differences between blocked and non-blocked cells were observed (Figure 13, Paper IV). In spheroplast samples, a higher fraction of cell-associated Hg(o) was observed after 4 h compared to 0.5 h with 45 pmol and 10 pmol Hg(o) cell-associated, respectively (Paper IV).

The higher Hg(o) formation in whole cells compared to spheroplasts was consistent with Paper III for liquid Hg(o) determination (Figure 12, Paper III). Overall, the reduction of Hg(II) to Hg(o) is linked to cytochromes as discussed in the previous section *Formation of liquid Hg(o)*. The reduction of Hg(II) by spheroplast samples was assumed to be linked to inner membrane cytochromes, however, in Paper III the lower formation of liquid Hg(o) was suggested to be linked to interrupted electron transfer due to the removal of the outer membrane. In this study we confirmed the results of Paper III with an overall lower formation in spheroplast samples, especially the cell-associated Hg(o) was lower after 0.5 compared to 4 h incubation time (Paper IV). In Paper III and IV, it was not identified if liquid and gaseous Hg(o) were both formed due to cytochromes in membranes and if liquid Hg(o) was part of the purgeable Hg fraction or not. However, the result of Paper IV showed, that there was a fraction of purgeable Hg(o) cell-associated, and this suggested that liquid Hg(o) might be purgeable (Figure 13, Paper IV). In addition, Paper IV showed that blocking cell surface thiols, both on the outer and inner membrane, were not impacting the formation of Hg(o).

Methylation of Hg(II)

In all samples MeHg was formed. For whole cells, the amount of formed MeHg increased between 0.5 and 4 h from 35 to 60 pmol and 35 to 120 pmol for blocked and unblocked samples (Figure 13, Paper IV) The major fraction of MeHg was cell-associated after 4 h with 80% of formed MeHg (Figure 13). In contrast, spheroplast samples showed lower formation of MeHg with differences in the amount of formed MeHg after 0.5 and 4 h with 11 and 13 pmol MeHg (Figure 13).

The formed MeHg in whole cells was in the same range as reported in Paper II and previous studies corresponding to ~5 nM MeHg.^{60, 120} The formation of MeHg of blocked whole cells showed decreased MeHg formation after 4 h. In contrast, a study by Thomas and co-workers showed overall low MeHg formation, ~1 nM, for blocked and non-blocked whole cell samples.¹⁵²

Formation of MeHg by spheroplasts was lower compared to whole cells with 15 compared to 120 pmol MeHg for non-blocked samples and 12 compared to 63 pmol MeHg for blocked samples after 4 h (Figure 13, Paper IV). Non-blocked spheroplasts showed a slightly higher formation of MeHg at the initial time point (0.5 h) compared to a previous study by Schaefer et al. with 28×10^{-12} mol protein⁻¹ compared to 10×10^{-12} mol protein⁻¹, respectively.⁵³ At longer incubation time, MeHg formation was lower compared to Schaefer et al. with 34×10^{-12} mol protein⁻¹ after 4 h compared to $\sim 75 \times 10^{-12}$ mol protein⁻¹ after 1.5 h, respectively.⁵³ The higher MeHg formation in Schaefer et al. study at longer incubation times was assumed to be linked of the addition of cysteine (50 μ M), since the uptake of Hg(II) across the inner membrane is hypothesized to be linked to Hg-cysteine complexes.^{53, 54} The rapid internalization of Hg and the low MeHg formation might be caused by strong sorption of Hg(II) to cellular material inside the cell, which is unavailability for Hg(II) methylation.⁵⁴

Overall, the decreased formation of MeHg for blocked whole cells over time suggested an impact of blocking on its formation. However, the partitioning of Hg was not affected by membrane surface thiols blocking as previously discussed. These results indicated that additional processes linked to the derivatization of qBBBr could influence the lower MeHg formation between blocked and non-blocked membranes.

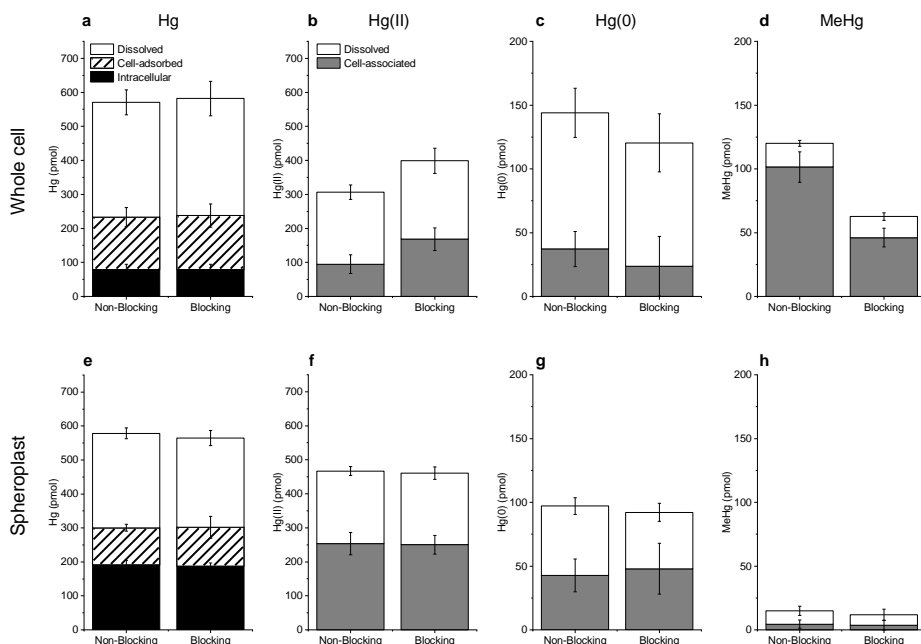


Figure 13: Mercury partitioning of whole cell (a-d) and spheroplast (e-h) assays of *G. sulfurreducens* after addition of 750 pM Hg(II) (corresponding to 30 nM Hg(II)) with and without blocking of cell surface thiol groups with qBBR after 4 h incubation (n=5; \pm standard deviation). (Adapted from Paper IV)

Physiology of qBBR derivatized samples

The impact of qBBR on cell physiology was previously not tested.^{152, 154, 178, 181} The cell density of whole cells increased between 0.5 and 4 h by 26% and 16% for non-blocked and blocked whole cells, respectively (Paper IV). Additionally, fluorescence microscopy of whole cells and spheroplasts with and without qBBR treatment showed viable cells (Paper IV).

Furthermore, the changes of biochemical fingerprint of cells were investigated by ATR-FTIR as previously studied in Paper II. Non-blocked whole cell spectra was comparable to the previous obtain spectra in Paper II (see *Cell physiology during Hg(II) methylation assays*) and showed a decrease in the glycogen band at 1189–956 cm^{-1} between 0.5 and 4 h (Figure 14a, Paper IV). Blocked whole cells, however, showed no changes in the glycogen band at 4 h compared to 0.5 h (Figure 14a, Paper IV). For spheroplast samples the overall biochemical composition was deviating from whole cells, while no difference between blocking and non-blocking was observed (Figure 14). One central difference was a pronounced glycogen band between 1189 and 956 cm^{-1} and a strong band for DNA and phospholipids between 998 and 915 cm^{-1} . The contribution of DNA and phospholipids at lower wavelength was likely linked to the removal of the outer membrane and the changes of the penetration depth of the infrared beam with greater spectral contribution of the cytosol.

Overall, the physiology of cells based on fluorescence microscopy and cell growth was not impacted by derivatization of cell surface thiols functional groups, whereas the biochemical composition showed an impact by qBBr by the removal of the outer cell membrane. These results could not identify how qBBr was impacting the metabolisms of cells but showed that it was likely contributed to impact the cell physiology as shown by ATR-FTIR. Especially, the lower formation of MeHg for blocked whole cells might be linked to the qBBr treatment and the impact on cell physiology, rather than to blocked cell surface thiols, since the partitioning and internalization of Hg was not affected by qBBr blocking (Figure 13, Paper IV).

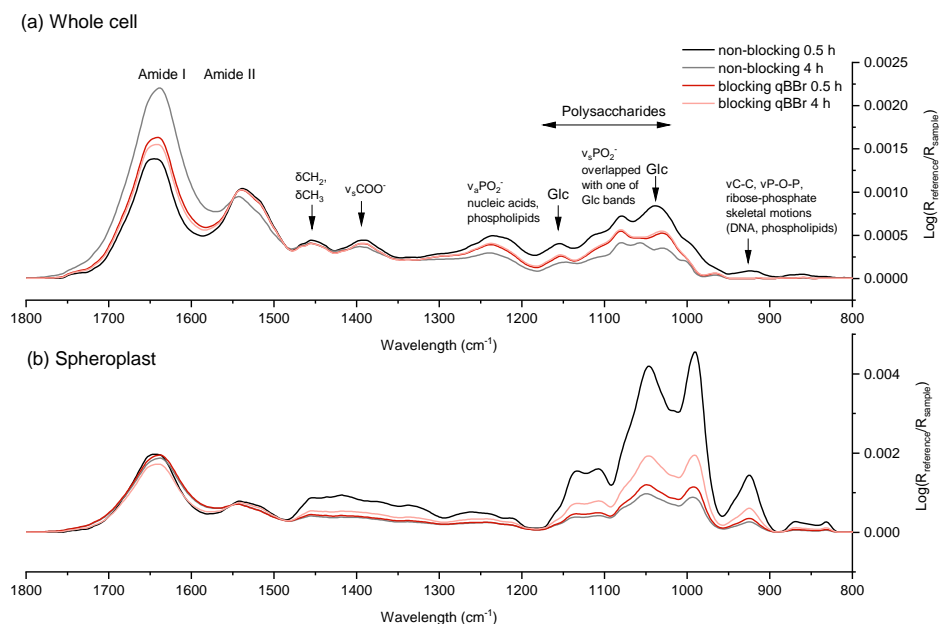


Figure 14: ATR-FTIR spectra of (a) whole cells and (b) spheroplasts with and without qBBr treatment after 0.5 and 4 h. Spectra were normalized to the amide II band at 1570-1515 cm^{-1} . Assignments of the different infrared bands are based on Quilès et al.²⁰¹ (Reproduced from Paper IV).

Concluding remarks: Interaction of Hg with the inner and outer membrane

Project III and IV investigated Hg interaction with the outer and inner membrane with the aim of describing the role of cell surface thiol functional groups on Hg(II) uptake, methylation and reduction.

The determination of the speciation by EXAFS and HERFD-XANES showed coherent results with two coordinated Hg-thiol structures at lower Hg exposure concentrations and with increasing Hg exposure concentrations less stable two coordinated Hg species with hydroxyl, carboxyl or amine functional groups were formed. The concentration of cell surface thiols on the outer and inner membrane were determined and showed a higher concentration for the latter. The distribution of Hg complexes with Mem_{ext}-R¹⁵S and Mem_{ext}-R¹⁷S varied between the two membranes with a higher amount and fraction of Hg(Mem_{ext}-R¹⁵S)₂ at the outer membrane. The blocking of cell surface thiol functionality groups did not impact the uptake, internalization and reduction of Hg(II). Whole cells showed an overall higher MeHg formation compared to spheroplasts and the formed MeHg remained cell-associated. Moreover, blocking of membrane surface thiols by qBBr altered the cell physiology as shown by changes in the biochemical composition. In addition, differences between Hg(II) reduction and methylation potential between whole cells and spheroplasts were observed. Paper III and IV showed the formation of either liquid or gaseous Hg(0), respectively. The outer membrane showed a higher Hg(II) reduction potential compared to the inner membrane and Hg(0) formation was independent of membrane surface thiols. A fraction of cell-associated Hg(0) was purgeable and suggested that liquid Hg(0) might be volatilize into gaseous Hg(0).

Conclusion

The formation of MeHg in the environment by *G. sulfurreducens* and other methylating organisms is dependent on biological, chemical and physical parameters as illustrated in Figure 2.^{2, 40} To detangle and to define the contribution of a single parameter and combination of parameters is challenging and requires a deep understanding of the biogeochemical processes of Hg. It is crucial to identify the key parameters to further predict rates of Hg transformation processes (Figure 1).^{2, 40, 41} This thesis emphasized the complex interplay of chemical and biological parameters and their impact on Hg(II) methylation by the model organisms *G. sulfurreducens*. The aim of the thesis was to unravel the importance of thiol compounds on Hg(II) speciation, uptake and transformation by this microorganism.

In the first part the role of dissolved LMM-thiols was investigated (Paper I and II). Overall, dissolved LMM-thiols showed a dynamic pattern during growth of *G. sulfurreducens* and in Hg(II) methylation assays (Figure 8 and 9). The composition of the growth medium with respect to Fe(II) was a driving factor for the formation and excretion of LMM-thiols, especially the small LMM-thiol cysteine showed, under iron depleted conditions, enhanced extracellular concentrations (Figure 8). In Paper I, we also showed the di-methylation of cysteine to penicillamine by *G. sulfurreducens* (Figure 9). Hg(II) methylation assays under altering nutrient concentrations showed that the formation and turnover of LMM-thiols was impacted by the assay composition and higher nutrient load led to a faster turnover of cysteine to penicillamine (Figure 9). The turnover was further amplified by the addition of exogenous cysteine. The formation and turnover of LMM-thiols were impacting the Hg(II) speciation in the extracellular media in Hg(II) methylation assays (Figure 10). Critical for the MeHg formation was the relative composition of Hg(Cys)₂ and Hg(PEN)₂ complexes, due to differences in the Hg(II) methylation rate constants with lower rates for Hg(PEN)₂ complexes.⁵² Overall, Hg(II) methylation was driven by LMM-thiols via (i) their impact on the Hg(II) speciation and (ii) the partitioning of Hg between the cell-associated and dissolved phase. In addition, Hg(II) methylation potential was affected by the cell physiology due to a higher metabolic activity in assays with higher nutrient concentrations (Figure 10 and 11). Both the Hg(II) speciation and cell physiology were driving parameters for Hg(II) methylation, however these two parameters were not additive. The results from Paper I and II showed the dynamic LMM-thiol metabolism, which is impacted by nutrient availability, and subsequently affected by the Hg(II) speciation and partitioning between the dissolved and cell-associated phase. The results of Paper I and II highlighted the importance of monitoring the fate of LMM-thiols in Hg(II) methylation experiments. Especially, the composition of individual LMM-thiol compounds was crucial for the Hg(II) methylation potential, due to differences in k_{meth} for small and branched Hg(RS)₂ complexes.⁵³ The results from Paper I and II suggest a critical interplay of LMM-thiol metabolism and Hg transformation in more complex environmental systems, i.e. natural biofilms. These environments show an overall high Hg(II) methylation potential, where the availability of nutrients and metabolites is constantly fluctuating.^{135, 137, 224}

The second part of this thesis focused on surface thiol on the outer and inner membrane (Paper III and IV). In Paper III, the Hg speciation was probed on the outer and inner membrane by EXAFS and HERFD-XANES and showed coherent results for these two methods (Figure 12). The speciation of Hg(II) with the outer and inner membrane was described by two coordinated Hg-thiol complexes $\text{Hg}(\text{Mem-RS})_2/(\text{Hg}(\text{Cys})_2$ complexes at lower Hg addition and the speciation shifted towards $\text{Hg}(\text{Mem-RO/N})_2/\text{Hg}(\text{acetate})_2$ with increasing Hg concentrations. This shift followed the thermodynamic stability of these complexes, where the functional groups forming the most stable complexes are saturated first.^{126, 155, 225} In addition, the concentrations of the outer and inner membrane were determined and showed a six times higher concentration of thiols on the inner membrane compared to the outer membrane (745 compared to 120 $\mu\text{mol g}^{-1}$ dry mass, Table 2). Overall, the determined thiol concentrations were in the same range as in previous studies on cell membrane fragments and whole cells of *G. sulfurreducens*.^{152, 154, 155} Outer membrane thiols were dominantly involved in two coordinated $\text{Hg}(\text{Mem}_{\text{ext-R}}\text{S})_2$ structures, whereas only a minor part of thiols in the inner membrane formed these complexes. Since $\text{Hg}(\text{Mem}_{\text{ext-R}}\text{S})_2$ complexes are much more stable compared to $\text{Hg}(\text{Mem}_{\text{ext-R}}\text{S})(\text{Mem}_{\text{ext-RO/N}})$ complexes,¹⁵⁵ this result suggested that Hg adsorption on the outer membrane is a Hg sink and less is available for uptake.^{54, 58, 60, 61}

Further, *G. sulfurreducens* is capable of Hg(II) reduction. We showed the formation of liquid Hg(0) on the outer and inner membrane by EXAFS and HERFD-XANES (Figure 12). In addition, the reduction of Hg(II) to gaseous Hg(0) was investigated and could be verified in whole cells and spheroplasts (Figure 13). The formation of gaseous Hg(0) was ascribed to membrane cytochromes.^{57, 60} In this work, the mechanism for the liquid Hg(0) formation were not identified and was hypothesized to be alike to gaseous Hg(0) formation. The linkage between gaseous and liquid Hg(0) may be important for the understanding of the global biogeochemical cycling of Hg, especially if the formation of liquid Hg(0) impacts the gaseous Hg(0) pool and if they are exchangeable. We showed in Paper IV that cell-adsorbed Hg(0) was purgeable, however to what extent was not determined.

Partition of Hg between the dissolved, cell-adsorbed, and intracellular phase was not impacted by blocking selectively surface thiols on the outer and inner membrane by qBBr (Figure 13). The blocking of outer membrane surface thiols decreased the formation of MeHg at longer incubation time. The biochemical composition of whole cells changed by blocking the outer membrane thiol groups, although cell growth was similar for both samples (Figure 14a). In contrast, no differences in MeHg formation were observed for spheroplast over time and the biochemical composition of spheroplasts did not alter with blocking or over time (Figure 13, Figure 14b). Overall, the combined results of blocked and non-blocked membrane surface thiols with respect to Hg partitioning, MeHg formation and cell physiology raised the crucial question if the blocking of membrane surface thiols was successful. The similar partitioning between blocked and non-blocked samples suggested that membrane surface thiols were partly derivatization with qBBr and qBBr inaccessible thiol groups were likely accessible for Hg(II). In a previous study it was discussed that the qBBr molecule may not block all membrane surface thiols, due to steric hindrance, and sites which are qBBr inaccessible may still potentially be accessible for Hg(II).¹⁸¹ The decreased formation of MeHg in blocked whole cell samples compared to

non-blocked, could be as well linked to changes in the cell physiology (Figure 14a). The overall low formation of MeHg in spheroplast samples proposed the importance of complexes between Hg(II) with dissolved LMM-thiols for Hg(II) internalization and subsequently methylation as shown in previous studies.⁵²⁻⁵⁴

The combined results of Paper I-IV showed the importance of dissolved and membrane surface thiol groups for Hg(II) speciation, uptake and transformation as illustrated in Figure 15. The formation, turnover and excretion of dissolved thiols is tightly coupled to the metabolisms of nutrients and essential trace metals (Paper I). This formation is important for the Hg(II) speciation in the dissolved phase and the partition between the dissolved and cell adsorbed phase in Hg(II) methylation assays (Paper II). In addition, cell physiology is crucial and a higher metabolic activity drives Hg(II) methylation and the turnover of LMM-thiols (Paper II). The characterization of the outer and inner membrane by EXAFS shows a higher thiol concentration on the inner membrane (Paper III). The distances of the outer membrane thiols are close enough to form dominantly two coordinated $\text{Hg}(\text{Mem}_{\text{ext}}\text{-R}^{\text{II}}\text{S})_2$ complexes, whereas the inner membrane dominantly formed $\text{Hg}(\text{Mem}_{\text{ext}}\text{-R}^{\text{I}}\text{S})(\text{Mem}_{\text{ext}}\text{-RO/N})$ complexes (Paper III). The outer and inner membrane thiols are hypothesized to play important roles for uptake, reduction, and methylation of Hg(II). The formation of liquid and gaseous Hg(0) is higher for whole cells and independent of membrane surface thiols (Paper III and IV). The partitioning between the different phases is not impacted by membrane surface thiol blocking (Paper IV). The formation of MeHg was highest for non-blocked whole cells (Paper IV). The blocking of membrane thiols with qBBr blocking changes the cell physiology and spheroplasts and whole cells show a different biochemical composition (Paper IV).

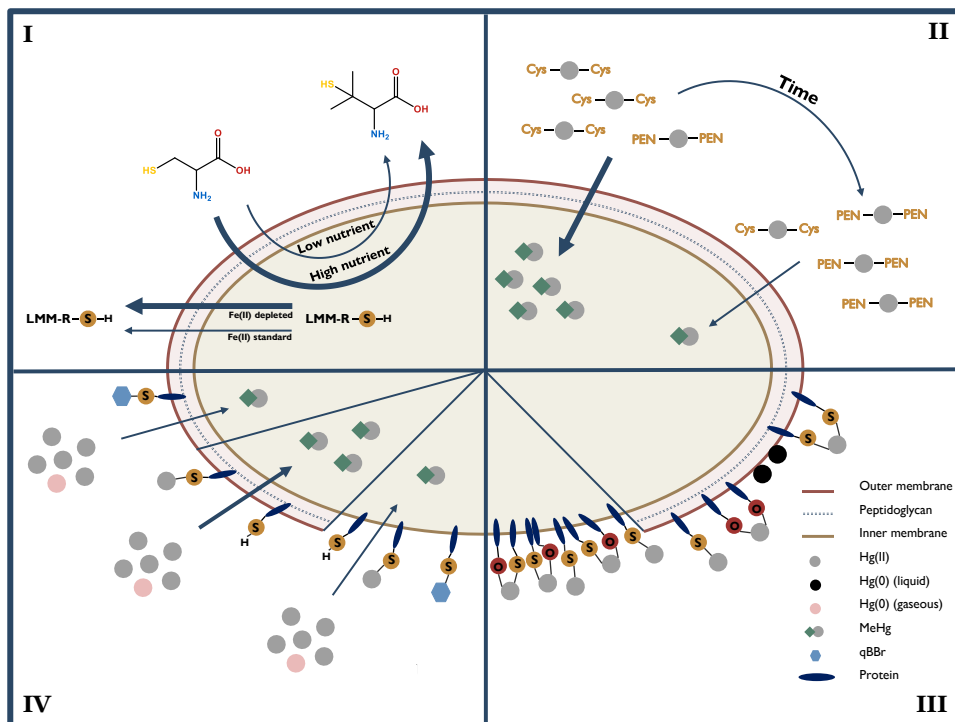


Figure 15: Illustration of the four thesis projects I – IV and their key findings. The focus of the different Papers are: (I) Turnover of thiol compounds under varying media composition, (II) The combined effect of Hg(II) speciation and physiology on MeHg formation, (III) Determination of the Hg speciation and membrane thiol concentration on the outer and inner membrane and (IV) the role of membrane thiols on Hg(II) uptake, methylation, and reduction.

Outlook

In this thesis, the transformation of Hg and the role of thiols by *G. sulfurreducens* was studied with new experimental approaches. This thesis showed the important role of dissolved and membrane surface thiols and highlighted the complexity and importance of the link between Hg and thiol compounds. The results form a basis on which knowledge gaps should be addressed in further research.

The dynamic turnover of LMM-thiols as investigated in Paper I and II emphasized the importance to monitor and measure LMM-thiols in laboratory experiments and in the environment to identify the speciation of Hg(II) with LMM-thiol compounds. Microenvironments, i.e. biofilms, contain enhanced concentration of LMM-thiols and are showing high Hg(II) methylation potential^{135, 137} and these biofilms are an important source of MeHg for macroinvertebrates.^{226, 227} Moreover, porewaters showed a similar relationship between LMM-thiols and methylation potential,¹³⁶ however the origin and metabolic turnover of LMM-thiols is unknown. The identification of the thiol composition is important for the prediction of Hg(II) availability and Hg(II) methylation potential, since specific thiol compounds promote Hg(II) uptake and methylation.^{51, 52, 62, 63, 120} To further understand the turnover and formation of LMM-thiols, e.g. of cysteine to penicillamine, the up- and/or downregulation of genes involved in thiol metabolism could give insight on a molecular level.

In addition, the microbial composition and the metabolic activity of microorganisms are central parameters.^{75-78, 150} However, a variety of Hg(II) methylating microorganisms are identified in various environmental niches.^{43, 44} Especially, sulfate-reducing microorganisms are key methylators. The relevance of LMM-thiol compounds in sulfidic environments for sulfate-reducing microorganisms is uncertain, especially when thiol concentrations are comparable to or exceeding sulfide concentrations and compete for Hg as a ligand. In addition, the flux and availability of nutrients is a varying factor within the biofilm²²⁸⁻²³⁰ and subsequently likely impact the metabolic activity and Hg(II) methylation potential. In a next step, mixed organism studies should be a major focus and to thereby investigate the thiol turnover, nutrient fluxes and their impact on metabolic activity to further predict Hg(II) methylation in microenvironments with a high methylation potential and nutrient flux.

The formation of liquid Hg(o) as shown in Paper III raised the question whether liquid Hg(o) formation is based on the same mechanism as gaseous Hg(o) formation. It is the second study showing liquid Hg(o) formation by bacteria.¹⁶² It is important to understand if there is a relationship between the formation of gaseous Hg(o) and liquid Hg(o). Gaseous Hg(o) is commonly determined as the purgeable Hg fraction.^{57, 60} However, it is not known if liquid Hg(o) adsorbed on membranes is part of the purgeable fraction. In case liquid Hg(o) is not purgeable the reduction potential of *G. sulfurreducens* was previously underestimated. In a broader perspective, it is unknown to what extent liquid Hg(o) is formed in environments with high Hg transformation potential, i.e. sediment, soil or biofilms. Volatilization of liquid Hg(o) to gaseous Hg(o) is observed in contaminated sites with liquid Hg(o) spills,²³¹ but studies on uncontaminated sites have focused mainly

on gaseous Hg(o) formation.^{232, 233} However, it raises the question if the liquid and gaseous Hg(o) are exchangeable and if liquid Hg(o) therefore can be a source of gaseous Hg(o) to the atmosphere also in environments not contaminated by local liquid Hg(o) sources.

The determination of the outer and inner membrane surface thiol concentrations in Paper III showed higher thiol concentration on the inner membrane, whereas on the outer membrane the distance of the thiol functional groups was closer to form dominantly Hg(Mem_{ext}-R^{II}S)₂ complexes. The role of outer and inner thiol compounds for the cellular uptake of Hg(II) was not fully identified. However, it raises the question if the thiol concentration plays a key role in the Hg(II) uptake mechanism and if it is further impacted by the coordination environment. Ligand exchange reactions with the membrane are considered crucial steps for the Hg(II) uptake across the outer and inner membrane.^{54, 140, 152, 156} Especially, previous studies showed higher uptake rates across the inner membrane compared to the outer membrane.⁵³ On the inner membrane, fewer stable complexes, Hg(Mem_{ext}-R^IS)(Mem_{ext}-RO/N), may be dominant under kinetically constrained conditions, and these complexes might be kinetically preferred for uptake. In addition, it is not identified if Hg is complexed as Hg(Mem_{ext}-R^{II}S)₂ on the outer membrane during Hg(II) uptake, since thiols and DOM in the extracellular media are competing for Hg. In Paper IV we attempted to resolve the role of the outer and inner membrane thiols for Hg(II) uptake and transformation. However, this study raised additional questions about whether the experimental strategy was successful. Selectively blocking of membrane thiol compounds with qBBr likely partly blocked membrane thiol groups and qBBr could only block specific surface thiols sites,¹⁸¹ and due to the size differences between qBBr and Hg(II), the qBBr inaccessible sides are in turn accessible for Hg(II). This knowledge gap could be further investigated with additional EXAFS study by determining the Hg speciation and coordination environment of Hg of qBBr blocked and non-blocked *G. sulfurreducens* cells.

Acknowledgement

First, I would like to thank my main supervisor Erik Björn for the great journey of mercury research during the past years at Umeå University! Thanks a lot for all the guidance and discussion, never being worried about time and always seeing “bad” results positive!

Second, I am thankful to have Ulf Skyllberg as a second supervisor at SLU Umeå. Your extreme drive and knowledge of synchrotron measurement is remarkable!! Thanks for sharing all the knowledge and helping me with the synchrotron project!

Third, I am grateful to have Jeffra Schaefer on the other side of the Atlantic as a third supervisor. It was a pleasure for me to visit you at Rutgers University and I am pleased with all these great insides on the microbiology part.

I would like to thank Malin Linder Nording and Madeline Ramstedt for their support in my yearly evaluation and all the important advice over the years!

Thanks to all current and former members of the mercury research group at Umeå University and SLU Umeå and I enjoyed all the great shuffleboard competition with you guys. Thanks as well to the internship boys from Münster University!

I am very grateful for the collaboration with Morgane Desmau. It was a pleasure for me to work together on the synchrotron project in Grenoble and Hamburg. Additionally, thanks to Olivier Proux for the support at the ESRF to make the beamtimes smooth and successful.

Thanks to my wonderful family back in Tübingen and for all the support during the last 30 years! And maybe I only finished this chapter to win the 16-year-old bet! I am looking forward to my cruise!

Thanks to my old friends aus´m Ländle for the great friendship: Sophie, Lisa, Muri, Teresa and Verena.

Thanks to Franzl and Maria for an amazing time in Leipzig and all the great skype discussion across Germany-UK-Sweden!

Thanks to Corinna and Hannah for an extremely enjoyable time in Oldenburg and the Blödit will never die!

And all of you, back in Germany, would never imagine that I will work in this particular peculiar language and that I stayed and survived some month in the country of my language enemies!

Thanks to all the great friends in Umeå and making this time in the country of reindeer wonderful: Thilde, Ioana, Isabel, Maria, Sofie, Fredrik, Linda, James, Måns, Mary, Elin & Valentin.

And my biggest thank you is to Mason. Without all your encouraging words, your amazing cooking skills and our wonderful outdoor adventures, I would have never finished this chapter!♥

References

1. Du Bray, E.A., *Preliminary compilation of descriptive geoenvironmental mineral deposit models*. 1995: US Geological Survey Denver, CO.
2. Bravo, A.G.;Cosio, C., *Biotic formation of methylmercury: A bio-physico-chemical conundrum*. *Limnol. Oceanogr.*, 2019. **65**(5): p. 1010-1027.
3. Jun, S.;Si, F.;Pugatch, R.;Scott, M., *Fundamental principles in bacterial physiology-history, recent progress, and the future with focus on cell size control: a review*. Reports on progress in physics. Physical Society (Great Britain), 2018. **81**(5): p. 056601.
4. Friedman, M., *The chemistry and biochemistry of the sulfhydryl group in amino acids, peptides and proteins*. 1973, Oxford: Pergamon Press.
5. Macielag, M.J., *Chemical Properties of Antimicrobials and Their Uniqueness*, in *Antibiotic Discovery and Development*, T.J. Dougherty;M.J. Pucci, Editors. 2012, Springer US: Boston, MA. p. 793-820.
6. Huxtable, R.J., *Thiols, Disulfides, and Thioesters*, in *Biochemistry of Sulfur*, R.J. Huxtable, Editor. 1986, Springer US: Boston, MA. p. 199-268.
7. OxfordEnglishDictionary, "*metabolite, n.*". Oxford University Press.
8. Templeton, D.M.;Fujishiro, H., *Terminology of elemental speciation – An IUPAC perspective*. *Coordination Chemistry Reviews*, 2017. **352**: p. 424-431.
9. WHO. *The 10 chemicals of major public health concerns*. [cited 2023 April 11]; Available from: <https://www.who.int/teams/environment-climate-change-and-health/chemical-safety-and-health/health-impacts/chemicals>.
10. Nies, D.H., *Efflux-mediated heavy metal resistance in prokaryotes*. *FEMS Microbiology Reviews*, 2003. **27**(2-3): p. 313-339.
11. Clarkson, T.W.;Magos, L., *The toxicology of mercury and its chemical compounds*. *Critical Reviews in Toxicology*, 2006. **36**(8): p. 609-62.
12. Zhang, H.;Feng, X.;Larssen, T.;Qiu, G.;Vogt, R.D., *In inland China, rice, rather than fish, is the major pathway for methylmercury exposure*. *Environ Health Perspect*, 2010. **118**(9): p. 1183-1188.
13. Sheehan, M.C.;Burke, T.A.;Navas-Acien, A.;Breyse, P.N.;McGready, J.;Fox, M.A., *Global methylmercury exposure from seafood consumption and risk of developmental neurotoxicity: a systematic review*. *Bulletin of the World Health Organization*, 2014. **92**(4): p. 254-269f.
14. Driscoll, C.T.;Mason, R.P.;Chan, H.M.;Jacob, D.J.;Pirrone, N., *Mercury as a global pollutant: sources, pathways, and effects*. *Environmental Science & Technology*, 2013. **47**(10): p. 4967-83.
15. Obrist, D.;Kirk, J.L.;Zhang, L.;Sunderland, E.M.;Jiskra, M.;Selin, N.E., *A review of global environmental mercury processes in response to human and natural perturbations: Changes of emissions, climate, and land use*. *Ambio*, 2018. **47**(2): p. 116-140.
16. UNEP, *Global mercury assesment 2018*. UN Environment Programme, Chemicals and Health Branch Geneva, Switzerland, 2019.
17. Pilson, M.E.Q., *An Introduction to the Chemistry of the Sea*. 2 ed. 2012, Cambridge: Cambridge University Press.
18. Mason, R.P.;Sheu, G.R., *Role of the ocean in the global mercury cycle*. *Global Biogeochemical Cycles*, 2002. **16**(4): p. 40-1-40-14.

19. Harada, M., *Minamata disease: methylmercury poisoning in Japan caused by environmental pollution*. Crit Rev Toxicol, 1995. **25**(1): p. 1-24.
20. Lindqvist, O.;Johansson, K.;Bringmark, L.;Timm, B.;Aastrup, M.;Andersson, A.;Hovsenius, G.;Håkanson, L.;Iverfeldt, Å.;Meili, M., *Mercury in the Swedish environment – Recent research on causes, consequences and corrective methods*. Water, Air, and Soil Pollution, 1991. **55**(1): p. xi-261.
21. Huisingsh, D., *Heavy Metals: Implications for Agriculture*. Annual Review of Phytopathology, 1974. **12**(1): p. 375-388.
22. Kurland, L.T.;Faro, S.N.;Siedler, H., *Minamata disease. The outbreak of a neurologic disorder in Minamata, Japan, and its relationship to the ingestion of seafood contaminated by mercuric compounds*. World Neurol, 1960. **1**: p. 370-395.
23. Abelson, P.H., *Methyl Mercury*. Science, 1970. **169**(3942): p. 237-237.
24. Saha, J.G.;McKinlay, K.S., *Use of mercury in agriculture and its relationship to environmental pollution*. Toxicological & Environmental Chemistry Reviews, 1973. **1**(4): p. 271-290.
25. Kimura, Y.;Miller, V., *Fungicide decomposition, degradation of organomercury fungicides in soil*. Journal of Agricultural and Food Chemistry, 1964. **12**(3): p. 253-257.
26. Booer, J.R., *THE ACTION OF MERCURY AS A SOIL FUNGICIDE*. Annals of Applied Biology, 1951. **38**(2): p. 334-347.
27. Selin, H.;Selin, N.E., *Mercury stories : understanding sustainability through a volatile element*. 2020, Cambridge, Massachusetts: The MIT Press.
28. SwedishChemicalAgency. *Swedish regulations on mercury and articles containing mercury*. [cited 2023 April 22]; Available from: <https://www.kemi.se/en/rules-and-regulations/rules-applicable-in-sweden-only/certain-swedish-restrictions-and-bans/mercury-and-articles-containing-mercury>.
29. UNEP. *Minimata convention on mercury*. [cited 2023 April 11]; Available from: <https://mercuryconvention.org/en/parties>.
30. Liu, G.;Cai, Y.;O'Driscoll, N.;Feng, X.;Jiang, G., *Overview of Mercury in the Environment*, in *Environmental Chemistry and Toxicology of Mercury*, G. Liu;Y. Cai;N. O´ Driscoll, Editors. 2011, John Wiley & Sons, Ltd. p. 1-12.
31. Skyllberg, U., *Chemical Speciation of Mercury in Soil and Sediment*, in *Environmental Chemistry and Toxicology of Mercury*, G. Liu;Y. Cai;N. O´ Driscoll, Editors. 2011, John Wiley & Sons, Ltd. p. 219-258.
32. Fitzgerald, W.F.;Clarkson, T.W., *Mercury and Monomethylmercury: Present and Future Concerns*. Environ Health Perspect, 1991. **96**: p. 159-166.
33. Barkay, T.;Turner, R.;Saouter, E.;Horn, J., *Mercury biotransformations and their potential for remediation of mercury contamination*. Biodegradation, 1992. **3**(2): p. 147-159.
34. Watras, C.J.;Back, R.C.;Halvorsen, S.;Hudson, R.J.;Morrison, K.A.;Wente, S.P., *Bioaccumulation of mercury in pelagic freshwater food webs*. Science of The Total Environment, 1998. **219**(2-3): p. 183-208.
35. Gosnell, K.J.;Mason, R.P., *Mercury and methylmercury incidence and bioaccumulation in plankton from the central Pacific Ocean*. Marine Chemistry, 2015. **177**: p. 772-780.
36. Moye, H.A.;Miles, C.J.;Phlips, E.J.;Sargent, B.;Merritt, K.K., *Kinetics and Uptake Mechanisms for Monomethylmercury between Freshwater Algae and Water*. Environmental Science & Technology, 2002. **36**(16): p. 3550-3555.

37. Reinfelder, J.R.;Fisher, N.S., *The Assimilation of Elements Ingested by Marine Copepods*. Science, 1991. **251**(4995): p. 794-796.
38. Watras, C.J.;Bloom, N.S., *Mercury and methylmercury, in individual zooplankton: Implications for bioaccumulation*. Limnol. Oceanogr., 1992. **37**(6): p. 1313-1318.
39. Weber, J.H., *Review of possible paths for abiotic methylation of mercury(II) in the aquatic environment*. Chemosphere, 1993. **26**(11): p. 2063-2077.
40. Regnell, O.;Watras, C.J., *Microbial Mercury Methylation in Aquatic Environments: A Critical Review of Published Field and Laboratory Studies*. Environmental Science & Technology, 2019. **53**(1): p. 4-19.
41. Hsu-Kim, H.;Kucharzyk, K.H.;Zhang, T.;Deshusses, M.A., *Mechanisms Regulating Mercury Bioavailability for Methylating Microorganisms in the Aquatic Environment: A Critical Review*. Environmental Science & Technology, 2013. **47**(6): p. 2441-2456.
42. Jensen, S.;Järnelöv, A., *Biological Methylation of Mercury in Aquatic Organisms*. Nature, 1969. **223**: p. 753-754.
43. Gilmour, C.C.;Podar, M.;Bullock, A.L.;Graham, A.M.;Brown, S.D.;Somenahally, A.C.;Johs, A.;Hurt, R.A., Jr.;Bailey, K.L.;Elias, D.A., *Mercury methylation by novel microorganisms from new environments*. Environmental Science & Technology, 2013. **47**(20): p. 11810-20.
44. Podar, M.;Gilmour, C.C.;Brandt, C.C.;Soren, A.;Brown, S.D.;Cralbo, B.R.;Palumbo, A.V.;Somenahally, A.C.;Elias, D.A., *Global prevalence and distribution of genes and microorganisms involved in mercury methylation*. Advances Science, 2015.
45. Gilmour, C.C.;Elias, D.A.;Kucken, A.M.;Brown, S.D.;Palumbo, A.V.;Schadt, C.W.;Wall, J.D., *Sulfate-Reducing Bacterium *Desulfovibrio desulfuricans* ND132 as a Model for Understanding Bacterial Mercury Methylation*. Appl. Environ. Microbiol., 2011. **77**(12): p. 3938-3951.
46. Gilmour, C.C.;Soren, A.B.;Gionfriddo, C.M.;Podar, M.;Wall, J.D.;Brown, S.D.;Michener, J.K.;Urriza, M.S.G.;Elias, D.A., *Pseudodesulfovibrio mercurii sp. nov., a mercury-methylating bacterium isolated from sediment*. International journal of systematic and evolutionary microbiology, 2021. **71**(3).
47. Graham, A.M.;Aiken, G.R.;Gilmour, C.C., *Dissolved Organic Matter Enhances Microbial Mercury Methylation Under Sulfidic Conditions*. Environmental Science & Technology, 2012. **46**(5): p. 2715-2723.
48. Graham, A.M.;Aiken, G.R.;Gilmour, C.C., *Effect of dissolved organic matter source and character on microbial Hg methylation in Hg-S-DOM solutions*. Environ Sci Technol, 2013. **47**(11): p. 5746-54.
49. Graham, A.M.;Bullock, A.L.;Maizel, A.C.;Elias, D.A.;Gilmour, C.C., *Detailed Assessment of the Kinetics of Hg-Cell Association, Hg Methylation, and Methylmercury Degradation in Several *Desulfovibrio* Species*. Appl. Environ. Microbiol., 2012. **78**(20): p. 7337-7346.
50. Janssen, S.E.;Schaefer, J.K.;Barkay, T.;Reinfelder, J.R., *Fractionation of Mercury Stable Isotopes during Microbial Methylmercury Production by Iron- and Sulfate-Reducing Bacteria*. Environmental Science & Technology, 2016. **50**(15): p. 8077-8083.
51. Schaefer, J.K.;Morel, F.M.M., *High methylation rates of mercury bound to cysteine by *Geobacter sulfurreducens**. Nat. Geosci., 2009. **2**(2): p. 123-126.
52. Schaefer, J.K.;Rocks, S.S.;Zheng, W.;Liang, L.Y.;Gu, B.H.;Morel, F.M.M., *Active transport, substrate specificity, and methylation of Hg(II) in anaerobic bacteria*. Proc. Natl. Acad. Sci. U. S. A., 2011. **108**(21): p. 8714-8719.

53. Schaefer, J.K.;Szczyka, A.;Morel, F.M.M., *Effect of Divalent Metals on Hg(II) Uptake and Methylation by Bacteria*. Environmental Science & Technology, 2014. **48**(5): p. 3007-3013.
54. Wang, Y.;Janssen, S.E.;Schaefer, J.K.;Yee, N.;Reinfelder, J.R., *Tracing the Uptake of Hg(II) in an Iron-Reducing Bacterium Using Mercury Stable Isotopes*. Environmental Science & Technology Letters, 2020. **7**(8): p. 573-578.
55. Wang, Y.W.;Schaefer, J.K.;Mishra, B.;Yee, N., *Intracellular Hg(0) Oxidation in Desulfovibrio desulfuricans ND132*. Environmental Science & Technology, 2016. **50**(20): p. 11049-11056.
56. An, J.;Zhang, L.;Lu, X.;Pelletier, D.A.;Pierce, E.M.;Johs, A.;Parks, J.M.;Gu, B., *Mercury Uptake by Desulfovibrio desulfuricans ND132: Passive or Active?* Environmental Science & Technology, 2019. **53**(11): p. 6264-6272.
57. Hu, H.;Lin, H.;Zheng, W.;Rao, B.;Feng, X.;Liang, L.;Elias, D.A.;Gu, B., *Mercury reduction and cell-surface adsorption by Geobacter sulfurreducens PCA*. Environmental Science & Technology, 2013. **47**(19): p. 10922-30.
58. Lin, H.;Lu, X.;Liang, L.;Gu, B., *Thiol-Facilitated Cell Export and Desorption of Methylmercury by Anaerobic Bacteria*. Environmental Science & Technology Letters, 2015. **2**(10): p. 292-296.
59. Lin, H.;Lu, X.;Liang, L.;Gu, B., *Cysteine Inhibits Mercury Methylation by Geobacter sulfurreducens PCA Mutant ΔomcBESTZ*. Environmental Science & Technology Letters, 2015. **2**(5): p. 144-148.
60. Lin, H.;Morrell-Falvey, J.L.;Rao, B.;Liang, L.;Gu, B., *Coupled Mercury–Cell Sorption, Reduction, and Oxidation on Methylmercury Production by Geobacter sulfurreducens PCA*. Environmental Science & Technology, 2014. **48**(20): p. 11969-11976.
61. Liu, Y.R.;Lu, X.;Zhao, L.;An, J.;He, J.Z.;Pierce, E.M.;Johs, A.;Gu, B., *Effects of Cellular Sorption on Mercury Bioavailability and Methylmercury Production by Desulfovibrio desulfuricans ND132*. Environmental Science & Technology, 2016. **50**(24): p. 13335-13341.
62. Yin, X.;Wang, L.;Liang, X.;Zhang, L.;Zhao, J.;Gu, B., *Contrary effects of phytoplankton Chlorella vulgaris and its exudates on mercury methylation by iron- and sulfate-reducing bacteria*. Journal of Hazardous Materials, 2022. **433**: p. 128835.
63. Zhao, L.;Chen, H.;Lu, X.;Lin, H.;Christensen, G.A.;Pierce, E.M.;Gu, B., *Contrasting Effects of Dissolved Organic Matter on Mercury Methylation by Geobacter sulfurreducens PCA and Desulfovibrio desulfuricans ND132*. Environmental Science & Technology, 2017. **51**(18): p. 10468-10475.
64. Zhao, Q.;Wang, J.;OuYang, S.;Chen, L.;Liu, M.;Li, Y.;Jiang, F., *The exacerbation of mercury methylation by Geobacter sulfurreducens PCA in a freshwater algae-bacteria symbiotic system throughout the lifetime of algae*. Journal of Hazardous Materials, 2021. **415**: p. 125691.
65. Wood, J.M.;Kennedy, F.S.;Rosen, C.G., *Synthesis of methyl-mercury compounds by extracts of a methanogenic bacterium*. Nature, 1968. **220**(5163): p. 173-4.
66. Choi, A.L.;Chase, T.;Bartha, R., *Metabolic Pathways Leading to Mercury Methylation in Desulfovibrio desulfuricans LS*. Appl. Environ. Microbiol., 1994. **60**(11): p. 4072-407.
67. Choi, S.-C.;Chase, T.J.;Bartha, R., *Enzymatic Catalysis of Mercury Methylation by Desulfovibrio desulfuricans LS*. Appl Environ Microbiol, 1994. **60**(4): p. 1342-1346.

68. Berman, M.;Chase, T.;Bartha, R., *CARBON FLOW IN MERCURY BIOMETHYLATION BY DESULFOVIBRIO-DESULFURICANS*. Appl. Environ. Microbiol., 1990. **56**(1): p. 298-300.
69. Choi, S.C.;Bartha, R., *Cobalamin-mediated mercury methylation by Desulfovibrio desulfuricans LS*. Appl Environ Microbiol, 1993. **59**(1): p. 290-5.
70. Ekstrom, E.B.;Morel, F.M.M., *Cobalt limitation of growth and mercury methylation in sulfate-reducing bacteria*. Environmental science & technology, 2008. **42** **1**: p. 93-9.
71. Parks, J.M.;Johs, A.;Podar, M.;Bridou, R.;Hurt, R.A.;Smith, S.D.;Tomanicek, S.J.;Qian, Y.;Brown, S.D.;Brandt, C.C.;Palumbo, A.V.;Smith, J.C.;Wall, J.D.;Elias, D.A.;Liang, L.Y., *The Genetic Basis for Bacterial Mercury Methylation*. Science, 2013. **339**(6125): p. 1332-1335.
72. Date, S.S.;Parks, J.M.;Rush, K.W.;Wall, J.D.;Ragsdale, S.W.;Johs, A., *Kinetics of Enzymatic Mercury Methylation at Nanomolar Concentrations Catalyzed by HgcAB*. Appl Environ Microbiol, 2019. **85**(13).
73. Villar, E.;Cabrol, L.;Heimbürger-Boavida, L.-E., *Widespread microbial mercury methylation genes in the global ocean*. Environmental Microbiology Reports, 2020. **12**(3): p. 277-287.
74. Gallorini, A.;Loizeau, J.-L., *Lake snow as a mercury methylation micro-environment in the oxic water column of a deep peri-alpine lake*. Chemosphere, 2022. **299**: p. 134306.
75. Goni-Urriza, M.;Corsellis, Y.;Lanceleur, L.;Tessier, E.;Gury, J.;Monperrus, M.;Guyoneaud, R., *Relationships between bacterial energetic metabolism, mercury methylation potential, and hgcA/hgcB gene expression in Desulfovibrio dechloroacetivorans BerOci*. Environ. Sci. Pollut. Res., 2015. **22**(18): p. 13764-13771.
76. Bravo, A.G.;Kothawala, D.N.;Attermeyer, K.;Tessier, E.;Bodmer, P.;Ledesma, J.L.J.;Audet, J.;Casas-Ruiz, J.P.;Catalan, N.;Cauvy-Fraunie, S.;Colls, M.;Deininger, A.;Evtimova, V.V.;Fonvielle, J.A.;Fuss, T.;Gilbert, P.;Herrero Ortega, S.;Liu, L.;Mendoza-Lera, C.;Monteiro, J.;Mor, J.R.;Nagler, M.;Niedrist, G.H.;Nydahl, A.C.;Pastor, A.;Pegg, J.;Gutmann Roberts, C.;Pilotto, F.;Portela, A.P.;Gonzalez-Quijano, C.R.;Romero, F.;Rulik, M.;Amouroux, D., *The interplay between total mercury, methylmercury and dissolved organic matter in fluvial systems: A latitudinal study across Europe*. Water Res, 2018. **144**: p. 172-182.
77. Kucharzyk, K.H.;Deshusses, M.A.;Porter, K.A.;Hsu-Kim, H., *Relative contributions of mercury bioavailability and microbial growth rate on net methylmercury production by anaerobic mixed cultures*. Environmental Science: Processes & Impacts, 2015. **17**(9): p. 1568-1577.
78. Xu, J.;Liem-Nguyen, V.;Buck, M.;Bertilsson, S.;Björn, E.;Bravo, A.G., *Mercury Methylating Microbial Community Structure in Boreal Wetlands Explained by Local Physicochemical Conditions*. Frontiers in Environmental Science, 2021. **8**:518662.
79. Celo, V.;Lean, D.R.;Scott, S.L., *Abiotic methylation of mercury in the aquatic environment*. Sci Total Environ, 2006. **368**(1): p. 126-37.
80. Munson, K.M.;Lamborg, C.H.;Boiteau, R.M.;Saito, M.A., *Dynamic mercury methylation and demethylation in oligotrophic marine water*. Biogeosciences, 2018. **15**(21): p. 6451-6460.
81. Barkay, T.;Miller, S.M.;Summers, A.O., *Bacterial mercury resistance from atoms to ecosystems*. FEMS Microbiology Reviews, 2003. **27**(2-3): p. 355-384.

82. Boyd, E.S.;Barkay, T., *The mercury resistance operon: from an origin in a geothermal environment to an efficient detoxification machine*. Front Microbiol, 2012. **3**: p. 349.
83. Osborn, A.M.;Bruce, K.D.;Strike, P.;Ritchie, D.A., *Distribution, diversity and evolution of the bacterial mercury resistance (mer) operon*. FEMS Microbiology Reviews, 1997. **19**(4): p. 239-262.
84. Lin, C.-C.;Yee, N.;Barkay, T., *Microbial Transformations in the Mercury Cycle*, in *Environmental Chemistry and Toxicology of Mercury*, G. Liu;Y. Cai;N. O' Driscoll, Editors. 2011, John Wiley & Sons, Ltd. p. 155-191.
85. Oremland Ronald, S.;Culbertson Charles, W.;Winfrey Michael, R., *Methylmercury Decomposition in Sediments and Bacterial Cultures: Involvement of Methanogens and Sulfate Reducers in Oxidative Demethylation*. Appl. Environ. Microbiol., 1991. **57**(1): p. 130-137.
86. Seller, P.;Kelly, C.A.;Rudd, J.W.M.;MacHutchon, A.R., *Photodegradation of methylmercury in lakes*. Nature, 1996. **380**(6576): p. 694-697.
87. Suda, I.;Suda, M.;Hirayama, K., *Degradation of methyl and ethyl mercury by singlet oxygen generated from sea water exposed to sunlight or ultraviolet light*. Archives of Toxicology, 1993. **67**(5): p. 365-368.
88. Poulain, A.J.;SM, N.C.;Ariya, P.A.;Amyot, M.;Garcia, E.;Campbell, P.G.;Zylstra, G.J.;Barkay, T., *Potential for mercury reduction by microbes in the high arctic*. Appl Environ Microbiol, 2007. **73**(7): p. 2230-8.
89. Siciliano, S.D.;O'Driscoll, N.J.;Lean, D.R., *Microbial reduction and oxidation of mercury in freshwater lakes*. Environ Sci Technol, 2002. **36**(14): p. 3064-8.
90. Nazaret, S.;Jeffrey, W.H.;Saouter, E.;Von Haven, R.;Barkay, T., *merA gene expression in aquatic environments measured by mRNA production and Hg(II) volatilization*. Appl Environ Microbiol, 1994. **60**(11): p. 4059-65.
91. Liang, X.;Zhu, N.;Johs, A.;Chen, H.;Pelletier, D.A.;Zhang, L.;Yin, X.;Gao, Y.;Zhao, J.;Gu, B., *Mercury Reduction, Uptake, and Species Transformation by Freshwater Alga Chlorella vulgaris under Sunlit and Dark Conditions*. Environ Sci Technol, 2022. **56**(8): p. 4961-4969.
92. Ben-Bassat, D.;Mayer, A.M., *Light-Induced Hg Volatilization and O₂ Evolution in Chlorella and the Effect of DCMU and Methylamine*. Physiologia Plantarum, 1978. **42**(1): p. 33-38.
93. Devars, S.;Avilés, C.;Cervantes, C.;Moreno-Sánchez, R., *Mercury uptake and removal by Euglena gracilis*. Arch Microbiol, 2000. **174**(3): p. 175-80.
94. Zhang, T.;Hsu-Kim, H., *Photolytic degradation of methylmercury enhanced by binding to natural organic ligands*. Nat Geosci, 2010. **3**(7): p. 473-476.
95. Vost, E.E.;Amyot, M.;O'Driscoll, N.J., *Photoreactions of mercury in aquatic systems*. Environmental chemistry and toxicology of mercury, 2012: p. 193-218.
96. Lalonde, J.D.;Amyot, M.;Kraepiel, A.M.;Morel, F.M., *Photooxidation of Hg(0) in artificial and natural waters*. Environ Sci Technol, 2001. **35**(7): p. 1367-72.
97. Whalin, L.;Kim, E.-H.;Mason, R., *Factors influencing the oxidation, reduction, methylation and demethylation of mercury species in coastal waters*. Marine Chemistry, 2007. **107**(3): p. 278-294.
98. Zheng, W.;Liang, L.;Gu, B., *Mercury reduction and oxidation by reduced natural organic matter in anoxic environments*. Environ Sci Technol, 2012. **46**(1): p. 292-9.

99. Gu, B.;Bian, Y.;Miller, C.L.;Dong, W.;Jiang, X.;Liang, L., *Mercury reduction and complexation by natural organic matter in anoxic environments*. Proc Natl Acad Sci U S A, 2011. **108**(4): p. 1479-83.
100. Jiang, T.;Skylberg, U.;Wei, S.;Wang, D.;Lu, S.;Jiang, Z.;Flanagan, D.C., *Modeling of the structure-specific kinetics of abiotic, dark reduction of Hg(II) complexed by O/N and S functional groups in humic acids while accounting for time-dependent structural rearrangement*. Geochim. Cosmochim. Acta, 2015. **154**: p. 151-167.
101. Coulibaly, M.;Mazrui, N.M.;Jonsson, S.;Mason, R.P., *Abiotic Reduction of Mercury(II) in the Presence of Sulfidic Mineral Suspensions*. Frontiers in Environmental Chemistry, 2021. **2**.
102. Wiatrowski, H.A.;Das, S.;Kukkadapu, R.;Ilton, E.S.;Barkay, T.;Yee, N., *Reduction of Hg(II) to Hg(O) by Magnetite*. Environmental Science & Technology, 2009. **43**(14): p. 5307-5313.
103. Mishra, B.;O'Loughlin, E.J.;Boyanov, M.I.;Kemner, K.M., *Binding of HgII to high-affinity sites on bacteria inhibits reduction to Hgo by mixed FeII/III phases*. Environmental Science & Technology, 2011. **45**(22): p. 9597-603.
104. Benoit, J.M.;Gilmour, C.C.;Mason, R.P.;A., H., *Sulfide controls on Mercury Speciation and Bioavailability to Methylating Bacteria in Sediment Pore Waters*. Environmental Science & Technology, 1999. **33**: p. 951-957.
105. Mason, R.P.;Reinfelder, J.R.;Morel, F.M., *Uptake, Toxicity, and Trophic Transfer of Mercury in a Coastal Diatom*. Environmental Science & Technology, 1996. **30**: p. 1835-1845.
106. Golding, G.R.;Kelly, C.A.;Sparling, R.;Loewen, P.C.;Rudd, J.W.M.;Barkay, T., *Evidence for facilitated uptake of Hg(II) by Vibrio anguillarum and Escherichia coli under anaerobic and aerobic conditions*. Limnol. Oceanogr., 2002. **47**(4): p. 967-975.
107. Benoit, J.M.;Gilmour, C.C.;Mason, R.P., *Aspects of bioavailability of mercury for methylation in pure cultures of Desulfobulbus propionicus (1pr3)*. Appl. Environ. Microbiol., 2001. **67**(1): p. 51-8.
108. Benoit, J.M.;Mason, R.P.;Gilmour, C.C., *Estimation of mercury-sulfide speciation in sediment pore waters using octanol-water partitioning and implications for availability to methylating bacteria*. Environ. Toxicol. Chem., 1999. **18**(10): p. 2138-2141.
109. Barkay, T.;Gillman, M.;Turner, R.R., *Effects of dissolved organic carbon and salinity on bioavailability of mercury*. Appl. Environ. Microbiol., 1997. **63**(11): p. 4267-4271.
110. Zhou, J.;Smith, M.D.;Cooper, S.J.;Cheng, X.L.;Smith, J.C.;Parks, J.M., *Modeling of the Passive Permeation of Mercury and Methylmercury Complexes Through a Bacterial Cytoplasmic Membrane*. Environmental Science & Technology, 2017. **51**(18): p. 10595-10604.
111. Gutknecht, J., *Inorganic mercury (Hg²⁺) transport through lipid bilayer membranes*. The Journal of Membrane Biology, 1981. **61**(1): p. 61-66.
112. Deonarine, A.;Hsu-Kim, H., *Precipitation of Mercuric Sulfide Nanoparticles in NOM-Containing Water: Implications for the Natural Environment*. Environmental Science & Technology, 2009. **43**(7): p. 2368-2373.
113. Drott, A.;Bjorn, E.;Bouchet, S.;Skylberg, U., *Refining thermodynamic constants for mercury(II)-sulfides in equilibrium with metacinnabar at sub-micromolar aqueous sulfide concentrations*. Environmental Science & Technology, 2013. **47**(9): p. 4197-203.

114. Zhang, T.;Kim, B.;Leyard, C.;Reinsch, B.C.;Lowry, G.V.;Deshusses, M.A.;Hsu-Kim, H., *Methylation of Mercury by Bacteria Exposed to Dissolved, Nanoparticulate, and Microparticulate Mercuric Sulfides*. Environmental Science & Technology, 2012. **46**(13): p. 6950-6958.
115. Mazrui, N.M.;Jonsson, S.;Thota, S.;Zhao, J.;Mason, R.P., *Enhanced availability of mercury bound to dissolved organic matter for methylation in marine sediments*. Geochim. Cosmochim. Acta, 2016. **194**: p. 153-162.
116. Slaveykova, V.I.;Wilkinson, K.J., *Predicting the Bioavailability of Metals and Metal Complexes: Critical Review of the Biotic Ligand Model*. Environ. Chem., 2005. **2**(1).
117. Zhao, C.-M.;Campbell, P.G.C.;Wilkinson, K.J., *When are metal complexes bioavailable?* Environ. Chem., 2016. **13**(3): p. 425-433.
118. Szczuka, A.;Morel, F.M.M.;Schaefer, J.K., *Effect of Thiols, Zinc, and Redox Conditions on Hg Uptake in Shewanella oneidensis*. Environmental Science & Technology, 2015. **49**(12): p. 7432-7438.
119. Ndu, U.;Barkay, T.;Mason, R.P.;Traore Schartup, A.;Al-Farawati, R.;Liu, J.;Reinfelder, J.R., *The Use of a Mercury Biosensor to Evaluate the Bioavailability of Mercury-Thiol Complexes and Mechanisms of Mercury Uptake in Bacteria*. PLoS One, 2015. **10**(9): p. e0138333.
120. Adediran, G.A.;Liem-Nguyen, V.;Song, Y.;Schaefer, J.K.;Skylberg, U.;Bjorn, E., *Microbial Biosynthesis of Thiol Compounds: Implications for Speciation, Cellular Uptake, and Methylation of Hg(II)*. Environmental Science & Technology, 2019. **53**(14): p. 8187-8196.
121. Thomas, S.A.;Catty, P.;Hazemann, J.L.;Michaud-Soret, I.;Gaillard, J.F., *The role of cysteine and sulfide in the interplay between microbial Hg(ii) uptake and sulfur metabolism*. Metallomics, 2019. **11**(7): p. 1219-1229.
122. Reeder, R.J.;Schoonen, M.A.A.;Lanzirotti, A., *Metal Speciation and Its Role in Bioaccessibility and Bioavailability*. Reviews in Mineralogy and Geochemistry, 2006. **64**(1): p. 59-113.
123. Hsu-Kim, H.;Eckley, C.S.;Acha, D.;Feng, X.B.;Gilmour, C.C.;Jonsson, S.;Mitchell, C.P.J., *Challenges and opportunities for managing aquatic mercury pollution in altered landscapes*. Ambio, 2018. **47**(2): p. 141-169.
124. Mason, R.P., *Trace metals in aquatic systems*. 2013, Hoboken, N.J: John Wiley & Sons Inc.
125. Skylberg, U., *Competition among thiols and inorganic sulfides and polysulfides for Hg and MeHg in wetland soils and sediments under suboxic conditions: Illumination of controversies and implications for MeHg net production*. J. Geophys. Res.-Biogeosci., 2008. **113**: p. 14.
126. Liem-Nguyen, V.;Skylberg, U.;Nam, K.;Bjorn, E., *Thermodynamic stability of mercury(II) complexes formed with environmentally relevant low-molecular-mass thiols studied by competing ligand exchange and density functional theory*. Environ. Chem., 2017. **14**(4): p. 243-253.
127. Smith, R.M., *NIST Critically Selected Stability Constant of metal complexes database*. Version 4, 1997.
128. Jalilehvand, F.;Leung, B.O.;Izadifard, M.;Damian, E., *Mercury(II) Cysteine Complexes in Alkaline Aqueous Solution*. Inorg. Chem., 2006. **45**(1): p. 66-73.

129. Cooke Andrews, J., *Mercury Speciation in the Environment Using X-ray Absorption Spectroscopy*, in *Recent Developments in Mercury Science*, D.A. Atwood, Editor. 2006, Springer Berlin Heidelberg: Berlin, Heidelberg. p. 1-35.
130. Li, Y.;Yin, Y.;Liu, G.;Cai, Y., *Advances in Speciation Analysis of Mercury in the Environment*, in *Environmental Chemistry and Toxicology of Mercury*, G. Liu;Y. Cai;N. O´ Driscoll, Editors. 2011, John Wiley & Sons, Ltd. p. 13-58.
131. Wang, F.;Lemes, M.;Khan, M.A.K., *Metallomics of Mercury: Role of Thiol- and Selenol-Containing Biomolecules*, in *Environmental Chemistry and Toxicology of Mercury*, G. Liu;Y. Cai;N. O´ Driscoll, Editors. 2011, John Wiley & Sons, Ltd. p. 517-544.
132. Hudson R, J.M.;Gherini, S.A.;Watras, C.J.;Porcella, D.B., *MODELING THE BIOGEOCHEMICAL CYCLE OF MERCURY IN LAKES THE MERCURY CYCLING MODEL MCM AND ITS APPLICATION TO THE MTL STUDY LAKES*. 1994, Hudson R, JM; Gherini, SA; Watras, CJ; Porcella, DB. p. 473-523.
133. Zhang, J.Z.;Wang, F.Y.;House, J.D.;Page, B., *Thiols in wetland interstitial waters and their role in mercury and methylmercury speciation*. *Limnol. Oceanogr.*, 2004. **49**(6): p. 2276-2286.
134. Hu, H.;Mylon, S.E.;Benoit, G., *Distribution of the thiols glutathione and 3-mercaptopropionic acid in Connecticut lakes*. *Limnol. Oceanogr.*, 2006. **51**(6): p. 2763–2774.
135. Leclerc, M.;Planas, D.;Amyot, M., *Relationship between Extracellular Low-Molecular-Weight Thiols and Mercury Species in Natural Lake Periphytic Biofilms*. *Environmental Science & Technology*, 2015. **49**(13): p. 7709-16.
136. Liem-Nguyen, V.;Skylberg, U.;Björn, E., *Methylmercury formation in boreal wetlands in relation to chemical speciation of mercury(II) and concentration of low molecular mass thiols*. *Science of The Total Environment*, 2021. **755**: p. 142666.
137. Bouchet, S.;Goni-Urriza, M.;Monperrus, M.;Guyoneaud, R.;Fernandez, P.;Heredia, C.;Tessier, E.;Gassie, C.;Point, D.;Guedron, S.;Acha, D.;Amouroux, D., *Linking Microbial Activities and Low-Molecular-Weight Thiols to Hg Methylation in Biofilms and Periphyton from High-Altitude Tropical Lakes in the Bolivian Altiplano*. *Environmental Science & Technology*, 2018. **52**(17): p. 9758-9767.
138. Kiene, R.P., *Evidence for the biological turnover of thiols in anoxic marine sediments*. *Biogeochemistry*, 1991. **13**(2): p. 117-135.
139. Kiene, R.P.;Malloy, K.D.;Taylor, B.F., *Sulfur-Containing Amino Acids as Precursors of Thiols in Anoxic Coastal Sediments †*. *Appl. Environ. Microbiol.*, 1990. **56**(1): p. 156-161.
140. Thomas, S.A.;Tong, T.Z.;Gaillard, J.F., *Hg(II) bacterial biouptake: the role of anthropogenic and biogenic ligands present in solution and spectroscopic evidence of ligand exchange reactions at the cell surface*. *Metallomics*, 2014. **6**(12): p. 2213-2222.
141. Lu, X.;Liu, Y.;Johs, A.;Zhao, L.;Wang, T.;Yang, Z.;Lin, H.;Elias, D.A.;Pierce, E.M.;Liang, L.;Barkay, T.;Gu, B., *Anaerobic Mercury Methylation and Demethylation by Geobacter bemedjiensis Bem*. *Environmental Science & Technology*, 2016. **50**(8): p. 4366-73.
142. Thomas, S.A.;Gaillard, J.-F., *Cysteine Addition Promotes Sulfide Production and 4-Fold Hg(II)-S Coordination in Actively Metabolizing Escherichia coli*. *Environmental Science & Technology*, 2017. **51**(8): p. 4642-4651.
143. Zhang, T.;Kucharzyk, K.H.;Kim, B.;Deshusses, M.A.;Hsu-Kim, H., *Net Methylation of Mercury in Estuarine Sediment Microcosms Amended with Dissolved, Nanoparticulate,*

- and Microparticulate Mercuric Sulfides. *Environmental Science & Technology*, 2014. **48**(16): p. 9133-9141.
144. Kari, C.;Nagy, Z.;Kovacs, P.;Hernadi, F., *Mechanism of the Growth Inhibitory Effect of Cysteine on Escherichia coli*. *Journal of General Microbiology*, 1971. **68**: p. 349-356.
145. Carlsson, J.;Granberg, G.P.;Nyberg, G.K.;Edlund, M.B., *Bactericidal effect of cysteine exposed to atmospheric oxygen*. *Appl Environ Microbiol*, 1979. **37**(3): p. 383-90.
146. Park, S.;Imlay, J.A., *High levels of intracellular cysteine promote oxidative DNA damage by driving the fenton reaction*. *J Bacteriol*, 2003. **185**(6): p. 1942-50.
147. Turnbull, A.L.;Surette, M.G., *Cysteine biosynthesis, oxidative stress and antibiotic resistance in Salmonella typhimurium*. *Research in microbiology*, 2010. **161**(8): p. 643-50.
148. Reitzer, L., *Death by Cystine: an Adverse Emergent Property from a Beneficial Series of Reactions*. *J Bacteriol*, 2015. **197**(23): p. 3626-8.
149. Yin, X.;Wang, L.;Zhang, L.;Chen, H.;Liang, X.;Lu, X.;DiSpirito Alan, A.;Semrau Jeremy, D.;Gu, B., *Synergistic Effects of a Chalkophore, Methanobactin, on Microbial Methylation of Mercury*. *Appl. Environ. Microbiol.*, 2020. **86**(11): p. e00122-20.
150. Bravo, A.G.;Bouchet, S.;Tolu, J.;Bjorn, E.;Mateos-Rivera, A.;Bertilsson, S., *Molecular composition of organic matter controls methylmercury formation in boreal lakes*. *Nat. Commun.*, 2017. **8**: p. 9.
151. Wright, D.R.;Hamilton, R.D., *Release of Methyl Mercury from Sediments: Effects of Mercury Concentration, Low Temperature, and Nutrient Addition*. *Canadian Journal of Fisheries and Aquatic Sciences*, 1982. **39**(11): p. 1459-1466.
152. Thomas, S.A.;Mishra, B.;Myneni, S.C.B., *Cellular Mercury Coordination Environment, and Not Cell Surface Ligands, Influence Bacterial Methylmercury Production*. *Environmental Science & Technology*, 2020. **54**(7): p. 3960-3968.
153. Gilmour, C.C.;Henry, E.A.;Mitchell, R., *Sulfate stimulation of mercury methylation in freshwater sediments*. *Environmental Science & Technology*, 1992. **26**(11): p. 2281-2287.
154. Mishra, B.;Shoenfelt, E.;Yu, Q.;Yee, N.;Fein, J.B.;Myneni, S.C.B., *Stoichiometry of mercury-thiol complexes on bacterial cell envelopes*. *Chem. Geol.*, 2017. **464**: p. 137-146.
155. Song, Y.;Adediran, G.A.;Jiang, T.;Hayama, S.;Bjorn, E.;Skylberg, U., *Toward an Internally Consistent Model for Hg(II) Chemical Speciation Calculations in Bacterium-Natural Organic Matter-Low Molecular Mass Thiol Systems*. *Environmental Science & Technology*, 2020. **54**(13): p. 8094-8103.
156. Dunham-Cheatham, S.;Mishra, B.;Myneni, S.;Fein, J.B., *The effect of natural organic matter on the adsorption of mercury to bacterial cells*. *Geochim. Cosmochim. Acta*, 2015. **150**: p. 1-10.
157. Song, Y.;Jiang, T.;Liem-Nguyen, V.;Sparrman, T.;Björn, E.;Skylberg, U., *Thermodynamics of Hg(II) Bonding to Thiol Groups in Suwannee River Natural Organic Matter Resolved by Competitive Ligand Exchange, Hg LIII-Edge EXAFS and ¹H NMR Spectroscopy*. *Environmental Science & Technology*, 2018. **52**(15): p. 8292-8301.
158. Dyrssen, D.;Wedborg, M., *The sulphur-mercury(II) system in natural waters*. *Water, Air & Soil Pollution*, 1991. **56**(1): p. 507-519.
159. Johnson, C.R.;Fein, J.B., *The effect of metal loading on bacterial Hg adsorption*. *Chem. Geol.*, 2018. **498**: p. 106-114.

160. Rao, B.;Simpson, C.;Lin, H.;Liang, L.;Gu, B., *Determination of thiol functional groups on bacteria and natural organic matter in environmental systems*. Talanta, 2014. **119**: p. 240-7.
161. Fein, J.B., *Advanced biotic ligand models: Using surface complexation modeling to quantify metal bioavailability to bacteria in geologic systems*. Chem. Geol., 2017. **464**: p. 127-136.
162. Isaure, M.P.;Albertelli, M.;Kieffer, I.;Tucoulou, R.;Petrel, M.;Gontier, E.;Tessier, E.;Monperrus, M.;Goñi-Urriza, M., *Relationship Between Hg Speciation and Hg Methylation/Demethylation Processes in the Sulfate-Reducing Bacterium Pseudodesulfobivibrio hydrargyri: Evidences From HERFD-XANES and Nano-XRF*. Front Microbiol, 2020. **11**: p. 584715.
163. Liang, X.;Johs, A.;Abernathy, M.J.;Zhao, J.;Du, H.;Ku, P.;Zhang, L.;Zhu, N.;Yin, X.;Brooks, S.;Zhao, L.;Sarangi, R.;Pierce, E.M.;Gu, B., *High methylation potential of mercury complexed with mixed thiolate ligands by Geobacter sulfurreducens PCA*. Geochim. Cosmochim. Acta, 2023. **342**: p. 74-83.
164. Wang, Y.W.;Yu, Q.;Mishra, B.;Schaefer, J.K.;Fein, J.B.;Yee, N., *Adsorption of Methylmercury onto Geobacter bemidjensis Bem*. Environmental Science & Technology, 2018. **52**(20): p. 11564-11572.
165. Caccavo, F., Jr.;Lonergan, D.J.;Lovley, D.R.;Davis, M.;Stolz, J.F.;McInerney, M.J., *Geobacter sulfurreducens sp. nov., a hydrogen- and acetate-oxidizing dissimilatory metal-reducing microorganism*. Appl Environ Microbiol, 1994. **60**(10): p. 3752-9.
166. Waite, D.W.;Chuvochina, M.;Pelikan, C.;Parks, D.H.;Yilmaz, P.;Wagner, M.;Loy, A.;Naganuma, T.;Nakai, R.;Whitman, W.B.;Hahn, M.W.;Kuever, J.;Hugenholtz, P., *Proposal to reclassify the proteobacterial classes Deltaproteobacteria and Oligoflexia, and the phylum Thermodesulfobacteria into four phyla reflecting major functional capabilities*. International journal of systematic and evolutionary microbiology, 2020. **70**(11): p. 5972-6016.
167. Knoche, K.L.;Renner, J.N.;Gellett, W.;Ayers, K.E.;Minteer, S.D., *A Self-Sufficient Nitrate Groundwater Remediation System: Geobacter Sulfurreducens Microbial Fuel Cell Fed by Hydrogen from a Water Electrolyzer*. Journal of The Electrochemical Society, 2016. **163**(7): p. F651.
168. Bond, D.R.;Lovley, D.R., *Electricity production by Geobacter sulfurreducens attached to electrodes*. Appl Environ Microbiol, 2003. **69**(3): p. 1548-55.
169. Lovley, D.R., *Electromicrobiology*. Annu Rev Microbiol, 2012. **66**: p. 391-409.
170. Kerin, E.J.;Gilmour, C.C.;Roden, E.;Suzuki, M.T.;Coates, J.D.;Mason, R.P., *Mercury methylation by dissimilatory iron-reducing bacteria*. Appl Environ Microbiol, 2006. **72**(12): p. 7919-21.
171. Caccova, F.;Lonergan, D.J.;Lovley, D.R.;Mark, D.;Stolz, J.F.;McInerney, M.J., *Geobacter sulfurreducens sp. nova., a Hydrogen- and Acetate-Oxidizing Dissimilatory Metal-Reducing Microorganism*. Appl. Environ. Microbiol., 1994. **60**: p. 3752-3759.
172. Magnuson, T.S.;Hodges-Myerson, A.L.;Lovley, D.R., *Characterization of a membrane-bound NADH-dependent Fe³⁺ reductase from the dissimilatory Fe³⁺-reducing bacterium Geobacter sulfurreducens*. FEMS Microbiology Letters, 2000. **185**(2): p. 205-211.
173. Methé, B.A.;Nelson, K.E.;Eisen, J.A.;Paulsen, I.T.;Nelson, W.;Heidelberg, J.F.;Wu, D.;Wu, M.;Ward, N.;Beanan, M.J.;Dodson, R.J.;Madupu, R.;Brinkac, L.M.;Daugherty,

- S.C.;DeBoy, R.T.;Durkin, A.S.;Gwinn, M.;Kolonay, J.F.;Sullivan, S.A.;Haft, D.H.;Selengut, J.;Davidsen, T.M.;Zafar, N.;White, O.;Tran, B.;Romero, C.;Forberger, H.A.;Weidman, J.;Khouri, H.;Feldblyum, T.V.;Utterback, T.R.;Van Aken, S.E.;Lovley, D.R.;Fraser, C.M., *Genome of Geobacter sulfurreducens: metal reduction in subsurface environments*. Science, 2003. **302**(5652): p. 1967-9.
174. DSMZ. 826: *GEOBACTER SULFURREDUCTENS MEDIUM*. [22.03.2023]; Available from: <https://www.dsmz.de/collection/catalogue/details/culture/DSM-12127>.
175. Coppi, M.V.;O'Neil, R.A.;Leang, C.;Kaufmann, F.;Methe, B.A.;Nevin, K.P.;Woodard, T.L.;Liu, A.;Lovley, D.R., *Involvement of Geobacter sulfurreducens SfrAB in acetate metabolism rather than intracellular, respiration-linked Fe(III) citrate reduction*. Microbiology, 2007. **153**(Pt 10): p. 3572-3585.
176. Kosower, E.M., *Bimane fluorescent labels: Labeling of normal human red cells under physiological conditions*. Cell Biology, 1979. **76**(7): p. 3382-3386.
177. Fahey, R.C.;Newton, G.L.;Dorian, R.;Kosower, E.M., *Analysis of Biological Thiols: Quantitative Determination of picomolar level based upon derivatization with monobromobimanes and separation by cation-exchange chromatography*. ANALYTICAL BIOCHEMISTRY, 1980. **111**: p. 357-365.
178. Joe-Wong, C.;Shoenfelt, E.;Hauser, E.J.;Crompton, N.;Myneni, S.C.B., *Estimation of Reactive Thiol Concentrations in Dissolved Organic Matter and Bacterial Cell Membranes in Aquatic Systems*. Environmental Science & Technology, 2012. **46**(18): p. 9854-9861.
179. Yu, Q.;Mishra, B.;Fein, J.B., *Role of bacterial cell surface sulfhydryl sites in cadmium detoxification by Pseudomonas putida*. Journal of Hazardous Materials, 2020. **391**: p. 122209.
180. Huynh, K.;Liem-Nguyen, V.;Feng, C.;Lindberg, R.;Björn, E., *Quantification of total concentration of thiol functional groups in environmental samples by titration with monobromo(trimethylammonio)bimane and determination with tandem mass spectrometry*. Talanta, 2020. **218**.
181. Yu, Q.;Szymanowski, J.;Myneni, S.C.B.;Fein, J.B., *Characterization of sulfhydryl sites within bacterial cell envelopes using selective site-blocking and potentiometric titrations*. Chem. Geol., 2014. **373**: p. 50-58.
182. Huang, T.T.;Kosower, N.S.;Yanagimachi, R., *Localization of thiol and disulfide groups in guinea pig spermatozoa during maturation and capacitation using bimane fluorescent labels*. Biology of reproduction, 1984. **31**(4): p. 797-809.
183. Cook, J.A.;Pass, H.I.;Russo, A.;Iype, S.;Mitchell, J.B., *Use of monochlorobimane for glutathione measurements in hamster and human tumor cell lines*. International journal of radiation oncology, biology, physics, 1989. **16**(5): p. 1321-4.
184. Tyagarajan, K.;Pretzer, E.;Wiktorowicz, J.E., *Thiol-reactive dyes for fluorescence labeling of proteomic samples*. Electrophoresis, 2003. **24**(14): p. 2348-58.
185. Sahaf, B.;Heydari, K.;Herzenberg, L.A.;Herzenberg, L.A., *Lymphocyte surface thiol levels*. Proceedings of the National Academy of Sciences, 2003. **100**(7): p. 4001-4005.
186. Mate, K.E.;Kosower, N.S.;White, I.G.;Rodger, J.C., *Fluorescent localization of thiols and disulfides in marsupial spermatozoa by bromobimane labelling*. Molecular Reproduction and Development, 1994. **37**(3): p. 318-325.
187. Gutensohn, M.;Desmau, M.;Proux, O.;Björn, E.;Skjllberg, U., *Determination of mercury speciation and thiol concentration on the outer and inner cell membrane surface of*

- Geobacter sulfurreducens* by EXAFS and HERFD-XANES, in *Manuscript in Preparation*. 2023.
188. Liem-Nguyen, V.;Bouchet, S.;Björn, E., *Determination of Sub-Nanomolar Levels of Low Molecular Mass Thiols in Natural Waters by Liquid Chromatography Tandem Mass Spectrometry after Derivatization with p-(Hydroxymercuri)Benzoate and Online Preconcentration*. *Anal. Chem.*, 2015. **87**(2): p. 1089-1096.
 189. Snell, J.P.;Stewart, I.I.;Sturgeon, R.E.;Frech, W., *Species specific isotope dilution calibration for determination of mercury species by gas chromatography coupled to inductively coupled plasma- or furnace atomisation plasma ionisation-mass spectrometry*. *Journal of Analytical Atomic Spectrometry*, 2000. **15**(12): p. 1540-1545.
 190. Heumann, K.G., *Book Review: Guidelines for Achieving High Accuracy in Isotope Dilution Mass Spectrometry (IDMS) Edited by Mike Sargent, Chris Harrington and Rita Harte*. *Angewandte Chemie International Edition*, 2003. **42**(14): p. 1564-1565.
 191. Björn, E.;Larsson, T.;Lambertsson, L.;Skylberg, U.;Frech, W., *Recent advances in mercury speciation analysis with focus on spectrometric methods and enriched stable isotope applications*. *Ambio*, 2007. **36**(6): p. 443-51.
 192. *Method 1631, Revision E: Mercury in Water by Oxidation, Purge and Trap, and Cold Vapor Atomic Fluorescence Spectrometry*. EPA: Washington, DC, 2002.
 193. Carrasco, L.;Vassileva, E., *Determination of methylmercury in marine biota samples: Method validation*. *Talanta*, 2014. **122**: p. 106-114.
 194. Lambertsson, L.;Bjorn, E., *Validation of a simplified field-adapted procedure for routine determinations of methyl mercury at trace levels in natural water samples using species-specific isotope dilution mass spectrometry*. *Analytical Bioanalytical Chemistry*, 2004. **380**(7-8): p. 871-5.
 195. Proux, O.;Lahera, E.;Del Net, W.;Kieffer, I.;Rovezzi, M.;Testemale, D.;Irar, M.;Thomas, S.;Aguilar-Tapia, A.;Bazarkina, E.F.;Prat, A.;Tella, M.;Auffan, M.;Rose, J.;Hazemann, J.L., *High-Energy Resolution Fluorescence Detected X-Ray Absorption Spectroscopy: A Powerful New Structural Tool in Environmental Biogeochemistry Sciences*. *J Environ Qual*, 2017. **46**(6): p. 1146-1157.
 196. Proux, O.;Biquard, X.;Lahera, E.;Menthonnex, J.J.;Prat, A.;Ulrich, O.;Soldo, Y.;Trivison, P.;Kapoujyan, G.;Perroux, G.;Taunier, P.;Grand, D.;Jeantet, P.;Deleglise, M.;Roux, J.P.;Hazemann, J.L., *FAME A New Beamline for XRay Absorption Investigations of VeryDiluted Systems of Environmental, Material and Biological Interests*. *Physica Scripta*, 2005: p. 970.
 197. Welter, E.;Chernikov, R.;Herrmann, M.;Nemausat, R., *A beamline for bulk sample x-ray absorption spectroscopy at the high brilliance storage ring PETRA III*. *AIP Conference Proceedings*, 2019. **2054**(1): p. 040002.
 198. Grasshoff, K.;Kremling, K.;Ehrhardt, M., *Methods of Seawater analysis*.
 199. Fonselius, S.H.;Dyrssén, D.;Yhlén, B., *Determination of hydrogen sulphide.*, in *Methods of Seawater Analysis*. 2007, Wiley-VCH: New York. p. 91-100.
 200. Bremer, P.J.;Geesey, G.G., *An evaluation of biofilm development utilizing non-destructive attenuated total reflectance Fourier transform infrared spectroscopy*. *Biofouling*, 1991. **3**(2): p. 89-100.
 201. Quilès, F.;Humbert, F.;Delille, A., *Analysis of changes in attenuated total reflection FTIR fingerprints of Pseudomonas fluorescens from planktonic state to nascent biofilm state*.

- Spectrochimica Acta Part A: Molecular and Biomolecular Spectroscopy, 2010. **75**(2): p. 610-616.
202. Karlsson, M.;Lindgren, J. [2020-06-06]; Available from: http://www.winsgw.se/WinSGW_eng.htm.
203. Kiene, R.P.;Taylor, B.F., *Demethylation of Dimethylsulfoniopropionate and Production of Thiols in Anoxic Marine Sediments* †. Appl. Environ. Microbiol., 1988. **54**(9): p. 2208-2212.
204. Chandrangsou, P.;Rensing, C.;Helmann, J.D., *Metal homeostasis and resistance in bacteria*. Nature Reviews Microbiology, 2017. **15**(6): p. 338-350.
205. Embree, M.;Qiu, Y.;Shieu, W.;Nagarajan, H.;O'Neil, R.;Lovley, D.;Zengler, K., *The iron stimulon and fur regulon of Geobacter sulfurreducens and their role in energy metabolism*. Appl Environ Microbiol, 2014. **80**(9): p. 2918-27.
206. Neilands, J.B., *Iron absorption and transport in microorganisms*. Annual review of nutrition, 1981. **1**: p. 27-46.
207. Khan, A.;Singh, P.;Srivastava, A., *Synthesis, nature and utility of universal iron chelator - Siderophore: A review*. Microbiological research, 2018. **212-213**: p. 103-111.
208. Bauerle, M.R.;Schwalm, E.L.;Booker, S.J., *Mechanistic Diversity of Radical S-Adenosylmethionine (SAM)-dependent Methylation**. Journal of Biological Chemistry, 2015. **290**(7): p. 3995-4002.
209. Ermler, U.;Grabarse, W.;Shima, S.;Goubeaud, M.;Thauer, R.K., *Crystal structure of methyl-coenzyme M reductase: the key enzyme of biological methane formation*. Science, 1997. **278**(5342): p. 1457-62.
210. Fyfe, C.D.;Bernardo-García, N.;Fradale, L.;Grimaldi, S.;Guillot, A.;Brewer, C.;Chavas, L.M.G.;Legrand, P.;Benjdia, A.;Bertheau, O., *Crystallographic snapshots of a B12-dependent radical SAM methyltransferase*. Nature, 2022. **602**(7896): p. 336-342.
211. Norambuena, J.;Wang, Y.;Hanson, T.;Boyd, J.M.;Barkay, T., *Low-Molecular-Weight Thiols and Thioresoxins Are Important Players in Hg(II) Resistance in Thermus thermophilus HB27*. Appl Environ Microbiol, 2018. **84**(2).
212. Rodríguez-Rojas, F.;Díaz-Vásquez, W.;Undabarrena, A.;Muñoz-Díaz, P.;Arenas, F.;Vásquez, C., *Mercury-mediated cross-resistance to tellurite in Pseudomonas spp. isolated from the Chilean Antarctic territory*. Metallomics, 2016. **8**(1): p. 108-17.
213. Gao, Y.;Peng, X.;Zhang, J.;Zhao, J.;Li, Y.;Li, Y.;Li, B.;Hu, Y.;Chai, Z., *Cellular response of E. coli upon Hg2+ exposure – a case study of advanced nuclear analytical approach to metalloproteomics*. Metallomics, 2013. **5**(7): p. 913-919.
214. Feldman, C., *Preservation of dilute mercury solutions*. Anal. Chem., 1974. **46**(1): p. 99-102.
215. Parker, J.L.;Bloom, N.S., *Preservation and storage techniques for low-level aqueous mercury speciation*. Science of The Total Environment, 2005. **337**(1): p. 253-263.
216. Olsen, T.A.;Muller, K.A.;Painter, S.L.;Brooks, S.C., *Kinetics of Methylmercury Production Revisited*. Environ Sci Technol, 2018. **52**(4): p. 2063-2070.
217. Jonsson, S.;Skylberg, U.;Nilsson, M.B.;Westlund, P.-O.;Shchukarev, A.;Lundberg, E.;Björn, E., *Mercury Methylation Rates for Geochemically Relevant HgII Species in Sediments*. Environmental Science & Technology, 2012. **46**(21): p. 11653-11659.
218. Preiss, J., *Bacterial glycogen synthesis and its regulation*. Annu Rev Microbiol, 1984. **38**: p. 419-58.

219. Preiss, J.;Romeo, T., *Physiology, biochemistry and genetics of bacterial glycogen synthesis*. Advances in microbial physiology, 1989. **30**: p. 183-238.
220. Sekar, K.;Linker, S.M.;Nguyen, J.;Grünhagen, A.;Stocker, R.;Sauer, U.;Cann, I., *Bacterial Glycogen Provides Short-Term Benefits in Changing Environments*. Appl. Environ. Microbiol., 2020. **86**(9): p. e00049-20.
221. Yu, Q.;Fein, J.B., *Controls on Bacterial Cell Envelope Sulfhydryl Site Concentrations: The Effect of Glucose Concentration During Growth*. Environmental Science & Technology, 2017. **51**(13): p. 7395-7402.
222. Ueki, T., *Cytochromes in Extracellular Electron Transfer in Geobacter*. Appl Environ Microbiol, 2021. **87**(10).
223. Ding, Y.H.;Hixson, K.K.;Giometti, C.S.;Stanley, A.;Esteve-Núñez, A.;Khare, T.;Tollaksen, S.L.;Zhu, W.;Adkins, J.N.;Lipton, M.S.;Smith, R.D.;Mester, T.;Lovley, D.R., *The proteome of dissimilatory metal-reducing microorganism Geobacter sulfurreducens under various growth conditions*. Biochim Biophys Acta, 2006. **1764**(7): p. 1198-206.
224. Lin, C.C.;Jay, J.A., *Mercury methylation by planktonic and biofilm cultures of Desulfovibrio desulfuricans*. Environ Sci Technol, 2007. **41**(19): p. 6691-7.
225. Skyllberg, U.;Bloom, P.R.;Qian, J.;Lin, C.-M.;Bleam, W.F., *Complexation of Mercury(II) in Soil Organic Matter: EXAFS Evidence for Linear Two-Coordination with Reduced Sulfur Groups*. Environmental Science & Technology, 2006. **40**: p. 4174-4180.
226. Cremona, F.;Hamelin, S.;Planas, D.;Lucotte, M., *Sources of Organic Matter and Methylmercury in Littoral Macroinvertebrates: A Stable Isotope Approach*. Biogeochemistry, 2009. **94**(1): p. 81-94.
227. Dominique, Y.;Maury-Brachet, R.;Muresan, B.;Vigouroux, R.;Richard, S.;Cossa, D.;Mariotti, A.;Boudou, A., *Biofilm and mercury availability as key factors for mercury accumulation in fish (Curimata cyprinoides) from a disturbed amazonian freshwater system*. Environ. Toxicol. Chem., 2007. **26**(1): p. 45-52.
228. Stoodley, P.;Sauer, K.;Davies, D.G.;Costerton, J.W., *Biofilms as complex differentiated communities*. Annu Rev Microbiol, 2002. **56**: p. 187-209.
229. Karatan, E.;Watnick, P., *Signals, regulatory networks, and materials that build and break bacterial biofilms*. Microbiology and molecular biology reviews : MMBR, 2009. **73**(2): p. 310-47.
230. Mah, T.-F.C.;O'Toole, G.A., *Mechanisms of biofilm resistance to antimicrobial agents*. Trends in Microbiology, 2001. **9**(1): p. 34-39.
231. Miller, C.L.;Watson, D.B.;Lester, B.P.;Howe, J.Y.;Phillips, D.H.;He, F.;Liang, L.;Pierce, E.M., *Formation of Soluble Mercury Oxide Coatings: Transformation of Elemental Mercury in Soils*. Environmental Science & Technology, 2015. **49**(20): p. 12105-12111.
232. Pannu, R.;Siciliano, S.D.;O'Driscoll, N.J., *Quantifying the effects of soil temperature, moisture and sterilization on elemental mercury formation in boreal soils*. Environmental Pollution, 2014. **193**: p. 138-146.
233. O'Connor, D.;Hou, D.;Ok, Y.S.;Mulder, J.;Duan, L.;Wu, Q.;Wang, S.;Tack, F.M.G.;Rinklebe, J., *Mercury speciation, transformation, and transportation in soils, atmospheric flux, and implications for risk management: A critical review*. Environment International, 2019. **126**: p. 747-761.

Appendix

Table A1: Overview of growth medium and assay buffer composition for the different studies. Standard growth medium and standard assay buffer were used in all Papers (I-IV). Modifications are indicated. The pH of all solutions was adjusted to 6.8. (Table adapted from Paper I and II)

Component	Unit	Standard growth medium	Iron depleted growth medium §	Standard assay buffer *,#	Metabolite assay buffer §	Nutrient assay buffer §	Spheroplast assay buffer *,§
MOPS	mM	10	10	10	10	10	10
NH ₄ Cl	mM	5.6	5.6	0.1	0.1	0.7	-
KCl	mM	1.3	1.3	1.3	1.3	1.3	5.1
CaCl ₂	μM	8	8	-	0.8	0.8	-
NaCl	mM	0.17	0.17	0.17	0.17	0.17	80
MgSO ₄	mM	0.12	0.12	0.15	0.15	0.15	-
MgCl ₂	mM	-	-	-	-	-	1.5
NaH ₂ PO ₄	mM	0.05	0.05	5	4.51-5.00	4.51	-
KH ₂ PO ₄	mM	-	-	-	-	-	3.09
K ₂ HPO ₄	mM	-	-	-	-	-	1.26
Acetate	mM	10	10	1	1.0-1.9	1.9	1
Fumarate	mM	40	40	1	1.0-3.9	3.9	1
Resazurin	μM	4	4	4	4	4	-
Sucrose	mM	-	-	-	-	-	350
NTA	μM	78.6	-	-	0-10	7.86	-
EDTA	μM	-	100	-	0-10	-	-
CoCl ₂	μM	4.24	4.24	-	0-0.42	0.42	-
CuSO ₄	μM	0.04	-	-	-	0	-
MnCl ₂	μM	29.8	29.8	-	0-2.98	2.98	-
AlK(SO ₄) ₂	μM	0.22	0.22	-	0-0.02	0.02	-
H ₃ BO ₃	μM	1.6	1.6	-	0-0.16	0.16	-
Na ₂ MoO ₄	μM	0.42	0.42	-	0-0.04	0.04	-
NiCl ₂	μM	0.44	0.44	-	0-0.04	0.04	-
ZnSO ₄	μM	3.48	3.48	-	0-0.35	0.35	-
FeSO ₄	μM	3.6	1.5	-	0-0.15	0.36	-
Na ₂ SeO ₃	μM	0.6	0.6	-	0-0.06	0.06	-

§Paper I & II, *no fumarate and acetate in Paper III, #no resazurin in Paper IV, ‡Paper III & IV

Table A2: Overview of different measured and calculated Hg fractions. Calculation varies among Paper II and IV due to differences in the measured Hg fraction. Details are described in Paper II and IV.

Measurements		Paper
Total Hg (THg)		II, III, IV
Total Dissolved Hg (DHg)		II, III, IV
Total MeHg (TMeHg)		II, IV
Dissolved MeHg (DMeHg)		IV
Non-purgeable – THg (NP-THg)		IV
Non-purgeable – DHg (NP-DHg)		IV
Total intracellular Hg (CHg)		IV
Calculations		
Total Hg losses	= Added Hg – Total Hg	II, IV
Total cell-adsorbed Hg	= THg – DHg – CHg	IV
Total cell-associated Hg	= THg – DHg	II, IV
Dissolved MeHg	= Fraction dissolved MeHg × Total MeHg	II
Cell-associated MeHg	= TMeHg – DMeHg	II, IV
Total Hg(o)	= THg – NP-THg	IV
Dissolved Hg(o)	= DHg – NP-DHg	IV
Cell-associated Hg(o)	= THg – NP-THg – dissolved Hg(o)	IV
Total Hg(II)	= Total Hg – Total MeHg	II
	NP-THg – TMeHg	IV
Dissolved Hg(II)	= Total dissolved Hg – dissolved MeHg	II
	NP-DHg – DMeHg	IV
Cell-associated Hg(II)	= Total cell-associated Hg – cell-associated MeHg	II
	Total Hg(II) – Dissolved Hg(II)	IV

Table A3: Overview of the different Hg species terminology used in EXAFS and HERFD-XANES studies for the outer and inner membrane of *G. sulfurreducens*. EXAFS data were analyzed by fitting *ab initio* models of known structures generating information about coordination number, bond distance and Debye-Waller factors (thermal and structural disorder). HERFD-XANES data were analyzed by optimizing LCF of pre-selected model compounds. Based on the different data treatment the Hg speciation was expressed by different terms in EXAFS and HERFD-XANES studies and describing equivalent structures.

EXAFS	HERFD-XANES	Description
Hg(Mem-RS) ₂	Hg(Cys) ₂ *	Hg coordinated with two -SH functional groups
Hg(Mem-RO/N) ₂	Hg(acetate) ₂	Hg coordinated with two -OH, -COOH or NH ₂ functional groups or a combination of these three functional groups
Liquid Hg(o)	Liquid Hg(o)	Elemental liquid Hg

* measured at pH 3 and 11